

LI

LABORATORY INVESTIGATION

THE BASIC AND TRANSLATIONAL PATHOLOGY RESEARCH JOURNAL

VOLUME 98 | SUPPLEMENT 1 | MARCH 2018

 USCAP 2018

ABSTRACTS

HEAD AND NECK PATHOLOGY

(1317-1386)

107TH ANNUAL MEETING

**GEARED
TO
LEARN**



MARCH 17-23, 2018

Vancouver Convention Centre
Vancouver, BC, Canada

Published by

SPRINGER NATURE

www.ModernPathology.org

 **USCAP**
Creating a Better Pathologist

AN OFFICIAL JOURNAL OF THE
UNITED STATES AND CANADIAN
ACADEMY OF PATHOLOGY

EDUCATION COMMITTEE

Jason L. Hornick, Chair
 Rhonda Yantiss, Chair, Abstract Review Board
 and Assignment Committee
 Laura W. Lamps, Chair, CME Subcommittee
 Steven D. Billings, Chair, Interactive Microscopy
 Shree G. Sharma, Chair, Informatics Subcommittee
 Raja R. Seethala, Short Course Coordinator
 Ilan Weinreb, Chair, Subcommittee for
 Unique Live Course Offerings
 David B. Kaminsky, Executive Vice President
 (Ex-Officio)
 Aleodor (Doru) Andea
 Zubair Baloch
 Olca Basturk
 Gregory R. Bean, Pathologist-in-Training
 Daniel J. Brat

Amy Chadburn
 Ashley M. Cimino-Mathews
 James R. Cook
 Carol F. Farver
 Meera R. Hameed
 Michelle S. Hirsch
 Anna Marie Mulligan
 Rish Pai
 Vinita Parkash
 Anil Parwani
 Deepa Patil
 Lakshmi Priya Kunju
 John D. Reith
 Raja R. Seethala
 Kwun Wah Wen, Pathologist-in-Training

ABSTRACT REVIEW BOARD

Narasimhan Agaram
 Christina Arnold
 Dan Berney
 Ritu Bhalla
 Parul Bhargava
 Justin Bishop
 Jennifer Black
 Thomas Brenn
 Fadi Brimo
 Natalia Buza
 Yingbei Chen
 Benjamin Chen
 Rebecca Chernock
 Andres Chiesa-Vottero
 James Conner
 Claudiu Cotta
 Tim D'Alfonso
 Leona Doyle
 Daniel Dye
 Andrew Evans
 Alton Farris
 Dennis Firchau
 Ann Folkins
 Karen Fritchie
 Karuna Garg
 James Gill
 Anthony Gill
 Ryan Gill
 Tamara Giorgadze
 Raul Gonzalez
 Anuradha Gopalan
 Jennifer Gordetsky
 Ilyssa Gordon
 Alejandro Gru

Mamta Gupta
 Omar Habeeb
 Marc Halushka
 Krisztina Hanley
 Douglas Hartman
 Yael Heher
 Walter Henricks
 John Higgins
 Jason Hornick
 Mojgan Hosseini
 David Hwang
 Michael Idowu
 Peter Illei
 Kristin Jensen
 Vickie Jo
 Kirk Jones
 Chia-Sui Kao
 Ashraf Khan
 Michael Kluk
 Kristine Konopka
 Gregor Krings
 Asangi Kumarapeli
 Frank Kuo
 Alvaro Laga
 Robin LeGallo
 Melinda Lerwill
 Rebecca Levy
 Zaibo Li
 Yen-Chun Liu
 Tamara Lotan
 Joe Maleszewski
 Adrian Marino-Enriquez
 Jonathan Marotti
 Jerri McLemore

David Meredith
 Dylan Miller
 Roberto Miranda
 Elizabeth Morgan
 Juan-Miguel Mosquera
 Atis Muehlenbachs
 Raouf Nakhleh
 Ericka Olgaard
 Horatiu Olteanu
 Kay Park
 Rajiv Patel
 Yan Peng
 David Pisapia
 Jenny Pogoriler
 Alexi Polydorides
 Sonam Prakash
 Manju Prasad
 Bobbi Pritt
 Peter Pytel
 Charles Quick
 Joseph Rabban
 Raga Ramachandran
 Preetha Ramalingam
 Priya Rao
 Vijaya Reddy
 Robyn Reed
 Michelle Reid
 Natasha Rekhman
 Michael Rivera
 Mike Roh
 Marianna Ruzinova
 Peter Sadow
 Safia Salaria
 Steven Salvatore

Souzan Sanati
 Sandro Santagata
 Anjali Saqi
 Frank Schneider
 Michael Seidman
 Shree Sharma
 Jeanne Shen
 Steven Shen
 Jiaqi Shi
 Wun-Ju Shieh
 Konstantin Shilo
 Steven Smith
 Lauren Smith
 Aliyah Sohani
 Heather Stevenson-Lerner
 Khin Thway
 Evi Vakiani
 Sonal Varma
 Marina Vivero
 Yihong Wang
 Christopher Weber
 Olga Weinberg
 Astrid Weins
 Maria Westerhoff
 Sean Williamson
 Laura Wood
 Wei Xin
 Mina Xu
 Rhonda Yantiss
 Akihiko Yoshida
 Xuefeng Zhang
 Debra Zynger

To cite abstracts in this publication, please use the following format: **Author A, Author B, Author C, et al. Abstract title (abs#). *Laboratory Investigation* 2018; 98 (suppl 1): page#**

1317 Subgemmal Neurogenous Plaque: A Clinical and Pathologic Review

Hussein Alnajar¹, Thomas R O'Toole², Diana M Lin³, Vijaya Reddy⁴, Pincas Bitterman⁵, Leonidas Arvanitis⁶, Ritu Gha⁷, Samer Al-Khudar⁸, Paolo Gattuso⁹. ¹Rush University Medical Center, Chicago, IL, ²University of Kansas Medical Center, ³University of Illinois at Chicago, Chicago, IL, ⁴Rush University Medical Center, Chicago, IL, ⁵Rush University Medical Center, ⁶Burr Ridge, IL

Background: In humans, subgemmal neurogenous plaque (SNP) is a well described structure normally found in association with the taste buds as subepithelial aggregates of ganglion cells and nerve plexus. They are usually asymptomatic, but occasionally they may be associated with an erythematous area, ulcer, white patch or a hyperplastic papule which may warrant a biopsy. The aim of this study is to look at the nature of neural neoplasms in the head and neck mucosal region and to correctly recognize SNP to potentially avoid misdiagnosis and unnecessary treatment.

Design: From 3/2000 to 6/2017 the surgical pathology archives were reviewed for head and neck mucosal neural lesions. The pathologic and clinical data were reviewed in details.

Results: A total of 26 cases were identified, 9 neuromas, 9 neurofibromas, 2 ganglioneuromas and 6 cases with hyperplastic subepithelial nerve bundle.

After reviewing the histologic material the 26 lesions were re-classified as follows: traumatic neuroma 3 cases and neurofibroma in 3 cases. The remaining 20 cases were reclassified as SNP.

In patients with the original diagnosis of neurofibroma (9 cases) and ganglioneuroma (2 cases) a full clinical investigation was done for neurofibromatosis or other multiple endocrine neoplasias. None of these patients had any clinical syndromes.

The 20 cases of SNP were 15 women and 5 men with a median age of 60 years (range 30-85 years). The location of SNP cases was as follows: 10 cases oral tongue (50%), 8 cases base of tongue (40%), 1 case each lip and tonsillar fossa (5%). The mean greatest dimension of SNPs was 2.0 mm (1-3 mm in diameter). Most of them were subjacent to taste buds (13 cases).

The clinical data was available in 19 cases; most common presenting complaints were: painless lesion in 8 patients, mouth or throat pain in 5, otalgia in 2, odynophagia in 2, and weight loss in 2.

Case	Gender	Age	Smoking status	Location	Original Histologic diagnosis	Size (mm)	Ganglion cells	Taste Buds	Chronic inflammation
1	F	63	unknown	oral tongue	neuroma	3	no	yes	no
2	F	35	no	base of tongue	neuroma	2	yes	no	yes
3	M	50	current daily	base of tongue	neurofibroma	2	no	yes	no
4	F	62	no	oral tongue	neurofibroma	2	no	yes	yes
5	F	38	current some day	oral tongue	ganglioneuroma	1	yes	no	no
6	F	46	no	oral tongue	neuroma	1	no	no	yes
7	F	53	current daily	glottis	neuroma	3	no	yes	yes
8	M	41	no	oral tongue	neurofibroma	2	yes	yes	yes
9	F	74	current daily	base of tongue	ganglioneuroma	2	yes	yes	yes
10	M	66	no	oral tongue	neurofibroma	2	no	yes	yes
11	F	76	former	tonsillar fossa	neuroma	1	no	no	no
12	M	85	no	base of tongue	neuroma	3	yes	no	no
13	F	69	former	base of tongue	subepithelial nerve plexus	3	yes	yes	yes
14	F	57	former	base of tongue	neurofibroma	2	no	yes	no
15	F	43	current daily	base of tongue	reactive ganglioneural proliferation	1	yes	no	no
16	F	56	no	oral tongue	neurofibroma	2	no	yes	yes
17	M	73	no	base of tongue	submucosal edema and peripheral nerve bundles	3	no	no	no
18	F	66	current daily	oral tongue	peripheral nerve bundle and ganglion cells	1	yes	yes	yes
19	F	30	no	oral tongue	peripheral nerve bundle	1	yes	yes	yes
20	F	62	former	oral tongue	peripheral nerve bundle	1	yes	yes	no

Conclusions: The result of this study confirms that neural tumors are rare in the head and neck mucosal region. Awareness of SNPs is important, as they are unique small subgemmal structures that are associated with taste buds and ganglion cells and usually found in tongue biopsies that show distinctive biphasic pattern, with superficial neurofibroma like plaques and deeper neuroma like areas. Caution should be exercised before calling lesions as ganglioneuromas, neurofibromas, mucosal neuromas, or traumatic neuromas especially in the lack a proper clinical setting to avoid unnecessary clinical investigations.

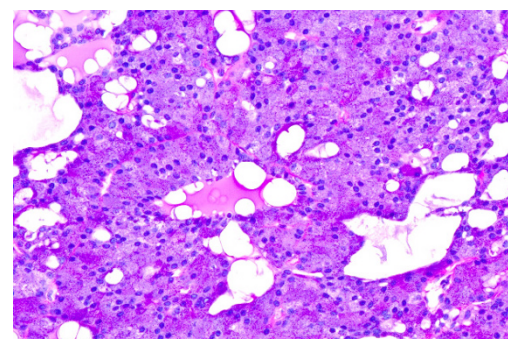
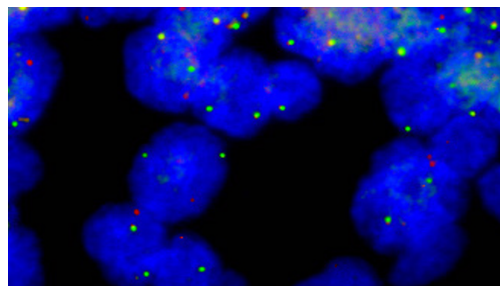
1318 Recurrent MSANTD3 Aberrations Defines a Subset of Acinic Cell Carcinomas of the Salivary Gland

Simon Andreassen¹, Sushama Varma², Linea C Melchior³, Tina K Agander⁴, Katalin Kiss⁵, Irene Wesse⁶, Preben Homøe⁷, Justin Bishop⁸, Jonathan Pollack⁹, Robert West⁷. ¹Rigshospitalet, Copenhagen, ²Stanford University School of Medicine, ³Rigshospitalet, Copenhagen University Hospital, ⁴Copenhagen University Hospital, Copenhagen, ⁵Zealand University Hospital, ⁶UT Southwestern Medical Center, Dallas, TX, ⁷Stanford University, Stanford, CA

Background: A growing number of salivary gland tumors are characterized by recurrent chromosomal rearrangements resulting in promoter swapping or generation of fusion genes, which has resulted in improved molecular taxonomy, diagnostic accuracy, and new venues for targeted therapies. However, no genetic characteristics have been identified in acinic cell carcinoma (AciCC), which is among the remaining genetic orphans among salivary gland carcinomas. Here, we report the finding of recurrent *MSANTD3* aberrations in a subset of AciCC.

Design: Whole-transcriptome sequencing of an index AciCC identified a *HTN3-MSANTD3* gene fusion. An expanded series of salivary gland AciCC ($n=126$, 3 with dedifferentiation) was collected and subjected to FISH using custom dual-color break-apart probes for the *MSANTD3* gene. All rearranged cases were subjected to a histochemical (PAS+D) and immunohistochemical (amylase, CK7, DOG-1, ki-67, mammaglobin, S-100) panel. The same panel was applied to 10 non-rearranged AciCC for comparison.

Results: A total of six AciCCs showed rearrangement and one case showed amplification of the *MSANTD3* gene 7/126, 5.6%) (Fig. 1). Histologically, tumors were lobulated and showed varied growth patterns including solid, microcystic, follicular (Fig. 2). In all cases, PAS-positive diastase-resistant granules were abundant in the neoplastic cells. Immunohistochemically, all cases were positive for CK7 in the non-acinar cells, and intense membranous DOG-1 positivity was observed in the acinar cells. Mammaglobin and S-100 were consistently negative. Ki-67 was low, ranging from 1-7%. The immunohistochemical profile of the 10 non-rearranged AciCCs was identical. Clinical information was available from 4 patients with *MSANTD3* aberrations and included 2 males and 2 females of which 3 tumors arose in the parotid and 1 in the submandibular gland. Three patients remained free of disease during follow-up (46-256 months) whereas the case with *MSANTD3* amplification developed pulmonary metastases after 6 years.



Conclusions: salivary gland. The oncogenic property of *MSANTD3* is unclear but is supported by the fulminant course case with selective *MSANTD3* gain. Collectively, *MSANTD3* is the first recurrent genetic

aberration reported in salivary gland AcicC and adds another branch to the molecular classification of salivary gland tumors. The prognostic significance of this subset of AcicC awaits the identification of additional cases.

1319 Human Papilloma-Virus Downregulates S100A8/A9 (Calprotectin) Expression in Oral Epithelial Dysplasia and Head and Neck Squamous Cell Carcinoma (HNSCC)

Prokopios Argyris¹, Xue (Cheryl) Wang², Christine Goergen³, Ioannis Koutlas⁴, Mark C Herzberg³. ¹University of Minnesota, Minneapolis, MN, ²University of Minnesota, Minneapolis, MN, ³University of Minnesota, ⁴Malcolm Moos Health Sci., Minneapolis, MN

Background: Calprotectin, a heterodimeric complex of the calcium-binding proteins S100A8 and S100A9 (S100A8/A9) appears to activate the G2/M cell cycle checkpoint and inhibits tumor cell proliferation, migration and invasion in HNSCC. In HNSCC patients, increased tumor grading, DNA methylation and poor overall survival rates are associated with decreased calprotectin levels. In HNSCC, HPV affects gene expression. Based on TCGA data, S100A8 and S100A9 expression is less in HPV(+) than in HPV(-) tumors, whereas S100A8/A9 may inhibit viral oncogenic activity *in vitro* by regulating CKII-mediated E7 phosphorylation. We sought to learn whether HPV infection affects S100A8/A9 levels in premalignant epithelial dysplasia and HNSCC *ex vivo*.

Design: S100A8 and S100A9 protein levels were compared using immunohistochemistry in HPV(+) oral epithelial dysplasias (OED, N=15) and HPV(+) non-keratinizing/basaloid (NK/BAS, N=6) HNSCCs with HPV(-) OED (N=16), HPV(-) well-differentiated (WD, N=19) HNSCCs and normal adjacent epithelial tissue (NAT). HPV positivity was marked by strong nuclear and cytoplasmic p16^{INK4a} staining in >75% of lesional cells; S100A8 and S100A9 immunoreactivity was quantified using Aperio Imagescope analysis. Ratios of strong positive (NSR) and total positive pixels (TPR) were analyzed using one-way ANOVA with post-hoc Tukey HSD test.

Results: The epidemiologic and histopathologic characteristics of all cases studied are summarized in Table 1. S100A8/A9 immunoreactivity in NAT was strong and diffuse in the nucleus and cytoplasm excepting basal cells, which were consistently negative. Both S100A8 (NSR; p<0.05, TPR; p<0.01) and S100A9 (NSR; p<0.01, TPR; p<0.01) were significantly lower in HPV(+) OEDs in the p16^{INK4a} (+) areas than in NAT and HPV(-) OEDs. Phenotypically resembling NAT, WD HNSCC displayed strong and diffuse S100A8/A9-high immunostaining. In contrast, HPV(+) NK/BAS tumors were consistently S100A8/A9-negative, resembling the immunophenotype of basal epithelial cells.

Table 1	Gender	Age (years)	Location	Histopathologic Classification
HPV (+) Oral Epithelial Dysplasia (N=15)	14M:1F	Mean=57.6 Range= 51-71	Lateral and ventral tongue (8, 53.3%) Floor of mouth (3, 20%) Palate (2, 13.3%) Buccal mucosa (1, 6.7%) Gingiva (1, 6.7%)	N/A
HPV (-) Oral Epithelial Dysplasia (N=16)	8M: 8F	Mean=60.9 Range= 44-77	Lateral and ventral tongue (11, 68.8%) Floor of mouth (2, 12.5%) Palate (1, 6.2%) Buccal mucosa (1, 6.2%) Retromolar trigone (1, 6.2%)	Mild (6, 37.5%) Moderate (9, 56.3%) Severe (1, 6.2%)
Head and Neck Squamous Cell Carcinoma (N=25)	13M: 12F	Mean=63.4 Range=43-85	Lateral and ventral tongue (10, 40%) Floor of mouth (4, 16%) Palate (4, 16%) Gingiva (4, 16%) Buccal vestibule (1, 4%) Base of tongue (1, 4%) Retromolar trigone (1, 4%)	Well-Differentiated (N=19) p16 ^{INK4a} (-): 19/19 Non-Keratinizing/Basaloid (N=6) p16 ^{INK4a} (+): 6/6

Conclusions: HPV appears to affect S100A8 and S100A9 expression

in oral premalignant epithelial dysplasias and HNSCC. Since calprotectin appears to function as a tumor suppressor in HNSCC, HPV-mediated downregulation of S100A8/A9 may represent an additional tumorigenic mechanism.

1320 Pathogenic SMARCA4 Mutations in Head and Neck and Thyroid Carcinomas are Rare

Javier A Arias-Stella¹, Satshil Rana¹, Mrinal M Gounder¹, Marc Ladanyi¹, Snjezana Dogan¹. ¹Memorial Sloan Kettering Cancer Center, New York, NY

Background: SMARCA4 gene encodes BRG1 a member of the SWI/SNF protein complex involved in chromatin remodeling, cell-cycle regulation, programmed cell death, differentiation, genomic instability, and DNA repair. SMARCA4 mutations with loss of BRG1 protein expression has been identified in small cell carcinoma of the ovary-hypercalcemic type, a subset of thoracic sarcomas, and approximately 5% of pulmonary squamous cell carcinomas (SqCC). Loss of SMARCA4 (BRG1) protein has been associated with an aggressive behavior and poor prognosis. Patients harboring SMARCA4/BRG1 deficient tumors may be eligible for molecular targeted therapy. Except for a single case report of SMARCA4/BRG1 deficient sinonasal carcinoma the frequency of pathogenic SMARCA4 mutation in head and neck (H&N) carcinomas remains unknown.

Design: We searched our clinical cohort of 20,981 solid tumor patient samples (January 2014 to September 2017) which underwent mutational profiling by hybridization exon-capture next-generation sequencing assay MSK-IMPACT™ targeting 341, 410 or 468 cancer-related gene panel to identify H&N and thyroid tumors harboring somatic alterations in SMARCA4. Immunohistochemistry for BRG1 was performed to assess the SMARCA4/BRG1 protein status.

Results: 878 H&N cases were retrieved including 358 (40.8%) thyroid tumors, 277 (31.5%) SqCC, 198 (22.6%) salivary gland tumors, and 45 (5.1%) other rare H&N entities. SMARCA4 mutations were overall detected in 20 (2.3%) cases including mostly (75%, n=15) putative passenger single nucleotide variants (SNV). The remaining 5 mutations included 2 amplifications (laryngeal and sinonasal SqCC), 1 LPAR2-SMARCA4 fusion (in myoepithelial carcinoma), 1 SMARCA4 L1161Sfs*3 (laryngeal SqCC), and 1 putative driver SNV SMARCA4 R1135L (sinonasal SqCC). BRG1 protein was retained in all tested (100%, n=10) cases including the latter 3. The cases with putative passenger SNV included 7 SqCC, 2 adenoid cystic carcinomas, 2 Hurthle cell carcinomas, 1 anaplastic and 1 medullary thyroid carcinoma, 1 high grade neuroendocrine carcinoma of parotid gland, and 1 nasopharyngeal carcinoma.

Conclusions: Oncogenic SMARCA4 mutations in cancers of H&N are rare. Although BRG1 is retained by immunohistochemistry in cases with putative oncogenic mutations, further studies are needed to explore if the mutated SMARCA4 protein in these cases remains functional.

1321 Retinoblastoma-1 Loss in Human Papillomavirus-negative Oropharyngeal Squamous Cell Carcinoma - A Cause of False Positive P16 as a Surrogate HPV Marker and a Favorable Prognosticator

Jeremie Berdugo¹, Simon Chiosea². ¹University of Pittsburgh Medical Center, Pittsburgh, PA, ²University of Pittsburgh, Pittsburgh, PA

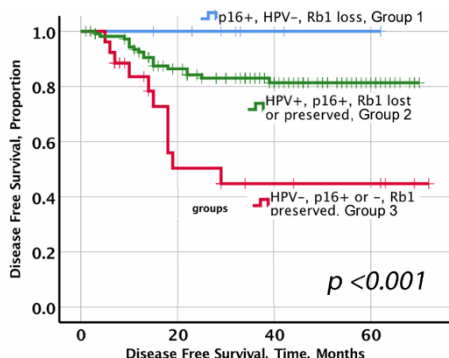
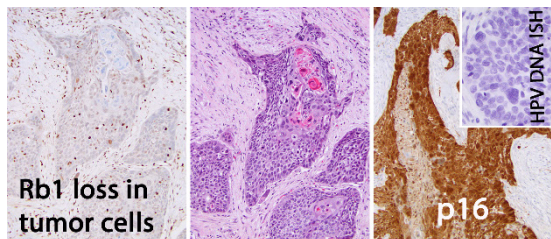
Background: P16 immunohistochemistry (IHC) is a surrogate marker for human papillomavirus (HPV) in oropharyngeal squamous cell carcinoma (OSCC). However, P16 expression in OSCC may be induced by Retinoblastoma-1 (Rb1) loss in the absence of HPV. We aimed to assess the prevalence and prognostic significance of Rb1 loss leading to false positive P16 in HPV-negative OSCC. The performance of the AJCC 8th Edition staging system among patients with P16-positive OSCC was evaluated.

Design: One hundred forty-five patients with OSCC were prospectively accrued from 2011 to 2015. Clinicopathologic parameters (including morphologic types, AJCC 8th Edition staging, and sub-sites) were indexed. IHC for Rb1 (clone 13A10) and P16 (clone E6H4) was performed. Rb1 IHC was scored as "lost" or "preserved". HPV status was assessed by HPV DNA In Situ Hybridization (ISH) (Enzo Life Sciences, wide spectrum). Of deceased patients (n=21), only 14 died of disease. Therefore, disease free survival (DFS) was the primary endpoint examined by Kaplan-Meier method.

Results: Based on the status of P16 IHC, Rb1 IHC, HPV ISH, and correlation with DFS, three clinicopathologic groups of OSCC emerged (Table 1, Figure 1). P16 was false-positive in 7 patients [7/145, 4.8%] (P16-positive, HPV-negative, Rb1-lost, i.e., group 1) (Table 1). In contrast to the other groups, no patient in group 1 had a disease recurrence (Figure 2). Compared to the 7th edition, the AJCC 8th Edition downstaged 93% of patients with P16-positive OSCC and 100% of patients in group 1. Our study cohort is likely representative of a larger population, because such known prognosticators as HPV and P16 correlated with DFS. For instance, the estimated mean DFS of all patients with P16-positive OSCC was 58 months (95% confidence

interval, CI, 56 - 64 months) compared to DFS for patients with p16-negative OSCC of 42 months (95% CI, 28 - 56)(p<0.001). Extent of keratinization, morphologic types of OSCC, and oropharyngeal subsites were evenly distributed among the 3 groups.

		GROUP 1	GROUP 2	GROUP 3
		p16+, HPV -, RB lost (n=7)	(HPV+, p16+, Rb1 preserved (n=80) or Rb1 lost (n=31))	(HPV-, Rb1 preserved, and p16+ (n=3) or p16- (n=24))
Male : Female ratio		2.5 : 1	6.4 : 1	1.7 : 1
Age at diagnosis, average, range		57.3 (50-68)	57.0 (36-80)	60.4 (40-79)
Subsite	Base of Tongue	4	34	5
	Tonsil	3	71	12
	Other	0	6	10
Smoking, yes		3	78	26
Alcohol use, yes		6	76	22
HISTOLOGY	NONKERATINIZING	5	107	10
	KERATINIZING	2	1	11
	BASALOID	0	0	2
	OTHER	0	3	4
Pathologic stage grouping (AJCC 7 th edition, p16+ cases only)	X	0	4	0
	I	0	7	0
	II	0	12	0
	III	1	21	0
	IV	6	67	3
Pathologic stage grouping (AJCC 8 th edition, p16+ cases only)	X	0	4	0
	I	5	91	2
	II	2	12	0
	III	0	4	1
Chemoradiotherapy, yes		7	89	13
Free of disease at 20 months, %		100%	85%	45%



Conclusions: False positive P16 expression due to Rb1 loss in HPV-negative OSCC was detected in 7/145 cases (for a false positive rate of P16, as a surrogate HPV marker, of 4.8%). Rb1 loss is independent of HPV status and is associated with better outcome in HPV-negative OSCC only. By selecting cases based on P16 alone, the AJCC 8th Edition downstages P16-positive, HPV-negative cases with Rb1 loss, reflecting the more favorable prognosis of this subset of HPV-negative OSCC.

1322 Salivary Intercalated Duct Lesions: a Single Institution Prospective Study of 230 Totally Submitted Superficial Parotid Glands

Jeremie Berdugo¹, Simon Chiosea², Robert Peel¹, Aaron Berg¹, Raja Seethala². ¹University of Pittsburgh Medical Center, Pittsburgh, PA, ²University of Pittsburgh, Pittsburgh, PA, ³University of Pittsburgh School of Medicine, Pittsburgh, PA

Background: Intercalated duct lesions (IDL) range from hyperplasia to adenoma. They have been implicated as precursor lesions since they have been reported most frequently in association with epithelial myoepithelial carcinomas (EMCA) and basal cell adenomas (BCA). However, the general prevalence of IDL and the strength of this association either with these tumors or other primary salivary epithelial neoplasms is not well tested. We report our experience with 230 consecutive cases of superficial parotidectomies accrued over a 7-year period.

Design: 230 superficial parotidectomies were accrued prospectively (2011- 2017) and submitted entirely for histologic evaluation (serially sectioned, 3-5mm intervals). General epidemiologic parameters were obtained. Cases were stratified into two groups: parotids with primary salivary epithelial tumors (Group 1), and parotids removed for other disease (i.e. non-neoplastic, non-primary and non-epithelial parotid tumors) (Group 2). For each case, the number of IDL per case, largest IDL per case, number of IDL per gram of parotid, sialadenitis and atrophy was assessed. Any expansile or nodular proliferation of intercalated ducts was accepted as an IDL. IDL were stratified into hyperplastic type and adenoma type as previously described (PMID:19542868).

Results: General characteristics are summarized in table 1. All but one of our IDL cases were of the hyperplastic type and one was of the adenoma type (0.6%). No statistically significant difference was found between group 1 and group 2 in terms of presence or absence of IDL, presence or absence of IDL of 0.3 cm and above, mean size of largest IDL, mean number of IDL per gram of parotid tissue and mean number of IDL per parotid (see table 1). Also, presence or absence of IDL was not related to atrophy or sialadenitis. None of our cases showed a transition between IDL and tumor. However, a subgroup consisting of EMCA, BCA and basal cell adenocarcinomas (BCAC) had a higher frequency (11/14, 78.6%) of IDL than the rest of group 1 (68/147, 46.3%) (p=0.02).

	Overall (n=230)	Group 1 (n=161)	Group 2 (n=69)
Mean age	58.8	56.5	64.1
M:F ratio	1.1:1	0.8:1	2.5:1
IDL	111 (48.3%)	79 (49.1%)	32 (46.4%)
IDL ≥ 3mm	15	10 (6.2%)	5 (7.2%)
Mean size of largest IDL per case	0.17	0.18cm	0.17cm
Mean IDL number per case	1.20	1.25	1.07
Mean IDL number per gram of parotid tissue per case	0.08	0.09	0.06
Atrophy	159 (69.0%)	113 (70.2%)	46 (66.7%)
Sialadenitis	148 (64.3%)	100 (62.1%)	48 (69.6%)

Conclusions: Minute IDL are frequent in parotids with and without primary salivary gland tumors. However, those ≥3mm as previously reported are rare, with an adenoma subtype being even rarer. IDL are not preferentially associated with primary salivary gland tumors in general, but may be associated with EMCA, BCA and BCAC as previously implied.

1323 Overt Radiographic Extranodal Extension Predicts a Poorer Survival in p16+ Oropharyngeal Squamous Cell Carcinoma

Onita Bhattasali¹, Hannah Herrera², Shawn Igane², Lester D Thompson³. ¹Southern California Permanente Medical Group, ²SCPMG, ³Southern California Permanente Medical Group, Woodland Hills, CA

Background: The AJCC 8th edition TNM classification for oropharyngeal squamous cell carcinoma (OPSCC) does not consider overt radiographic extranodal extension (ORENE) as a specific characteristic in the nodal staging for p16+ nonsurgically treated patients managed with definitive chemoradiation. Survival outcomes were analyzed among patients with p16+ OPSCC with or without ORENE.

Design: All patients in Southern California Permanente Medical Group diagnosed with OPSCC between 2006 and 2012 with a minimum of 5 years follow-up were included. Radiographic findings and pathology diagnoses with central p16 evaluation were compared for stage-matched patients with and without ORENE.

Results: 302 males and 40 females ranging in age from 35-81 years comprised the cohort of 342 p16+ OPSCC patients. Nonkeratinizing (n=290), with maturation (n=35) and keratinizing (n=17) histologies were identified. The overall mean survival was 71.0 months for all

342 patients. Among these patients, ORENE was associated with poor survival (HR=2.79 [1.67-4.67]; p<0.001). After adjusting for TNM group stage, ORENE remained a significant prognostic factor for poor survival (HR=2.33 [1.37-3.98]; p=0.002. This finding proved significant in multivariate analysis also with a HR of 1.95 [1.10-3.46]; p=0.02).

Stage	# of patients	Mean overall survival (months)
I	130	75.1
I-ORENE	22	64.9
II	76	77.5
II-ORENE	7	61.0
III	51	64.3
III-ORENE	23	43.6

Conclusions: Based on this cohort of 342 patients with p16+ OPSS, irrespective of histologic type or tumor site, the presence of ORENE predicts a poorer survival outcome when compared with otherwise similar stage patients. This suggests that the nodal staging system may need to be modified or upstaged to account for ORENE.

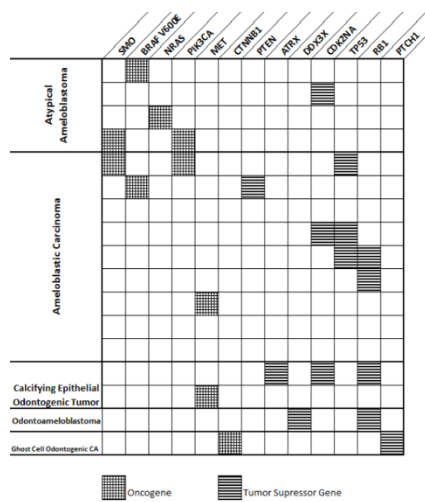
1324 Molecular Profiling of Rare Odontogenic Tumors

Elizabeth A Bilodeau¹, Simon Chiosea¹, Aaron Berg², Susan Muller³, Bibiana Purgina⁴, Raja Seethala⁵. ¹University of Pittsburgh, Pittsburgh, PA, ²University of Pittsburgh Medical Center, Pittsburgh, PA, ³Atlanta, GA, ⁴University of Ottawa, Ottawa Hospital, Ottawa, ON, ⁵University of Pittsburgh School of Medicine, Pittsburgh, PA

Background: Ameloblastomas are now known to demonstrate frequent *BRAF* V600E or other MAPK (mitogen-activated protein kinase) pathway mutations (usually mandibular) as well as *SMO* mutations (usually maxillary). However, the mutational profile for atypical ameloblastomas, ameloblastic carcinomas as well as other rare odontogenic neoplasms is less characterized.

Design: 19 odontogenic tumors (11 ameloblastic carcinomas (AC) from 9 patients including 1 metastasis, 4 atypical ameloblastomas (AA) from 4 patients, 2 calcifying epithelial odontogenic carcinomas (CEOT) from 2 patients, 1 odontoameloblastoma (OA), and 1 ghost cell odontogenic carcinoma (GCOC) were successfully tested by next generation sequencing (DNA for point mutations in 30 tumor-related genes (>1360 hot spots), copy number alterations in 24 genes, PMID: 26681766). Anatomic site was indexed and clinical follow-up was obtained. *CDK2NA* and *RB1* abnormalities were corroborated with fluorescent in-situ hybridization (FISH) and immunohistochemistry (IHC). *TP53*, *CTTNB1*, and *ATRX* abnormalities were corroborated with IHC.

Results: Only a small percentage of AA and AC had *BRAF* (p.V600E) mutations (2/13 patients, 15.4%; 1/4 AA, 1/9 AC), and 1/4 AA had a *NRAS* mutation (p.Q61R). *SMO* mutations (p.L412F, p.W535L) were seen in 2 patients (1/9 AC and 1/4 AA) in conjunction with a *PIK3CA* mutation (p.C420R, p.E545K) in both cases. *CDK2NA* mutation (p.R144C) was present in 1/4 AA with loss in 1/9 AC and 1/2 CEOT confirmed with FISH. *TP53* mutation (p.R273C n=2, p.G245C, p.P85Lfs*38) was present in 4 ACs from 3 patients. *MET* mutation (p.E168D, p.M35L) was present in 1 AC and 1 CEOT. *RB1* loss was present in 5 cases in 4 patients (3 AC in 2 patients, 1 CEOT, 1 OA) and was confirmed with FISH and IHC. A *DDX3X* mutation (p.V271I) was detected in an additional 1/1 OA. 1/2 CEOT exhibited an *ATRX* mutation (p.I360fs) with loss confirmed via IHC. The GCOC exhibited a *CTNNB1* mutation (p.S33C) with nuclear beta-catenin on IHC and a *PTCH1* mutation (p.V1413P).



Conclusions: The data suggests a pathogenesis for AA/AC distinct from ameloblastoma with alterations more commonly noted in *PIK3CA*, *TP53*, *CDKN2A*, and *RB1* and a lower rate of MAPK pathway

mutations. As expected GCOC demonstrates *CTTNB1* mutation. Novel mutations noted include *DDX3X* mutation in OA. The presence of *ATRX* mutation in CEOT implies a role for the alternative telomerase lengthening pathway in its pathogenesis.

1325 Utility of Direct Immunofluorescence in the Diagnosis of Immunobullous Diseases of the Oral Cavity

Scott C Bresler¹, Roxanne Bavarian², Sook-Bin Woo³, Scott R Granter² ¹Brigham & Women's Hospital, Boston, MA, ²Brigham and Women's Hospital, ³Brigham and Women's Hospital, Boston, MA

Background: Oral immunobullous disorders (OIBD), including mucous membrane pemphigoid (MMP), pemphigus vulgaris (PV), paraneoplastic autoimmune multiorgan syndrome (PAMS), and others, show considerable clinical overlap with diseases such as lichen planus and others that may cause desquamative gingivitis. Currently, it is common practice to obtain fresh biopsies for direct immunofluorescence (DIF) alongside tissue for histologic examination. As DIF is extremely expensive, in large part due to the amount of antibody needed, we sought to determine if H&E alone would be sufficient to distinguish between OIBD and clinical mimics, keeping in mind that definitive characterization would theoretically be deferred to follow-up.

Design: We searched the pathology records at our hospital, a large tertiary care facility, for patients with suspected OIBD who underwent biopsies for concurrent H&E and DIF studies and who had at least one follow-up visit. Cases were separated into high suspicion (HS) and low suspicion (LS) subgroups based on clinical findings and impression of 10 anatomic regions of the oral cavity.

Results: There were 149 cases and 141 were definitively diagnosed. There were 27 LS and 122 HS cases. Overall, the sensitivity of H&E alone (using a combination of clinical follow up and DIF as a gold standard) was just 0.811, with a negative predictive value of 0.882. The LS group contained no H&E false negatives. Just one LS case showed positive DIF, and the H&E exhibited non-specific chronic inflammation with eosinophils; however, focal subepithelial separation was noted. DIF showed strong linear IgG and C3 along the basement membrane, consistent with MMP. Of the HS cases, 57 (46.7%) were found to be consistent with OIBD, with a total of 11 H&E false negatives. 8 cases, all in the HS subgroup, showed indeterminate DIF results. However, under close clinical follow-up, and in some cases re-biopsy, these cases were eventually diagnosed as MMP (3 cases), PV (1 case), and PAMS (1 case), with 1 case determined to be non-OIBD (chronic graft versus host disease).

Conclusions: In patients with a low clinical suspicion for OIBD, it is reasonable and more cost-effective to perform a biopsy for H&E alone. However, if the suspicion for OIBD is high, additional sampling for DIF is recommended, as H&E alone fails to recognize a number of cases. Our analysis also indicates that DIF is not a stand-alone test, as close clinical follow up (including re-biopsy) may assist in proper identification of patients with OIBD.

1326 Alterations in Labial Salivary Gland in Adult Patients with Common Variable Immunodeficiency. A Single Center Experience

Lourdes Cabrera¹, Ana Macias-Robles², Nora-Hilda Segura-Mendez². ¹Hospital Infantil de Mexico Federico Gomez, Buena Park, CA, ²Hospital de Especialidades CMN SXXI, IMSS, Mexico

Background: Common variable immunodeficiency (CVID) is the most common humoral immunodeficiency in adults and is associated to an increased predisposition to develop infections, autoimmune disease. Sjögren's syndrome (SS) has been reported in 20.6 % of CVID patients and although orofacial alterations including labial salivary gland enlargement had been reported in previous clinical investigation, histological findings are lacking. The aim of this study was to describe the histopathological alterations and to characterize the cellular infiltrates in labial salivary gland biopsy (LSGB) in adult patients with CVID.

Design: 18 patients with diagnosis of CVID on clinical follow-up at Allergy and Immunology Service at Hospital de Especialidades in CMN SXXI, IMSS in whom a LSGB was performed. Clinical and demographic data were reviewed. Inflammatory infiltrates grade evaluation with Chisholm and Mason score on FFPE was performed on H&E stained tissue sections corresponding to: Grade 0= Absent, Grade 1= mild and Grade 2= moderate inflammatory infiltrate, Grade 3= 1 focus of 50 cells and Grade 4 = > 1 focus all per 4mm². We also assessed other morphological changes including glandular atrophy, interstitial fibrosis, ductal changes, and immunohistochemical stains on TMA sections with anti CD3, CD4, CD8, to identify T cells, CD19 and CD20 for B cells and CD68 for macrophages, qualitatively scoring them as present or absent.

Results: There were 10 female and 8 male, age ranged from 19-69 years (mean 37 years). IHC showed in 11 (61%) patients a mixture of lymphocytes and macrophages, with the following global distribution

of the different cell types CD4 83 %, CD3 56 %, CD8 11%, CD20 11 % and CD68 28% positive and none express CD19. Inflammatory infiltrates were associated to glandular atrophy in 8 patients (focal, 2, and diffuse 6) and interstitial fibrosis was present in 10 cases.

Chisholm and Mason score	Number of Patients	Sex M/F	Glandular atrophy	Fibrosis	Ductal dilatation
0	7	2 / 5	0	1	3
1	7	4 / 3	4	5	6
2	1	1 / 0	1	1	1
3	1	1 / 0	1	1	1
4	2	2 / 0	2	2	1
Total	18	10 / 8	8 / 18	10 / 18	12/18

Conclusions: Our study demonstrated labial salivary glands lesions in 61 % in CVID, 17% of patients showed inflammatory grade 3 and 4 consistent with secondary Sjögren's syndrome. Interestingly SS frequency on LSGB is lower than reported and all patients were male.

1327 Identification of a Novel Fusion Transcript Involving F-box Protein 32 (FBXO32) and Pleomorphic Adenoma Gene 1 (PLAG1) in Pleomorphic Adenoma

Tiffany Y Chen¹, Rebecca N Wehrs¹, Shahm Raslan¹, Michael Rivera², Jean Lewis³, Jason Lewis³, David J Schembri-Wismayer¹, Kevin Halling¹, Joaquin Garcia¹. ¹Mayo Clinic, Rochester, MN, ²Mayo Clinic, ³Ponte Vedra, FL

Background: Fusion transcripts have been used to characterize benign and malignant neoplasms of hematomalymphoid, mesenchymal, and epithelial origin. Pleomorphic adenoma (PA), the most common salivary gland neoplasm overall, has previously exhibited *PLAG1* or *HMG2A* rearrangement in a significant portion of cases. We report a novel fusion transcript involving F-box protein 32 (*FBXO32*) and pleomorphic adenoma gene 1 (*PLAG1*) in PA.

Design: Total RNA was extracted from frozen tissue in 11 cases previously diagnosed as PA (9) or cellular PA (2) using a Qiagen® miRNeasy Micro kit. RNA quality (RNA Integrity Number, RIN) was determined using an Agilent 2100 Bioanalyzer (Agilent Genomics) and RNA quantity was determined using a Qubit 2.0 fluorometer (Thermo Fisher Scientific). Poly(A) mRNA selection and cDNA synthesis were performed on a Janus® Automated Workstation (Perkin Elmer) and NGS libraries were prepared with a Biomek® FXp Liquid Handler (Beckman Coulter) using custom-built protocols and a TruSeq® RNASample Preparation v2 Kit (Illumina). Paired-end, 101 bp-read sequencing was performed on a HiSeq 2500 (Illumina) in Rapid Run mode. Data analysis utilized a custom suite of alignment, fusion detection, filtering, and annotation programs (MAP-Seq) to detect fusions in 573 genes.

Results: One of 11 cases did not meet the RIN cutoff and was unable to begin cDNA synthesis. Two cases failed library prep and were unable to be sequenced. No fusion transcript was identified in 5 cases. The remaining 3 cases demonstrated the following fusion transcripts: *HMG2A-WIF1*, *HMG2A-NFIB*, and *FBXO32-PLAG1*. The *FBXO32-PLAG1* fusion transcript has not been previously described. The *PLAG1* breakpoints observed in this novel fusion are the same as those seen with previously described fusion partners. *FBXO32* contributes its 5' untranslated region to the chimeric transcript.

Conclusions: This study describes identification of a novel fusion transcript, *FBXO32-PLAG1*, in PA using RNA Seq. This finding broadens the cytogenetic diversity of PA and supports the clinical utility of RNA Seq in the evaluation of salivary gland neoplasms.

1328 Evaluating the Impact of AJCC Staging Modifications on the Clinical Management of Oropharyngeal Squamous Cell Carcinoma

Tiffany Y Chen¹, Shahm Raslan¹, Michael Rivera², Jean Lewis³, Jason Lewis³, David J Schembri-Wismayer¹, Daniel Ma², Joaquin Garcia¹. ¹Mayo Clinic, Rochester, MN, ²Mayo Clinic, ³Ponte Vedra, FL

Background: In 2017, the 8th Edition of the American Joint Committee on Cancer (AJCC) made modifications to the previous staging schema for patients with oropharyngeal squamous cell carcinomas (OPSCC). In HPV-mediated (p16+) OPSCC, previously designated T4a and T4b have been consolidated into T4 and nodal staging is determined by number [pN1 (≤4) and pN2 (≥5)] rather than size of involved lymph nodes. In p16-negative OPSCC, T classification remains unchanged while extra nodal extension (ENE) is a recorded parameter in lymph node assessment. This retrospective study evaluates the potential impact of these staging modifications on the clinical management of HPV-mediated (p16+) and p16-negative OPSCC.

Design: Surgical pathology reports from patients with

OPSCC diagnosed between 2006 and 2014 were reviewed. Immunohistochemistry for p16INK4a was performed on formalin-fixed, paraffin-embedded tissue sections. RNA ISH for high-risk HPV E6/E7 mRNA was manually performed. Staging stratification was performed using the 7th and 8th Editions of the AJCC staging criteria.

Results: A total of 154 patients with OPSCC were evaluated. All patients received surgery prior to radiation treatment. The mean ages for the HPV-mediated (p16+) and p16-negative cases were 64 and 66 years, respectively. Of the 144 HPV-associated cases, there were 18 (12.5%) females and 126 (87.5%) males; 76 (53%) were smokers (mean 30 pack years). Of the 10 p16-negative cases, 3 (30%) were female (30%), 7 (70%) were male, and 9 (90%) were smokers (mean of 30 packs years). In HPV-mediated (p16+) cases, 143 (99.3%) were downstaged and 1 case was staged the same (stage I). 123 cases previously IVa were downstaged to III (8%), II (33%), and I (59%). 8 cases previously IVb were downstaged to III (25%), II (37.5%), and I (37.5%). 12 cases previously III were downstaged to II (33%) and I (67%). For p16-negative OPSCC, 6 (60%) were upstaged from IVa to IVb and 4 (40%) remained the same (IVa). Of the 6 upstaged, all had ENE present.

Conclusions: Recommendations for adjuvant treatment and inclusion criteria for clinical trials are often based upon AJCC staging. Our study reveals that a significant portion of patients previously classified as Stage IV were downstaged to Stages I-III (91%). This downstaging phenomenon impacts which patients are eligible for potential dose de-intensification studies, as well as those requiring more aggressive care due to risk for distant disease.

1329 Hypoxia Induced Centrosome Amplification as a Surrogate Marker in HPV Negative Oropharyngeal Squamous Cell Carcinomas

Da H Choi¹, Karuna Mittal², Guan hao wei³, Brian D Melton¹, Christopher Griffith⁴, Sergey Klimov⁵, Michelle Reid⁶, Pawel Golusinski⁷, Padmashree Rida², Ritu Aneja². ¹Georgia State University, ²Georgia State University, Atlanta, GA, ³Georgia State University, ⁴Emory University, Atlanta, GA, ⁵Roswell, GA, ⁶Emory University Hospital, Atlanta, GA, ⁷Greater Poland Cancer Center

Background: The identification of HPV DNA presence in the host genome of oropharyngeal squamous cell carcinomas (OPSCC) patient tumors is imperative for making treatment decisions. Current methods widely utilize p16 immunohistochemistry (IHC) as a surrogate marker for active oncogenic HPV infection. However, it can yield false positive/negative results, accentuating the need for other markers that can complement p16 IHC. Previous studies have shown higher expression of HIF-1α in HPV negative tumors and also, the role of hypoxia activated transcription factor HIF-1α in inducing numerical centrosome amplification (CA), but this unique relationship has not been studied in OPSCC. As a result, we aim to investigate the clinical relevance of HIF-1α induced CA in OPSCC and whether CA can serve as a complementary surrogate marker for determining HPV status.

Design: We immunohistochemically stained 40 p16 positive (+ve) and 40 p16 negative (-ve) OPSCC samples for HIF-1α and calculated the weighted indices (WIs) for the nuclear HIF-1α. Adjacent serial sections from the same tumors were also immunofluorescently labeled for γ-tubulin and CA was calculated. CA was defined as nuclei with more than 2 centrosomes and nuclei that fit the definition were counted to provide a percentage score. To further assess the clinical relationships between HIF-1α, CA and p16 status, survival analysis was performed. Additionally, we performed in silico analysis to substantiate the biological relationship between hypoxia and CA in OPSCC.

Results: A significant correlation was found between the nuclear HIF-1α and CA in p16-ve clinical samples. In line with the literature, p16-ve OPSCC had poorer overall survival when compared with the p16+ve OPSCC (p<0.0005). We further divided p16-ve OPSCC in high and low hypoxia groups (based on log rank test). Interestingly, we saw that the high hypoxia, high CA group was associated with worse overall survival when compared with low hypoxia, low CA group (p<0.0035). In silico analysis showed that the 26 hypoxia gene (DOI:10.1158/1078-0432.CCR-13-0542) signatures were positively correlated with 20 CA gene (DOI: 10.1038/s41598-017-00363-w) signatures (n=84; p<0.0046).

Conclusions: Collectively our findings suggest that HIF-1α induced CA within each p16 status can further serve as prognostic markers for treatment decisions and de-escalations.

1330 Genetic and Histologic Spectrum of SMARCB1-Deficient Carcinomas of the Head and Neck Including Sinonasal Tract, Thyroid and Skin

Paolo Cotzia¹, Ryan Ptashkin¹, Mrinal M Gounder¹, David G Pfister¹, Michael F Berger¹, Marc Ladanyi¹, Ronald Ghossein¹, Cristina R Antonescu¹, Snejzana Dogan¹. ¹Memorial Sloan Kettering Cancer Center, New York, NY

Background: *SMARCB1* is a tumor-suppressor gene located at 22q11.2 that leads to loss of protein expression through deletion, mutation or epigenetic silencing. *SMARCB1*-deficient sinonasal

carcinoma (SNC) have previously been described, however the frequency and spectrum of *SMARCB1* alterations in other head and neck (H&N) carcinomas are unknown.

Design: 21 H&N carcinomas with *SMARCB1* loss of expression and/or genetic alterations were collected from our surgical pathology and molecular diagnostic service from January 2014 to June 2017. 15 cases were analyzed by hybridization exon-capture next-generation sequencing (NSG) MSK-IMPACT™ assay targeting 279, 410 or 468 cancer-related genes. FACETS analysis to determine the loss of heterozygosity (LOH) status and cancer cell fraction (CCF) was performed in 13 cases. 6 cases were examined by FISH for *SMARCB1* copy number changes. INI1 protein status was determined by immunohistochemistry using Baf-47 (INI1) antibody.

Results: Nuclear expression of INI-1 protein was lost in all cases. Pathogenic *SMARCB1* alterations were detected in 20 (92%) including 14 SNCs, 1 anaplastic thyroid carcinomas, 1 papillary thyroid carcinoma, cribriform-morular variant with associated undifferentiated component, 1 poorly differentiated carcinoma of skin, and in 3 carcinomas of unknown primary origin. Among the cases profiled by NGS *SMARCB1* deletion was found in 9 (60%), while 6 cases harbored truncating *SMARCB1* mutations (stop codon, frameshift and splice site) coupled with LOH in 5 of 6 cases. 5 cases lacking NGS profiling showed either homozygous and heterozygous *SMARCB1* deletions by FISH, in 3 and 2 cases, respectively. *SMARCB1*-deficient SNCs showed predominantly basaloid, rhabdoid/oncocytic or (pseudo-)glandular features. Two SNCs were strongly positive for neuroendocrine markers synaptophysin and chromogranin.

Conclusions: *SMARCB1*-deficient carcinomas of H&N are not limited to the sinonasal tract and can also arise in the thyroid and skin. A significant proportion of *SMARCB1*-deficient cases harbour pathogenic *SMARCB1* mutations associated with LOH. *SMARCB1*-deficient SNCs are morphologically diverse and can exhibit *bona fide* neuroendocrine differentiation. A histogenetic variety of poorly-/undifferentiated carcinomas of H&N may potentially be amenable to EZH2 targeted therapy.

1331 Expression of PD-L1 22C3 in Head and Neck Squamous Cell Carcinomas, in Relation to p16 and HR-HPV DNA Status

Georgios Deftereos¹, Wenhua Zhou², Leslie Rowe², Sheryl R Tripp³, Mohamed Salama⁴, Anna P Matynia¹, Benjamin Witt⁵. ¹University of Utah, Salt Lake City, UT, ²ARUP Laboratories, Salt Lake City, UT, ³ARUP Laboratories, Salt Lake City, UT, ⁴Salt Lake City, UT, ⁵Huntsman Cancer Hospital, Salt Lake City, UT

Background: Head and neck squamous cell carcinomas (HNSCCs) are a group of tumors pathogenetically divided into high-risk human papillomavirus (HR-HPV) positive and HR-HPV negative. Generally, HR-HPV positive HNSCCs carry better prognosis and higher sensitivity to chemoradiotherapy. Current methods of HR-HPV status determination, p16 immunohistochemistry (IHC) and HPV DNA in situ hybridization have limitations related to sensitivity, specificity and interpretation. Recently, the use of immune checkpoint inhibitors has shown promise in HNSCC. However, the recent US Food and Drug Administration (FDA) approval of PD-L1 28-8 for the use with nivolumab as a complementary diagnostic has uncertain clinical utility. Our aim was to assess expression and correlations between p16 IHC, HR-HPV DNA and 22C3 IHC.

Design: 47 cases (31 p16 positive, 16 p16 negative) underwent HR-HPV DNA testing on the Roche cobas® HPV genotyping assay, currently under validation for use in this setting, and PD-L1 22C3 IHC. Correlations between p16 expression, 22C3 expression, HR-HPV DNA detection and HR-HPV genotype were investigated. Membranous 22C3 staining in ≥1% of tumor cells was considered positive.

Results: Using p16 as gold standard, cobas® sensitivity was 93.5% (29/31 cases), while specificity was 91.7% (11/12 cases). Four p16 negative cases failed to amplify on cobas®, possibly due to scant tissue. One p16 negative case was HPV16 positive by cobas®. 28/47 (59.6%) total cases showed expression of PD-L1 22C3. No correlation was seen between 22C3 and p16 expression (p=0.3655) or between 22C3 expression and HR-HPV detection by cobas® (p=0.3318). Finally, no association between 22C3 expression HPV16 genotype was noted (p=0.2279).

Conclusions: The Roche cobas® HPV assay shows high sensitivity and specificity for HR-HPV detection in HNSCC. As p16 IHC is a surrogate marker for HPV, rare cases identified as false positive/false negative by cobas® may better reflect HPV infection status than p16. Finally, PD-L1 22C3 status does not appear to depend on HR-HPV status or genotype.

1332 Skull Base Chordoma: Understanding Wnt- Upwind or Downwind?

Franco DeMonte¹, Ehab Y Hanna¹, Shaan M Raza¹, Achim H Bell¹, Victor Prieto¹, Gregory Fuller¹, Diana Bell¹. ¹UT - MD Anderson Cancer Center, Houston, TX

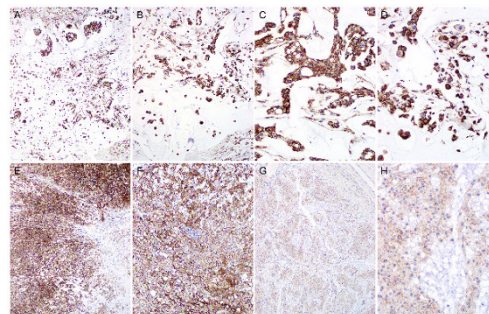
Background: Chordomas are rare, slowly growing, locally aggressive bone neoplasms that arise from embryonic remnants of the notochord and manifest a dual epithelial-mesenchymal differentiation. These tumors typically occur in the axial skeleton and have a predilection for the sphenoid-occipital and sacral regions.

Wnt/ β -catenin is an essential signaling pathway that functions in embryonic development. Aside from their role in early development, WNTs and their downstream effectors are involved in critical processes that are fundamental for cancer cell progression (tumor initiation, tumor growth, cell senescence, cell death, differentiation and metastasis). Overexpression of constitutively activated β -catenin can lead to tumorigenesis.

A mounting body of evidence, including our transcriptome data, indicate that the Wnt/ β -catenin signaling pathway is active in chordoma; however, the role of the pathway has yet to be elucidated. RNAseq data has shown differential upregulation of Wnt/ β -catenin/TCF4 in skull base versus spine chordoma. Herein, we further characterize the Wnt pathway at the protein level by examining the expression of direct targets β -catenin, LMX4, and brachyury.

Design: Immunohistochemistry was performed on 20 chordoma samples using anti- β -catenin, anti-LMX4 and anti-brachyury antibodies.

Results: According to anatomic location and histology, study chordomas were categorized as follows: 12 skull base (predominantly sphenoid-occipital; 6 chondroid and 6 conventional), and 8 spine (conventional, predominantly sacral). Strong nuclear expression of brachyury and LMX4 was detected in all 20 chordomas. Conventional chordomas (both skull base and spine) show membranous and cytoplasmic β -catenin expression; however, in the spine samples (Fig. 1 G-H), expression intensities were much weaker compared to those seen in skull base samples (Fig. 1 A-F). Of interest, β -catenin nuclear staining (5%, scattered focal) was observed only in chondroid-type skull base chordoma, and was confined to the cartilaginous component (Fig. 1 A-B).



Conclusions: Downstream targets brachyury and LMX4 are expressed in all chordomas. While variable membranous and cytoplasmic presence of β -catenin is detected in all chordomas, activated nuclear β -catenin is confined to the cartilaginous component of chondroid chordomas. Our current ongoing efforts track and jibe the genomic crosstalk between skull base chondroid chordoma and chondrosarcoma.

1333 Novel ETV6-RET Gene Fusion in Secretory Carcinoma of the Salivary Glands

Julie M Guilmette¹, Jochen Lennerz², Vania Nosé³, Peter Sadow¹. ¹Massachusetts General Hospital, Boston, MA, ²Massachusetts General Hospital and Harvard Medical, Boston, MA, ³Boston, MA

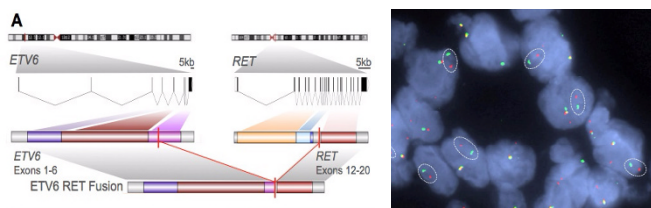
Background: Secretory carcinoma (SC) of the salivary gland is a low-grade malignancy with characteristic histomorphology, immunohistochemistry and cytogenetics. Although it holds a well-known cytogenetic translocation (12; 15) (p13; q25) resulting in an *ETV6-NTRK3* gene fusion, other *ETV6* partners have been described. *ETV6-RET* gene fusion is a novel translocation and likely belongs to the SC family.

Design: With IRB approval, we retrieved 11 cases of SC from the pathology files of the Massachusetts General Hospital. Fluorescence hybridization in situ (FISH) molecular analyses are performed on all SC to confirm their cytogenetic translocation.

Results: FISH demonstrates predominantly (12; 15) (p13; q25) translocations with *ETV6-NTRK3* gene fusion. One case without classical *ETV6* gene rearrangement harbored a gene rearrangement with *RET* (10q11.2), a proto-oncogene encoding a tyrosine kinase receptor. *ETV6-NTRK3* cases showed typical immunohistochemistry compatible with that previously described in SC; whereas, the *ETV6-RET* case revealed only focal mammaglobin staining.

FISH demonstrates predominantly (12; 15) (p13; q25) translocations with *ETV6-NTRK3* gene fusion. One case without classical *ETV6* gene rearrangement harbored a gene rearrangement with *RET* (10q11.2),

a proto-oncogene encoding a tyrosine kinase receptor. *ETV6-NTRK3* cases showed typical immunohistochemistry compatible with that previously described in SC; whereas, the *ETV6-RET* case revealed only focal mammaglobin staining.



Conclusions: FISH assay to detect potential gene fusion is the method of choice for molecular confirmation of SC. Although *ETV6-NTRK3* gene fusion is canonical for SC, *ETV6* gene occasionally partners with non-*NTRK3* genes, such as *RET*. Consequently, if variable molecular mechanisms are found within SC, these alternative pathways might present opportune therapeutic targets for persistent or recurrent disease. These findings provide novel insight into the oncogenesis, histopathology, and molecular diagnosis of this newly recognized carcinoma.

1334 MicroRNAs Expression Model Predicts Time to Local Recurrence in Head and Neck Squamous Cell Carcinoma

Marketa Hermanova¹, Parwez Ahmad², Jiri Sana², Marek Slavik⁴, Tetiana Shatokhina¹, Ondrej Slaby². ¹St. Anne's University Hospital and Faculty of Medicine, Masaryk University, Brno, Czech Republic, ²Central European Institute of Technology, Masaryk University, Brno, Czech Republic, ³Masaryk Memorial Cancer Institute and Faculty of Medicine, Masaryk University, Brno, Czech Republic

Background: MicroRNAs (miRNAs) represent promising prognostic and predictive biomarkers in many tumor types including head and neck squamous cell carcinoma (HNSCC). The objective of our study was to define a miRNAs profile efficient in prediction of locoregional control (LRC) – time to local recurrence, and radiotherapy treatment outcomes in patient with HNSCC.

Design: Our retrospective study included HNSCC patients who underwent a definitive radiotherapy in curative intent as a main treatment modality. Patients were divided into 2 groups according to LRC as follows: short (n = 22; median 5.1 months) versus long (n = 21; 60.4) LRC groups. Global miRNA expression profiles were examined in 43 formalin-fixed, paraffin-embedded primary biopsy tumor tissue samples. The miRNA expression analyses were carried out by the hybridization microarray technology. Data were pre-processed and statistically analyzed, all data were log2-transformed.

Results: Twenty-four of 2578 miRNAs analyzed were significantly differentially expressed between both examined groups (p < 0.05; Average Expression > 1; Average logFold Change = 0.42). Similarly, 24 miRNAs were significantly associated with LRC (p < 0.05). Based on these results, the model of four miRNAs (miR-212-3p, miR-331-5p, miR-1228-3p, and miR-4786-3p) highly associated with LRC was suggested (HR = 2.72, 95%CI for HR (1.78-4.16), p < 0.001, Cox regression analysis). Kaplan-Meier analysis confirmed that Risk Score calculated based on this miRNA model is able to stratify patients with early and later local recurrence after RT (p < 0.001, Risk Score threshold = 0.8566632).

Conclusions: Based on our results, the suggested set of miRNAs seems to represent a very promising tool for prediction of local recurrence and radiotherapy treatment outcomes in patients with HNSCC.

This work was financially supported by the Czech Ministry of Health, Grant no. 15-31627A, Project MZ CR – RVO (MOU, 00209805), and by the Ministry of Education, Youth and Sports of the Czech Republic under Project CEITEC 2020 (LQ1601).

1335 Radical Neck Dissections: The Necessity and Cost Effectiveness of the Standard Protocol

Ashley Illingworth¹, Debbie Walley¹, Lana Jackson¹, Varsha Manucha¹. ¹University of Mississippi Medical Center, Jackson, MS

Background: Neck dissection in squamous cell carcinomas of the head and neck is the therapeutic when nodal metastasis has been found during physical examination and diagnostic when lymph node (LN) involvement has not been found clinically or by imaging. Gross and microscopic evaluation of the neck dissection specimen is therefore critical in staging head and neck carcinomas. In order to conduct a thorough and accurate assessment of the lymph nodes, pathologists typically submit the entire neck dissection specimen and examine it microscopically, including tissue that does not contain palpable LNs. This practice increases the cost of pathologic evaluation and increases the anatomic laboratory's work load, but may not increase

the diagnostic yield compared to focused pathologic examination of palpable LN.

Design: All neck dissections performed for head and neck squamous cell carcinomas between 2014- 2016 were retrieved. Specimens were classified as group I, if they were evaluated grossly by the lead pathologist assistant (PA), or group II, if grossly prosected by pathology residents or physician assistant students. The PA and residents identified LNs using a standard palpation technique. All surgeries were performed by the same surgeon and microscopic evaluation was performed by the same pathologist. Results were tabulated as palpable/non palpable and positive/negative for metastatic carcinoma. The number of glass slides for each group was also documented. For purpose of comparison, bilateral neck dissections were evaluated as separate specimens.

Results: There were 291 radical neck dissection specimens that were received by the Department of Pathology between the years 2014-2016. Of these, 82 specimens were included in group I and 57 in group II. 2,771 palpable LN (levels II to IV) were identified, of which 109 (3.9%) were positive for metastatic carcinoma. 2,088 non-palpable microscopically identified LNs were found in 1174 additional glass slides, costing an additional \$21,202. None of the non-palpable LN was positive for metastatic carcinoma. Soft tissue microscopic deposits were seen in 3 cases with metastatic LNs. There was no major difference in the number of LNs retrieved between the two groups.

	Group I	Group II	Glass slides prepared
Number of specimens	82	57	
Palpable LN	1690	1081	1242
Palpable LN/specimen	20.6	19.0	
Palpable LN with metastatic disease (%)	78 (4.6)	31 (2.9)	-
Non-palpable LN	868	1220	1174
Non-palpable LN with metastatic disease	0	0	

Conclusions: While submission of the entire neck dissection specimen increases the number of LN examined, it does not contribute to the pathologic stage of the cancer. The number of palpable LN retrieved is not affected by the level of training of the gross prosector.

1336 NKX3.1 Expression in Salivary Gland Neoplasms: A Marker for Mucinous Differentiation and a Potential Diagnostic Pitfall

Anna-Karoline Israel¹, Abberly Lott Limbach². ¹URMC, Rochester, NY, ²University of Rochester Medical Center, Rochester, NY

Background: NKX3.1 plays an important role in prostate development and proliferation and is currently used as a diagnostic biomarker for prostate cancer. Expression of NKX3.1 has been reported in salivary gland tissue and submucosal bronchial glands, but not in salivary gland neoplasms. In our study, we examine the expression of NKX3.1 in select salivary gland neoplasms.

Design: The pathology laboratory information system was searched and 38 cases of salivary gland neoplasms (pleomorphic adenoma, warthin tumor, acinic cell carcinoma, adenoid cystic carcinoma, oncocytoma, mucoepidermoid carcinoma, salivary duct carcinoma, epithelial-myoeplithelial carcinoma and polymorphous low-grade adenocarcinoma) were identified. Immunohistochemical staining for NKX3.1 was performed and any amount and any intensity of nuclear staining was considered positive. The number of tumors with positive staining as well as the number of cases with staining in the background normal gland was recorded.

Results: There were 38 salivary neoplasms from 17 males and 21 females (age range of 20-94 years, average 60.7 years). The cases included both benign and malignant tumors (see table 1). We observed strong positive staining in one case of acinic cell carcinoma with high grade transformation. Additionally, positive staining was seen in mucoepidermoid carcinoma, salivary duct carcinoma, epithelial-myoeplithelial carcinoma, pleomorphic adenoma, and warthin tumor, (see table 1). There were 8 cases with strong positivity in the background mucous glands of the submandibular and minor salivary glands.

Tumor Type (n)	NKX3.1 Positive in tumor	NKX3.1 Positive in background gland
Pleomorphic adenoma (5)	2	2
Warthin tumor (5)	5	0
Oncocytoma (5)	0	0
Acinic cell carcinoma (5)	3	1
Adenoid cystic carcinoma (5)	3	2
Mucoepidermoid carcinoma (6)	3	2
Salivary duct carcinoma (3)	2	0
Epithelial-myoepithelial carcinoma (3)	2	0
Polymorphous low-grade adenocarcinoma (1)	1	1

Conclusions: In this study we assessed NKX3.1 expression in 38 representative cases of salivary gland neoplasms. Interestingly, there was strong expression in acinic cell carcinoma with high grade transformation, but only weak or no expression in conventional acinic cell carcinoma. Unsurprisingly, some low grade mucoepidermoid carcinomas showed positivity in the mucinous cells. The focal staining in salivary gland neoplasms as well as mucinous glands in the submandibular gland and minor salivary glands with NKX3.1 may represent a diagnostic pitfall when assessing primary salivary neoplasms and metastatic disease.

1337 Expression of PAX3 Distinguishes Biphenotypic Sinonasal Sarcoma from Histologic Mimics

Vickie Y Jo¹, Adrian Marino-Enriquez, Christopher D Fletcher², Jason L Hornick². ¹Brigham & Women's Hospital, Boston, MA, ²Brigham and Women's Hospital, Boston, MA

Background: Biphenotypic sinonasal sarcoma (BSNS) is a distinctive, anatomically restricted, low-grade spindle cell sarcoma that shows considerable histologic overlap with other highly cellular spindle cell neoplasms. This tumor type shows both myogenic and neural differentiation, which can be demonstrated by immunohistochemistry (IHC); however, the available diagnostic markers are relatively non-specific. BSNS is characterized by PAX3 gene rearrangements, most commonly with a MAML3 fusion partner (more rarely NCOA2 or FOXO1). The purpose of this study was to determine whether IHC for PAX3 could distinguish BSNS from potential histologic mimics, as well as to evaluate a widely available polyclonal PAX8 antibody, which is known to cross-react with other paired box transcription factor family members.

Design: IHC for PAX3 (mouse monoclonal antibody; clone 274212) and PAX8 (rabbit polyclonal antibody) was performed on whole sections from 13 cases of BSNS, and 10 cases of each of the following tumor types: malignant peripheral nerve sheath tumor (MPNST), monophasic synovial sarcoma, spindle cell rhabdomyosarcoma (RMS), solitary fibrous tumor, cellular schwannoma, and alveolar RMS (which harbors PAX3 or PAX7 gene rearrangements). Diagnoses were confirmed by review of H&Es and relevant ancillary studies. Nuclear staining was recorded according to extent (0, no staining; 1+, <5%; 2+, 5%-50%; 3+, >50%) and intensity; 5% or more nuclear immunoreactivity was considered positive.

Results: All thirteen BSNS were positive for PAX3 (7 cases 3+ including 2 moderate and 5 strong; 6 cases 2+ including 4 moderate and 2 weak). PAX3 was also positive in 1 (10%) spindle cell RMS (2+ moderate). All other histologic mimics of BSNS were completely negative for PAX3. In contrast, nuclear staining for PAX8 was seen in all 13 (100%) BSNS, 7 (70%) MPNST, 3 (30%) cellular schwannomas, 1 (10%) synovial sarcoma, 1 (10%) spindle cell RMS, and 1 (10%) solitary fibrous tumor. As expected, all cases of alveolar RMS were positive for PAX8, and most were also positive for PAX3 (8; 80%).

Conclusions: Expression of PAX3 detected by IHC is highly sensitive (100%) and specific (98%) for BSNS. BSNS also shows positivity with a polyclonal PAX8 antibody (due to cross-reactivity with PAX3) but has much lower specificity (76%) and should be interpreted with caution in the context of an inclusive IHC panel, especially in the distinction from MPNST.

1338 Immunohistochemistry Using a Pan-TRK Antibody Distinguishes Secretory Carcinoma of Salivary Gland from Acinic Cell Carcinoma

Vickie Y Jo¹, Yin P. (Rex) Hung¹, Jason L Hornick¹. ¹Brigham and Women's Hospital, Boston, MA

Background: Secretory carcinoma (previously known as mammary

analog secretory carcinoma) is a low-grade malignant salivary gland neoplasm characterized by ETV6 gene rearrangements, most often ETV6-NTRK3 fusion. Secretory carcinoma shows histologic overlap with other salivary gland tumors, in particular acinic cell carcinoma, and can be difficult to diagnose without genetic confirmation. A recently developed pan-TRK antibody (which recognizes a conserved sequence near the C-terminus of TRK proteins) shows promise for identifying tumors with NTRK fusions. The aim of this study was to evaluate the potential diagnostic utility of pan-TRK immunohistochemistry (IHC) for secretory carcinoma.

Design: We evaluated whole-tissue sections from 83 tumors including 12 secretory carcinomas (11 from parotid glands, 1 oral cavity; 5 with confirmed ETV6 rearrangement by fluorescence *in situ* hybridization, 1 confirmed ETV6-NTRK3 fusion by next-generation sequencing), 13 acinic cell carcinomas, 18 polymorphous low-grade adenocarcinomas (PLGA), 20 low-grade mucoepidermoid carcinomas, and 20 pleomorphic adenomas. IHC was performed following heat-induced antigen retrieval using a pan-TRK rabbit monoclonal antibody (clone EPR17341; Abcam).

Results: Immunoreactivity with pan-TRK was detected in 8 (67%) secretory carcinomas, all with a nuclear pattern, 4 showing diffuse staining (>50% of cells). Among the 6 confirmed ETV6-rearranged secretory carcinomas, 4 (67%) were positive with pan-TRK. All acinic cell carcinomas were entirely negative with pan-TRK. Of the other tumor types, pan-TRK immunoreactivity was observed in all 20 (100%) pleomorphic adenomas (nearly exclusively in myoepithelial cell-rich areas with prominent myxoid stroma), 14 (78%) PLGA, and 4 (20%) low-grade mucoepidermoid carcinomas. However, the pattern of pan-TRK staining in these tumors was predominantly membranous and cytoplasmic, with nuclear immunoreactivity noted focally (<10% of cells) in only 7 cases (6 PLGA and 1 low-grade mucoepidermoid carcinoma).

Conclusions: Nuclear staining with a pan-TRK antibody distinguishes secretory carcinomas from other salivary gland tumors, including acinic cell carcinomas. Membranous expression of TRK is common in salivary gland neoplasms other than acinic cell carcinomas, suggesting that TRK signaling may play a pathogenetic role. The lack of pan-TRK immunoreactivity in a subset of secretory carcinomas, including those with confirmed ETV6 gene rearrangements, suggests the presence of non-NTRK fusion partners.

1339 Prognostic Utility of Current Grading and Staging Systems in Esthesioneuroblastoma

Tanvee S Kulkarni¹, Asawari Patil¹, Swapnil Rane¹, Munita Bal¹, Shubhada Kane¹. ¹Tata Memorial Centre, Mumbai, Maharashtra, India

Background: Esthesioneuroblastoma (ENB) is a rare sinonasal malignant neoplasm arising from the specialized olfactory neuroepithelium with a diverse biological behaviour. Multiple staging (Modified Kadish, Dulgerov's and Biller's TNM staging) and grading (Hyams grading, Gallagher et al grading) systems have been proposed for optimal management of ENB patients; each with variable correlation with survival.

Design: A retrospective review of clinico-radiological and histopathological parameters including architecture, necrosis, rosettes, mitosis, calcification, neurofibrillary matrix, glandular hyperplasia, spindle cell morphology, apoptosis and currently available staging and grading systems was done in 73 ENB cases diagnosed over the period of 10 years (2006 to 2016). Histological parameters were assessed more quantitatively using percentages (e.g. necrosis, architecture) and count/hpf (e.g. mitosis, apoptosis) to increase objectivity. These were correlated with overall survival (OS) in 58 cases where follow up data was available.

Results: The age at diagnosis ranged from 4 to 72 years with a single peak in 4th decade (mean: 41.7 years). Male to female ratio was 2.3:1. Epistaxis and nasal obstruction were the most common presenting symptoms. Distribution of cases across the grading and staging systems along with their co-relation with OS is described in Table 1. A positive correlation between the Hyams grade and Kadish Morita stage (p=0.012) and Dulgerovs and Billers T stage (p= 0.001 and p= 0.002) was established with higher grade tumors exhibiting higher T stage at presentation. Cervical node metastasis was seen in 20.5% cases and 8.2% cases developed distant metastasis, most frequently to the axial skeleton. Recurrence was seen in 23.2% cases. Presence of distant metastasis was found to be a significant predictor of worse OS (p=0.000153). Presence of necrosis (p=0.006) and diffuse architecture (p= 0.049) at diagnosis was significantly associated with occurrence of distant metastasis. On univariate analysis of all the histopathological parameters, only mitotic count/hpf correlated significantly with OS (p=0.02). On further subgrouping, taking 2 mitosis/hpf as the cut off, significantly distinct survival outcomes were obtained between the two groups (p=0.000275).

Table 1: Distribution of cases across grading and staging systems and correlation with OS

Grading and Staging systems		Distribution (%)	Mean survival (Months)	p value
Hyam's Grading	I	0%	-	p = 0.205
	II	28.8%	110.1	
	III	53.4%	96.2	
	IV	17.8%	67.9	
Gallagher et al Grading	Low	11%	No deaths	p = 0.355
	Intermediate	56.2%	110.1	
	High	32.8%	67.5	
Modified Kadish Staging	A	0%	-	p = 0.443
	B	30.1%	86.5	
	C	47.9%	93.0	
	D	22%	97.0	
Dulgerov's T Staging	I	4.1%	No deaths	p = 0.822
	II	30.1%	81.5	
	III	50.7%	112.6	
	IV	15.1%	77.9	
Biller's T Staging	I	34.2%	82.6	p = 0.953
	II	43.8%	113.4	
	III	9.6%	77.9	
	IV	12.4%	28.6	

Conclusions: Current grading and staging systems did not show significant association with OS in our cohort. A grading system based on mitotic count alone, may prove to be an objective and prognostically significant stratification system.

1340 Salivary Duct Carcinoma with Rhabdoid Features is a Salivary Counterpart of Pleomorphic Lobular Carcinoma of the Breast: No or Aberrant expression of E-cadherin and the Gene Mutation of CDH1

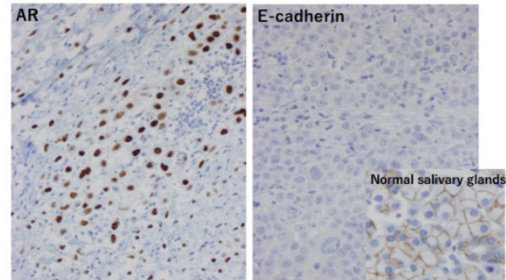
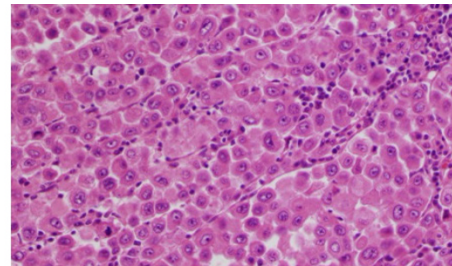
Kimihide Kusafuka¹, Takuya Kawasak², Haruhiko Sugimura³, Matsuyoshi Maeda⁴, Koji Yamaneg⁵, Akira Ishihara⁶, Tomoyuki Ohuchi⁷, Satoshi Baba⁸, Hiroshi Inagak⁹, Takashi Nakajima¹⁰, Takashi Sugino². ¹Shizuoka Cancer Center, Sunto-gun, Shizuoka, Japan, ²Shizuoka Cancer Center, ³Hamamatsu University School of Medicine, ⁴Toyohashi Municipal Hospital, Toyohashi, Aichi, ⁵Hyogo Medical University, ⁶Miyazaki Prefectural Nobeoka Hospital, Nobeoka, ⁷Keiyukai Sapporo Hospital, ⁸Hamamatsu University School of Medicine Hospital, ⁹Nagoya City University, ¹⁰Shizuoka Cancer Center, Nagazumi, Shizuoka, Japan

Background: Salivary duct carcinoma (SDC), which is high-grade malignancy of the salivary glands, has several histological variants. Previously, we reported nine cases of SDC as "salivary duct carcinoma with rhabdoid features (SDCRF)", which is extremely rare. We elucidate the morphological, immunohistochemical and genetic characteristics of SDCRF.

Design: We extracted SDCRF cases from pathology files of our institutions during 1995-2016. We examined them histologically and immunohistochemically. Immunostains were performed for cytokeratin (CK), GCDFP-15, androgen receptor (AR), Her-2, EGFR, vimentin, SMARCB1, E-cadherin, and Ki-67. We also examined the point mutation of E-cadherin (*CDH1*) gene in four cases, using PCR and direct sequence method with DNA extract from FFPE samples.

Results: Eleven cases of SDCRF were selected. Nine cases were male with a mean of 69 years (range: 36-85 years), which included eight parotid gland cases and three submandibular gland cases. Histologically, the carcinoma components showed diffuse proliferation of less-coherent large ovoid atypical cells with eosinophilic cytoplasm and eccentric nuclei. Immunohistochemically, such "rhabdoid cells" were positive for CK, GCDFP-15, and AR in all cases, but negative for vimentin. Intact nuclear expression of SMARCB1 was seen in all cases. No or decreased/cytoplasmic expression of E-cadherin was seen in six or three cases, respectively. Four cases could be examined genetically, and *CDH1* gene showed the mutations in all cases (Case 1, exon 4, & 14; Case 2, exon 3, 15, & 16; Case 6, exon 2 & 16; Case 7, exon 4).

Case No.	Exon	Nucleotide change	Amino Acid change	genotype
Case 1	4	c.490 C>T	p.(Pro164Ser)	c/t
	5	c.540C>T	p.(=)	c/t
	14	c.2173C>T	p.(=)	c/t
Case 2	3	c.220C>T	p.(Arg74Ter)	c/t
	15	c.2370C>T	p.(=)	t/t
	16	c.2528C>T	p.(Ala843Val)	c/t
Case 6	2	c.150C>5	p.(=)	c/t
	16	c.2476C>T	p.(Pro826Ser)	t/t
Case 7	4	c.388G>A	p.(Ala130Thr)	g/a
	4	c.489C>T	p.(=)	c/t



Conclusions: The morphogenesis of "rhabdoid cells" in SDCRF is related to the down-regulation of E-cadherin expression, which is induced from the *CDH1* gene mutation. From the similarity in morphology, immuno-phenotype and genotype, SDCRF is a salivary counterpart of pleomorphic lobular carcinoma of the breast.

1341 Impact on Clinical Follow-up of the Milan System for Salivary Gland Cytology: A Comparison with a Traditional Diagnostic Classification

Lester Layfield¹, Zubair Baloch², Sharon Hirschowitz³, William Faquin⁴, Esther Ross⁵. ¹University of Missouri, Columbia, MO, ²Hospital of Univ. of PA, Philadelphia, PA, ³David Geffen School of Medicine at UCLA, Los Angeles, CA, ⁴Massachusetts General Hospital, Boston, MA, ⁵Catholic University, Rome, Italy

Background: The recently proposed Milan System for Reporting Salivary Gland Cytopathology (MSRSGC) offers a uniform classification with known malignancy risks and corresponding management recommendations. We compared FNA diagnoses given in a prior study which assigned specific diagnoses (i.e. recapitulating surgical pathology diagnosis) with categorical diagnoses of MSRSGC.

Design: One-hundred and sixty-four cases from a prior cytologic study with histologic follow-up were re-reviewed by one of the authors (LL, also an author of the prior study) blinded to prior diagnoses. He assigned each specimen to one of the MSRSGC categories: Non-Diagnostic, Non-Neoplastic, AUS, Neoplasm: Benign, Neoplasm: Salivary Lesions of Uncertain Malignant Potential (SUMP), Suspicious for Malignancy and Malignant. The diagnoses and the associated

recommended follow-up were compared between MSRSGC and original diagnoses.

Results: The MSRSGC system classified 25 specimens as non-diagnostic (histologically shown to be 7 benign salivary gland, 2 non-mucinous cysts, 10 sialadenitis, 2 benign mixed tumors, 1 hemangioma, 1 lymphoma, 1 adenoid cystic carcinoma, 1 squamous carcinoma). The original study diagnosed these lesions as: 7 benign cysts, 15 benign salivary gland tissue, 1 benign neoplasm and 2 insufficient for diagnosis. In 15 cases, MSRSGC disagreed with original diagnoses and surgical resection showed lesions where optimal follow-up was more consistent with original cytologic diagnosis. In eight cases (32%) where disagreement occurred, the MSRSGC was associated with a more appropriate follow-up based on the surgical diagnosis.

Malignancy risks for the Milan Categories were: Non-Diagnostic (12%), Non-Neoplastic (0%), AUS (19%), Neoplasm, Benign (5%), Neoplasm (SUMP) (40%), Suspicious for Malignancy (60%) and Malignant (87%).

Conclusions: Despite the intraobserver variability and differences in assignment of the non-diagnostic category, both MSRSGC and the original series had high accuracy (93% and 92%) for distinguishing benign from malignant lesions. Both diagnostic approaches for classifying salivary gland lesions led to appropriate clinical management in a majority of cases.

1342 The Expression of PTEN, Androgen Receptor, HER2, Cytokeratin 5/6, Estrogen Receptor-beta, HMGA2 and PLAG1 in Salivary Duct Carcinoma

Li Liang¹, Michelle Williams¹, Diana Bell¹. ¹The University of Texas, MD Anderson Cancer Center, Houston, TX

Background: Salivary duct carcinoma (SDC) is an uncommon, but aggressive neoplasm. It can develop de novo or from the malignant transformation of pleomorphic adenoma (PA).

Design: We performed immunohistochemical stains for PTEN, androgen receptor, HER2, cytokeratin 5/6, estrogen receptor-beta, HMGA2 and PLAG1 on tissue microarray samples of 75 SDCs and 31 adenocarcinomas, NOS.

Results: Our data was summarized in the table below. Fisher's exact test was used to compare the two groups (SDC versus adenocarcinoma, NOS). In addition, we further studied the expression of HMGA2 in patients with SDCs. There is no statistically significant difference in the age of onset between HMGA2-positive (range: 32-85; mean: 64.3; median: 64.5) and HMGA2-negative SDCs (range: 41-79; mean: 62.5; median: 64.5). There is also no statistically significant difference in the overall survival between HMGA2-positive and HMGA2-negative SDCs (follow-up period ranging from 3 to 201 months (mean: 49.8 months; median: 30 months). Among ten patients with definite pleomorphic adenoma component (SDC ex-pleomorphic adenoma), six were positive for HMGA2, and four were negative for HMGA2.

Marker	Salivary duct carcinoma	Adenocarcinoma, NOS	P value
Loss of PTEN	17/60 (28.3%)	14/27 (51.9%)	0.0521
AR	43/62 (69.4%)	8/25 (32%)	0.0018
HER2	25/58 (43.1%)	6/28 (21.4%)	0.0584
CK5/6	14/54 (25.9%)	5/21 (23.8%)	1.0000
ER-beta	37/56 (66.1%)	7/25 (28%)	0.0018
HMGA2	29/63 (46%)	11/23 (47.8%)	1.0000
PLAG1	0/62 (0%)	1/24 (4.1%)	0.2791

Conclusions: In our cohort of patients, HMGA2 was expressed in approximately half of SDCs. The expression of HMGA2 is not associated with patients' age or overall survival. In the next step, we will further verify these findings using FISH analysis. In addition, loss of PTEN was found in a subset of both SDCs and adenocarcinoma, NOS. HMGA2 and PTEN are promising therapeutic targets for salivary gland tumors.

1343 Predictive Value of the 8th Edition American Joint Commission Cancer (AJCC) Nodal Staging System for Patients with Cutaneous Squamous Cell Carcinoma of the Head and Neck

Jessica Liu¹, Ardalan Ebrahim², Tsu-Hui (Hubert) Low², Kan Gao², Carsten E Palme², Sydney Ch'ng², Bruce G Ashford², N Gopalakrishna Iyer³, Jonathan Clark², Ruta Gupta⁴. ¹Royal Prince Alfred Hospital, Camperdown, NSW, ²Chris O'Brien Lifehouse, ³Singhealth Duke-NUS Head and Neck Centre, ⁴Royal Prince Alfred Hospital, Sydney, NSW

Background: The 8th edition American Joint Committee on Cancer (AJCC8) provides the same nodal staging system for mucosal and

cutaneous squamous cell carcinoma of the head and neck (HNCSCC) and includes extranodal extension (ENE) as an adverse prognostic criterion. This study evaluates the prognostic efficacy of the AJCC8 pathologic nodal staging system (pN) for HNCSCC.

Design: Univariate analysis of 382 patients with metastatic HNCSCC staged according to both the 7th (AJCC7) and the 8th edition staging systems.

Results: The AJCC7 pN3 category was associated with reduced disease specific survival (DSS HR 5.49; 95% CI: 1.83-16.53; p = 0.002) and overall survival (OS HR 3.42; 95% CI: 1.54-7.58; p = 0.002) as compared with pN1. However, no difference was observed between pN1, pN2 and pN3 categories as defined by the AJCC8. Also, when comparing Stage III and IV as defined by AJCC8, there was no difference in DSS (HR 0.75; 95% CI: 0.34-1.67; p = 0.478) or OS (HR 0.88; 95% CI: 0.51-1.51; p = 0.648).

Conclusions: The AJCC8 performed poorly as a prognostic indicator for patients with metastatic HNCSCC in this cohort. HNCSCC would benefit from a staging system that accounts for its unique biologic characteristics distinct from mucosal SCC.

1344 Acinic Cell Carcinoma of Salivary Gland Expresses Low Levels of PD-L1 with Retained MMR Proteins: A Potential Biomarker for Therapy

Abberly Lott Limbach, Rochester, NY

Background: Salivary gland neoplasms are rare tumors; acinic cell carcinomas (ACC) are the third most common salivary gland malignancy. The typical treatment is complete surgical resection, which may not be possible in all cases. New biomarkers, such as PD-L1 (programmed death ligand 1), may be useful to direct treatment.

PD-L1 is a transmembrane protein involved in recognition of self by the immune system. Disruption of the binding of PD-1 to PD-L1 can increase tumor cell death and high PD-L1 expression has been associated with response to pembrolizumab immunotherapy. A number of other tumors have been shown to have high expression of PD-L1. Mismatch repair proteins (MMR) have been used to screen for Lynch syndrome in other tumors (e.g. colon adenocarcinoma and endometrial carcinoma). Recently, mismatch repair deficiency has also been shown to be associated with response to immune checkpoint inhibitors.

Our study seeks to document expression of PD-L1 as well as mismatch repair proteins in acinic cell carcinomas.

Design: The pathology LIS was searched for cases of ACC from 1/1/2007 to 7/1/2017. The slides were reviewed to confirm diagnosis, and immunostains for S100 and mammaglobin was performed to rule out mammary analogue secretory carcinoma. Immunohistochemistry for PD-L1 was scored using similar scoring criteria to that used in lung carcinoma. Any amount and any intensity of membrane staining was considered as positive staining. The percent tumor staining was recorded as well as the percent staining of tumor infiltrating lymphocytes (TILS). Immunohistochemistry for MMR proteins (MLH1, PMS1, MSH2, MSH6) was scored with >1% nuclear positivity as retained expression (MMR proficient).

Results: Fifteen cases of ACC were found consisting of 10 females and 5 males ranging in age 15-74 years (56.3 years, average age). Nine cases (60%) stained for PD-L1. The percent tumor positivity ranged from 10-90%. A majority of cases (8) had 10% of tumor cells staining, one case had 90% of tumor cells staining. There were 6 cases (40%) with staining of TILS, ranging from 5%-50%. All cases showed retained expression of all MMR proteins.

Conclusions: There was expression of PD-L1 in 60% of cases of ACC, with low expression in 53.3% of cases and high expression in 6.6% of cases. All cases of ACC had retained expression of MMR. These findings suggest that PD-L1 expression could open new options for therapy of acinic cell carcinoma, but MMR status cannot be used as a surrogate marker.

1345 A Quantitative Histomorphometric Classifier (QuHbIC) for Risk Stratification in p16-Positive Oropharyngeal Squamous Cell Carcinoma

Cheng Lu¹, Jingqin Luo², Justin Bishop³, Wade Thorstad⁴, Anant Madabhushi¹, James S Lewis⁴. ¹Case Western Reserve University, Cleveland, OH, ²Washington University in St. Louis, ³UT Southwestern Medical Center, Dallas, TX, ⁴Vanderbilt University Medical Center, Nashville, TN

Background: Identifying patients with aggressive tumors is critical in human papillomavirus-related (p16-positive) oropharyngeal squamous cell carcinoma (OPSCC), but this is difficult clinically and no biomarkers exist. This work is a validation study for a quantitative histomorphometric-based image classifier (QuHbIC or kyoo-bik) using digitally-scanned H&E for risk stratification.

Design: A TMA of 160 primary OPSCC (previously published) was

utilized for further image classifier modeling and refinement. Six tumor nuclear morphologic features were considered: global/local architecture, orientation, statistics of shape and texture, and complexity of cluster, and fractal dimension of segmented masks. The features most discriminative of outcome within each were utilized. An independent, multi-institutional, whole slide cohort of 234 p16 positive OPSCC patients was then created for validation. Tumor regions of the whole slide image were annotated and then broken down into smaller image tiles in order to mimic the TMA spot image in modeling set. Each digitized spot was assigned a probability of recurrence from 0 to 1. A patient was labeled as positive if any digitized spot had the predicted probability >0.5.

Results: 55 patients developed recurrence, and 22 died with disease. QuHbIC was positive in 9 of these latter patients (40.1%) versus only 13 of the remaining 212 (6.1%). This translated to a positive likelihood ratio of dying of disease if QuHbIC positive of 6.67 (PPV = 40.9%; NPV = 93.9%). QuHbIC positive patients had poorer overall and disease-specific survival (HR 2.5, p=0.005 and HR 2.8, p=0.015) in the univariate Cox model. Using an institution-stratified multivariate Cox model with adjustment for the major prognostic variables (including smoking and AJCC 8th ed.stage), positive QuHbIC results were independently predictive of poorer overall and disease-specific survival [HR (95% CI) = 3.2 (1.12-9.23), p=0.029 and 3.46 (0.67-17.76), p=0.13], including among just the AJCC 8th ed. stage I/II patients [HR (95% CI) = 5.0 (1.47-17.22); p=0.01 and 11.53 (1.07-124.38), p=0.04].

Conclusions: This study validates that computer-extracted nuclear morphologic features from digitally-scanned tumor H&E slides are strongly and independently associated with disease recurrence in p16+ OPSCC. This testing could be utilized for treatment decisions, especially regarding de-escalation in patients who, on clinical and other currently available grounds, would otherwise be considered low or intermediate risk.

1346 Comparison of Clinically Relevant Somatic Mutations in Primary and Metastatic Head and Neck Cutaneous Squamous Cell Carcinoma

Peter P Luk¹, Velimir Gayevskiy², Bruce G Ashford³, N Gopalakrishna Iyer⁴, Marie Ranson⁵, Tsu-Hui (Hubert) Low², Kerwin Shannon⁶, Sydney Ch'ng³, Carsten E Palme³, Jonathan Clark³, Mark Cowley⁷, Ruta Gupta⁸. ¹Royal Prince Alfred Hospital, Camperdown, NSW, ²Kinghorn Cancer Centre and Garvan Institute of Medical Research, Darlinghurst, Sydney, Australia, ³Chris O'Brien Lifehouse, ⁴Singhealth Duke-NUS Head and Neck Centre, ⁵University of Wollongong, ⁶Chris O'Brien Lifehouse, Sydney, Australia, ⁷Garvan Institute of Medical Research, ⁸Royal Prince Alfred Hospital, Sydney, NSW

Background: The head and neck is the most common site for cutaneous squamous cell carcinoma (HNCSCC). Approximately 10,000 HNCSCC develop regional metastasis annually and require radical surgery and post-operative radiotherapy. The currently used clinical and pathologic parameters do not reliably predict the risk of metastases. The genetic mechanism of metastases has been poorly studied for HNCSCC. The current study aims to compare the genetic profile of primary HNCSCC and their metastases.

Design: Using the TruSeq Amplicon Cancer Panel, targeted sequencing of 48 clinically relevant genes was performed on DNA extracted from formalin fixed and paraffin embedded primary HNCSCCs and their corresponding metastases. An in-house analytical pipeline (The Kinghorn Cancer Center) was used to identify somatic variants after deducting the normal/germline variants observed in the matched normal samples from those observed in the tumor samples. Variant positions with at least 500x read depth and variant alleles observed >5% were included in the analysis. The association of the somatic variants with clinicopathologic features was evaluated and the somatic variant profiles of the primary HNCSCC and their corresponding metastases were compared.

Results: The study includes 10 patients (median age 70, M:F:6:4) with a mean follow up of 22 months and median overall survival of 20 months. A total of 613 variants were identified with 496 (81%) being C/T and G/A transitions, characteristic of UV mediated DNA damage. The UV signature was seen in primary tumours as well as their corresponding metastases. A total of 93 functionally relevant variants were identified across 25 genes in the primary tumors whereas 179 variants across 38 genes were identified in the metastases. Within primary tumors, TP53 was mutated in 90% of patients; ATM (60%), CDKN2A (50%), APC (40%), EGFR (40%), HNF1A (40%). In metastases, TP53 mutation was most common (100%), followed by APC (50%), ATM (50%), CDKN2A (50%), FLT3 (40%), HNF1A (40%), KDR (40%), KIT (40%), PIK3CA (40%), PTEN (40%), RET (40%). Similar incidences of CDKN2A mutations were observed compared with that described in metastatic HNCSCC in the literature.

Conclusions: HNCSCC metastases demonstrate larger numbers of functionally relevant somatic mutations as compared to their concurrent primaries. The metastases retain the UV signature characteristic of primary HNCSCC. The implications of these findings for development of targeted therapy for progressive HNCSCC require further analyses.

1347 Targeted Genomic Profiling of Sinonasal Melanoma Reveals Novel Oncogenic Alterations, Including Focal Very High Copy Number Gains of KRAS and MET

Zaid Mahdi¹, Komal Kunder², Jonathan McHugh³, Rajiv Patel⁴, Scott Tomlins⁵, Aaron M Udager⁶. ¹Michigan Medicine, ²University of Michigan, ³University of Michigan Health System, Ann Arbor, MI, ⁴Univ. of Michigan, Ann Arbor, MI, ⁵University of Michigan, Ann Arbor, MI, ⁶University of Michigan Medical School, Ann Arbor, MI

Disclosures:

Scott Tomlins: *Employee*, Strata Oncology

Background: Malignant melanoma is an uncommon primary tumor of the sinonasal tract that often has a poor long-term clinical outcome. Conventional chemotherapy is typically ineffective for locally-advanced or metastatic sinonasal melanoma (SM), necessitating the development of novel targeted therapeutic approaches for these aggressive tumors. In this study, we utilized targeted next-generation DNA sequencing (DNaseq) to identify possible targetable oncogenic alterations in SM.

Design: SM from a single large academic institution between June 2013 and June 2017 were retrospectively identified, and representative formalin-fixed paraffin-embedded tissue was selected for targeted DNaseq using the OncoPrint Comprehensive Assay and an Ion Torrent Proton sequencer. Somatic variants and copy number alterations (CNA) were identified via in-house bioinformatics pipelines, and prioritized alterations were nominated by manual curation using previously established criteria.

Results: 10 SM were available for the purposes of this study. Sequencing data was available for 9 tumors (90.0%) and demonstrated a total of 12 prioritized somatic variants (median per tumor = 1; range = 1-2), including oncogenic alterations in NRAS (n = 4), BRAF (n = 1), KIT (n = 1), and HRAS (n = 1); prioritized tumor suppressor mutations included CDKN2A (n = 1), NF1 (n = 1), ATM (n = 1), TET2 (n = 1), and DDR2 (n = 1). All oncogenic somatic variants were mutually exclusive. A total of 44 CNA were identified (median per tumor = 5; range = 0-9). Recurrent CNA included MYC (gain; n = 5), MCL1 (gain; n = 4), and CDKN2A (loss; n = 3), and the sole KIT-mutated tumor showed no CNA. Focal very high copy number gains of KRAS (22-fold; n = 1) and MET (25-fold; n = 1) were detected in two tumors without prioritized oncogenic somatic variants. Therefore, overall, all sequenced tumors harbored either an oncogenic somatic variant or focal very high copy number gain.

Conclusions: SM shows a very high rate of potentially targetable oncogenic alterations in growth factor signaling pathway genes, including frequent somatic mutations (77.8%) and occasional focal very high copy number gains (22.2%), providing a rational basis for therapeutic targeting of downstream MAPK/MEK activity in these aggressive tumors. Comprehensive genomic profiling with targeted DNaseq may be indicated for "triple-negative" SM without oncogenic NRAS, KIT, or BRAF mutations to identify other less common targetable oncogenic alterations.

1348 Is transcriptionally active high-risk human papillomavirus associated with sinonasal inverted papillomas?

Mitra Mehrad¹, Rebecca Chernock², Xiaowei Wang³, James S Lewis¹. ¹Vanderbilt University Medical Center, Nashville, TN, ²Washington University School of Medicine, Saint Louis, MO, ³Washington University School of Medicine

Background: Inverted papilloma (IP) is the most frequent papilloma of the sinonasal tract. Recurrences are common and malignant transformation occurs in ~5-10% of patients overall. Whether IPs are among the group of head and neck tumors caused by high-risk human papillomavirus (hrHPV) and associated with transcriptionally-active virus is an ongoing area of debate. Detection rates for HPV DNA and mRNA vary in studies from 0 to 100%. In this study, we sought to determine the association between IPs and transcriptionally-active hrHPV using p16 immunohistochemistry (IHC) and well-characterized and highly sensitive and specific reverse transcriptase polymerase chain reaction (RT-PCR) testing for E6/E7 mRNA.

Design: IP cases over a ten-year period were identified, re-reviewed, and assessed for p16 by IHC with a 70% staining cutoff and for hrHPV mRNA by RT-PCR capable of identifying 12 of the most common types. Six cases of non-keratinizing squamous cell carcinoma (NKSCC), as defined by the WHO, with "papilloma-like" (papillary and inverted) growth patterns were included as controls.

Results: Overall, 53 IPs were identified, including 5 (9.4%) with carcinoma. Patients were predominantly male (42, 79.2%) with an age range of 29 to 83 years (median 59). Tumors arose from nasal cavity (32, 60.3%) and maxillary (10, 18.8%), ethmoid (6, 11.3%), sphenoid (3, 5.6%), and frontal (2, 3.7%) sinuses. The NKSCC patients were male, and all tumors arose in the nasal cavity. Transcriptionally-active HPV was not detected in any of the 53 IPs but was present in 5 of the 6 NKSCCs [HPV16 (x2), 33, 35 and 56]. Similarly, p16 was negative in IPs but was

positive in all 5 of the NKSCCs which were positive for HPV mRNA. The five HPV(+) NKSCCs had nonkeratinizing, full thickness, high nuclear to cytoplasmic ratio cells (similar to oropharyngeal tumors), while the one HPV(-) NKSCC had more abundant cytoplasm and limited degrees of surface keratinization. All of the carcinomas arising from IP had keratinization and were moderately to well differentiated.

Conclusions: Our data further support the more recent literature that IPs, including those with carcinoma, are not driven by transcriptionally-active hrHPV. Some NKSCC will grow like sinonasal papillomas, but these are usually associated with transcriptionally-active hrHPV and are not the pattern of dysplasia and/or carcinoma that typically develops from pre-existing IP. p16 IHC and/or assessment for high risk HPV mRNA may be helpful to distinguish the two.

1349 Immunohistochemical Detection and Molecular Characterization of IDH-Mutant Sinonasal Undifferentiated Carcinomas

Jeffrey Mito¹, Justin Bishop², Peter Sadow³, Edward Stelow⁴, William Faquin³, Stacey Mills⁵, Jeffrey Krane¹, Jason L Hornick¹, Lynette Sholf⁶, Vickie Y Jo⁶. ¹Brigham and Women's Hospital, Boston, MA, ²UT Southwestern Medical Center, Dallas, TX, ³Massachusetts General Hospital, Boston, MA, ⁴Univ. of Virginia Health System, Charlottesville, VA, ⁵University of Virginia Health System, Charlottesville, VA

Background: Recent studies have identified recurrent *IDH2* mutations in a subset of sinonasal undifferentiated carcinomas (SNUC); however, the true frequency of *IDH* mutations in SNUC is unknown. We evaluate the utility of mutation-specific IDH1/2 immunohistochemistry (IHC) in a large multi-institutional cohort of SNUC and morphologic mimics, and perform targeted next generation sequencing (NGS) on a subset of tumors.

Design: IHC using a multispecific antibody for IDH1/2 (R132/172) mutant protein was performed on 193 sinonasal tumors (whole sections), including 53 SNUCs, 8 poorly differentiated carcinomas (PDCAR), 17 squamous cell carcinomas, 14 melanomas, 14 nasopharyngeal carcinomas, 13 alveolar rhabdomyosarcomas, 12 olfactory neuroblastomas, 10 NUT carcinomas, 10 adenoid cystic carcinomas, 8 neuroendocrine carcinomas, 6 basaloid carcinomas, 6 intestinal-type adenocarcinomas, 6 HPV-associated squamous cell carcinomas, 5 SMARCB1-deficient sinonasal carcinomas, 4 extranodal NK/T-cell lymphomas, 3 HPV-related multiphenotypic sinonasal carcinomas, 3 non-intestinal sinonasal adenocarcinomas, and 1 Ewing sarcoma. Targeted NGS of 447 cancer related genes was performed on 16 cases of SNUC/PDCAR, which were selected based on morphologic and/or IHC features.

Results: Mutant IDH1/2 IHC was positive in 20/53 SNUCs (38%) and 2/8 PDCARs (25%) but was absent in all other tumor types (0/132). Targeted NGS on a subset of SNUC/PDCAR (6 positive for IDH1/2 IHC, 3 equivocal, 7 negative) showed frequent *IDH2* R172X mutations (10/16) and a single *IDH1* R132C mutation. All 6 cases with positive IDH1/2 IHC had *IDH2* R172S/G mutations. Among the other 10 cases evaluated by NGS, all 3 cases with equivocal IHC had *IDH2* R172T mutations, while the 7 cases negative by IHC included 1 case each with *IDH2* R172T and *IDH1* R132C, and 1 case with *SMARCA4* truncating deletion (with loss of *SMARCA4* by IHC). *IDH*-mutant carcinomas had frequent mutations in *TP53* (55%) and activating mutations in *KIT* (45%) or the PI3K pathway (36%).

Conclusions: Mutation-specific IDH1/2 IHC identifies *IDH* mutations in morphologic SNUC (and reclassifies a subset of PDCAR), however, it has lower sensitivity for the full range of *IDH* mutations. Frequent *KIT* and PI3K pathway mutations were also observed in *IDH*-mutant tumors. *IDH*-mutant sinonasal carcinoma may represent a distinct pathobiologic entity with therapeutic implications, and can be identified by a combined approach of multispecific IDH1/2 IHC and sequencing.

1350 Clinicopathological Characteristics of Ossifying Fibromas of the Head and Neck Region

Neha Mittal¹, Munita BaP, Asawari PatiP, Shubhada Kane². ¹Mumbai, Maharashtra, ²Tata Memorial Hospital, Mumbai, India

Background: Ossifying fibromas of the jaw are classified as cemento-ossifying fibroma (COF) (odontogenic origin), and two types of juvenile ossifying fibromas: juvenile trabecular ossifying fibroma (JTOF), and juvenile psammomatous ossifying fibroma (JPOF). The potential for recurrence in JTOF and JPOF, and discovery of newer molecular signatures necessitates accurate histological classification.

Design: The aim of our study was to review the clinical parameters and radiological findings in cases of ossifying fibromas of the jaw and correlate them with histomorphological features. A total of 48 patients with 51 tumors were retrieved from the archives of a single tertiary care oncology center, from 2005-2017 (12 years), and reviewed for relevant clinical and histological parameters.

Results: Of the 48 cases, COF comprised 17 cases (35.4%); there were 15 cases of JPOF (31.3%), and 16 cases (33.3%) of JTOF. M:F

ratio was 1.32 with an age range of 6-66 years (mean: 24.6, median; 18.1 years). Most common site for COF was mandible, for JTOF was maxilla, and for JPOF was ethmoid sinus. One case of mixed JTOF and JPOF histology was seen. Aneurysmal bone cyst like areas were seen in 22.9% cases. A unique histological finding of abnormal blood vessels lacking muscular wall, akin to those seen in angiomatoid fibromas of kidney, were seen in 4 cases of JTOF and 10 cases of JPOF. Follow up was available in 22 cases, and ranged from 4-120 months. Three cases of JPOF had recurrence and one patient with JTOF had residual disease after surgery.

	COF (N=17)	JTOF (N=16)	JPOF (N=15)
AGE RANGE (YEARS)	10-66	6-57	12-48
T SIZE	3-12 cm	4-10 cm	3-6.2 cm
SITE	mandible (10 cases)	maxilla (9 cases)	ethmoid sinus (8 cases)
RADIOLOGY FINDING	radiolucent, lytic lesion	radiolucent, lytic lesion with peripheral arc like calcification	solid cystic lesion with ground glass appearance
TYPE OF CALCIFICATION	cementum	ossicles	psammomatous
BONY TRABECULAE	mature (periphery of the lesion)	immature (direct ossification of cells)	osteoid seams with superimposed calcification
ABC LIKE AREAS	2 cases (11.7%)	2 cases (12.5%)	7 cases (46.6%)
ABNORMAL BLOOD VESSELS	not seen	4 cases (25%)	10 cases (66.6%)
MITOSIS	occasional	occasional	0-2/10hpf
NECROSIS	not seen	not seen	not seen
RECURRENCE	none	none	3 cases (20%)

Conclusions: COF, JTOF, and JPOF are clinically, radiologically and histologically distinct entities. Abnormal thick walled venous channels lacking a muscular wall were seen in ossifying fibromas of bony origin. JPOF has higher incidence of recurrence as compared to JTOF and COF, and hence need a more aggressive follow up.

1351 Analysis and Comparison of the 8th Edition American Joint Committee on Cancer (AJCC) Nodal Staging System in Cutaneous and Oral Squamous Cell Cancer of the Head and Neck

Nikolaus Moeckelmann¹, Richard Dirven¹, Jessica Liu², Ardan Ebrahimi³, Tsu-Hui (Hubert) Low³, Bruce G Ashford³, Sydney Ch'ng³, Carsten E Palme³, Ruta Gupta⁴, Jonathan Clark³. ¹Chris O'Brien Lifehouse, ²Royal Prince Alfred Hospital, Camperdown, NSW, ³Chris O'Brien Lifehouse, ⁴Royal Prince Alfred Hospital, Sydney, NSW

Background: The American Joint Committee on Cancer (AJCC) uses the same nodal staging system for cutaneous and mucosal squamous cell carcinoma of the head and neck in its 8th edition (AJCC 8) despite differences in the etiology, risk factors and clinical behavior of squamous cell carcinoma from these sites. This study aims to evaluate and compare the performance of the AJCC 8 nodal staging system in cutaneous squamous cell carcinoma (cSCC) and oral cavity squamous cell carcinoma (oSCC).

Design: Patients with metastatic cSCC (N=382) and oSCC (N=325) were identified from a prospective head and neck cancer-center database (year 1987-2016). Multivariable analysis was performed using Cox proportional hazards competing risk model adjusting for the effect of adjuvant radiotherapy. To assess staging system performance an explained variation measure (Proportion of explained variation, PVE) as well as a discrimination measure (Harrell's concordance index, C-index) were used.

Results: The inclusion of extranodal extension (ENE) in AJCC 8 has increased the proportion of patients in the N3b category (48.7% in cSCC, 40.3% in oSCC). AJCC 8 stratifies poorly with regards to risk of death from cSCC and oSCC and shows limited monotonicity of the nodal categories. The estimates for model performance reveal modest predictive capacity of AJCC 8 for overall survival (OS) and disease specific survival (DSS) in oSCC (Harrell's C of 0.67 and 0.66, respectively) and weak predictive capacity in cSCC (Harrell's C of 0.58 and 0.61, respectively).

Conclusions: The AJCC 8 nodal staging system performs poorly in terms of stratifying survival by N category in cSCC. Whilst ENE is an important prognostic factor, further modelling is needed to determine how best to include it in staging. The data indicate that cSCC merits an independent nodal staging system that takes its biology and anatomy of its nodal basin into consideration.

1353 Spindle Epithelial Tumor with Thymus-like Differentiation (SETTLE): A Next-generation Sequencing (NGS) Study

Diana Morlote¹, Zoran Gatalica², Jeffrey Swensen³, Michelle Ellis⁴, Carlos Prieto-Granada⁵, Shuko Harada⁶, Andrew Folpe⁷, Todd M Stevens⁸. ¹University of Alabama at Birmingham, ²Caris Life Sciences, Phoenix, AZ, ³Caris Life Sciences, Phoenix, AZ, ⁴Caris Life Sciences, Phoenix, AZ, ⁵University of Alabama at Birmingham, Birmingham, AL, ⁶Univ. of Alabama at Birmingham, Birmingham, AL, ⁷Mayo Clinic, Rochester, MN

Disclosures:

Jeffrey Swensen: *Employee, Caris Life Sciences*

Background: SETTLE is an extremely rare, histologically distinctive, biphasic malignant tumor of the thyroid or neck, which typically occurs in young patients and has a propensity for late metastasis. The molecular pathogenesis of SETTLE has not been studied in depth, although it is known that they lack synovial sarcoma-associated molecular events, and a single example with a *KRAS* mutation has been reported. We studied a series of well-characterized SETTLEs by NGS with the goals of identifying specific genetic events and/or "actionable" mutations.

Design: Five morphologically and immunohistochemically typical cases of SETTLE (Figure, for representative images) underwent direct sequence analysis of 592 genes performed on genomic DNA isolated from FFPE tumor samples using the Illumina NextSeq platform. Fusion gene analysis of 52 genes commonly fused in tumors was performed on mRNA isolated from FFPE tumor samples using the Archer FusionPlex Solid Tumor Panel and the Illumina MiSeq (Caris Life Sciences). Cases 1, 4 and 5 were tested for *SS18* alteration by either break-apart FISH or RT-PCR.

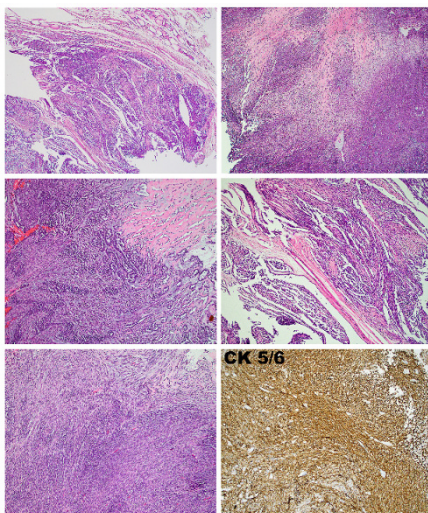
Results: Four pathogenic mutations were detected across 2 cases (Table 1). Case 1 had two pathogenic mutations in *KMT2D*, one an intron splice site mutation c.674-1A>G and the other a frameshift variant, p.M2829fs. Case 1 also had a pathogenic missense variant in the *KMT2C* gene, p.R1237X. Case 2 had a pathogenic *NRAS* mutation, p.Q61R variant.

No gene fusions, DNA microsatellite instability, or gene amplifications were detected. Cases 1, 4 and 5 were negative for *SS18* rearrangement.

Table 1. Summary of next-generation sequencing results of 5 cases of SETTLE.

ND: none detected

Case	Age	Sex	Location	Pathogenic genetic alterations
1	20	M	Mediastinum	KMT2D (c.674-1A>G & p.M2829fs), KMT2C (p.R1237X)
2	73	F	Neck	NRAS (p.Q61R)
3	40	M	Neck	ND
4	49	F	Thyroid	ND
5	10	F	Thyroid	ND



Conclusions: We did not identify disease-specific genomic events or "actionable" molecular targets in 5 cases of well-defined SETTLE. The study confirmed that SETTLE lacks *SS18* and *RET* alterations, which is

a useful distinction from synovial sarcoma and the spindle cell variant of medullary carcinoma, respectively.

1354 Beta-Catenin Expression and a CTNNB1 Mutation in Basal Cell Adenoma and Basal Cell Adenocarcinoma

Masato Nakaguro¹, Makoto Urano², Toshitaka Nagao³. ¹Nagoya University Graduate School of Medicine, Nagoya city, Aichi pref., ²Fujita Health University, Toyoake-shi, Aichi, Japan, ³Tokyo Medical University, Tokyo

Background: Basal cell adenoma (BCA) is a benign salivary gland tumor composed of luminal and basaloid epithelial components. Recent studies of BCA tumors detected expression of beta-catenin by immunohistochemistry and a *CTNNB1* (beta-catenin encoding gene) exon 3 mutation. Basal cell adenocarcinoma (BCAC) is considered the malignant counterpart of BCA. BCAC shows cytological or architectural findings similar to BCA and extracapsular invasion. However, expression of beta-catenin and *CTNNB1* mutations have not yet been studied well in BCAC.

Design: 16 BCA and 15 BCAC cases were retrieved from institution cases and consultation files. Pathological diagnoses were reconfirmed by three authors using morphological analysis. Beta-catenin immunohistochemistry and direct DNA sequencing of *CTNNB1* exon3 were performed.

Results: To confirm pathological diagnosis of BCAC, the following morphologies were observed: invasion to surrounding tissue (14 cases, 93.3%), lymphovascular invasion (4 cases, 26.7%), and an increase in mitosis and remarkable nuclear atypia (9 cases, 60%). Immunohistochemistry showed nuclear expression of beta-catenin in 13 (81.3) and 12 (80%) cases of BCA and BCAC, respectively. The point mutation, p.I35T (c.104T>C), in exon 3 of *CTNNB1* was detected in 6 (37.5%) and 7 (46.7%) cases of BCA and BCAC, respectively. No other mutations in *CTNNB1* were detected. The ratio of samples positive for beta-catenin expression or *CTNNB1* exon 3 mutation was not significantly different between BCAs and BCACs (p=1.00, 0.72, respectively). In BCAs, solid type and cribriform type (4/5 cases) showed significantly higher positive ratio of *CTNNB1* exon 3 mutation than tubular type and trabecular type (2/11 cases, p=0.035).

Conclusions: The ratio of BCAC and BCA cases expressing beta-catenin or containing a *CTNNB1* exon 3 mutation is not significantly different. These data could suggest that BCAC and BCA share a common tumorigenesis pathway or that BCAC may arise from BCA.

1355 HPV and EGFR Mutation in Schneiderian Papillomas and Related SCC: Who Plays the Games?

Giorgia Ottini¹, Carla Facco¹, Nora Sahnane¹, Anna Maria Chiaravalli¹, Roberta Cerutti¹, Mario Turri-Zanon², Apostolos Karligkiotis¹, Chiara Albeni¹, Lucio Lettig¹, Paolo Castelnovo¹, Daniela Furlan¹, Silvia Uccella³, Fausto Sessa¹. ¹University of Insubria, Varese, Italy, ²ASST Sette Laghi, Varese, Italy, ³University of Insubria, Varese, Italy, ³Varese

Background: Inverted sinonasal papilloma (ISP) is a distinctive neoplasm arising from sinonasal epithelium. Although considered benign, these tumors show unlimited potential for growth, local invasion and destruction of contiguous structures. In addition, approximately 10% to 25% of patients with ISP present a synchronous or metachronous sinonasal squamous cell carcinoma (SCC). In literature, HPV infection is closely associated with recurrence and progression of ISP.

The aim of this study was to investigate the etiopathogenetic role of high risk and low risk HPV genotypes in a well characterized series of ISP, *de novo* SCC and ISP-associated SCC. In addition, EGFR mutation was investigated, as well as p16 and p53 immunohistochemical expression.

Design: 54 cases, including 29 ISPs, 15 ISP-associated SCCs and 10 *de novo* SCCs of the sinonasal region, were analyzed for high risk (HR) and low risk (LR) HPV infection by in situ hybridization (ISH, Ventana). In addition, EGFR mutations, namely exon 20 insertions and complex mutations in exon 19, were investigated using Myriapod® Lung Status kit (Diatech) by mass-spectrometry. p16 and p53 immunohistochemical expression was assessed using specific antibodies.

Results: The male-to-female prevalence was 4:1, with a median age of 62 years at presentation, in all the three lesions studied. EGFR mutations were present in 25% of ISPs and in both components of 80% ISP-associated SCCs. By contrast, no EGFR mutation was detected in *de novo* SCCs. HR-HPV was not detected in any cases, while LR-HPV was observed in 24% of ISPs, 6% of ISP-associated SCCs and in none of SCCs. p16 was positive in 44% of ISPs, 4 of which were also LR-HPV positive, 6% of ISP-associated SCCs and 10% of SCCs. p53 was expressed in 3.44% of ISPs, 6% of ISP-associated SCCs and 40% of SCCs.

Conclusions: Our results suggest that:

- HPV infection is not a driving event in the etiopathogenesis of ISP and SCC and, despite LR-HPV has been found in 24% of ISP, it doesn't seem to be correlated with the malignant progression to SCC. Importantly, p16 expression is not a surrogate marker of HPV infection in the sinonasal region as it is in oropharyngeal cancer.
- EGFR exon 20 mutations seems to have a pivotal role in the pathogenesis of ISP and ISP-associated SCC.
- Finally, even if ISP has always been considered as a benign lesion by literature, our molecular results show that it should be considered a preneoplastic lesion and treated as such.

1356 NKX3.1 Expression in Salivary Gland Neoplasms (a Potential Diagnostic Pitfall)

Irina Perjar¹, Sara E. Wobker², Kevin G Greene³, Sherry Tang².
¹UNC Hospitals, Chapel Hill, NC, ²UNC Chapel Hill, Chapel Hill, NC, ³University of North Carolina School of Medicine, Durham, NC

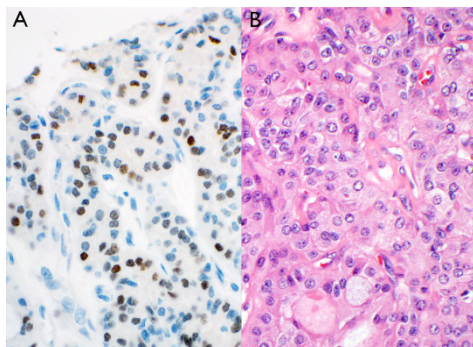
Background: NKX3.1 is an androgen-regulated, homeobox-containing transcription factor that functions as a negative regulator of epithelial cell growth in prostatic tissue. Nuclear expression of NKX3.1 by IHC is considered to be highly sensitive and specific for prostatic differentiation. Clinically, NKX3.1 IHC is a valuable tool for recognizing prostatic adenocarcinoma at metastatic sites. NKX3.1 expression has also been observed in non-neoplastic mucinous epithelium of minor salivary glands. Furthermore, targeted disruption of the *NKX3-1* gene has led to morphogenetic defects in minor salivary glands in mice. Androgen receptor expression by IHC has also been demonstrated in salivary gland neoplasms. Despite these observations, a 2010 study showed an absence of NKX3.1 expression in a variety of salivary gland neoplasms. The purpose of this study is to evaluate for NKX3.1 expression in five subtypes of salivary gland neoplasms using contemporary IHC methods.

Design: Two tissue microarrays (TMA) are created that contain eight unique examples of the following neoplasms: salivary duct carcinoma (SDC), mucoepidermoid carcinoma (MEC), adenoid cystic carcinoma (ACC), and polymorphous low-grade adenocarcinoma (PLGA). IHC for NKX3.1 (Biocare, predilute, Leica BOND III) is performed on the TMAs and on whole sections from two unique mammary analogue secretory carcinomas (MASC). Nuclear expression in neoplastic cells is scored as 0 (absent), 1+ (weak), 2+ (moderate), and 3+ (strong), and the percentage of positive cells is noted.

Results: Please refer to Table 1 for a summary of the staining results.

Figure 1: Mucoepidermoid carcinoma. A, NKX3.1 IHC. B, H&E stain.

Table 1	SDC	MEC	ACC	PLGA	MASC
Number of cases with NKX3.1 expression	4 of 8	3 of 8	1 of 8	3 of 8	2 of 2
Range of expression in positive cases	1+(1%) to 2+(5%)	2+(1%) to 2+(30%)	1+(1%)	1+(1%) to 2+(5%)	1+(5%) to 2+(10%)



Conclusions: In our study, at least focal NKX3.1 expression is present in each of the tumor subtypes tested. The intensity of staining in salivary gland neoplasms tends to be weaker than in non-neoplastic epithelium, which is similarly observed in prostatic tissue. Unlike in prostatic adenocarcinoma, where expression is usually diffuse, salivary gland neoplasms demonstrate patchy staining. In our series, the greatest expression is seen in a case of MEC (2+ staining in 30% of neoplastic cells). We believe that in a limited biopsy, or cell block FNA, a metastatic salivary gland neoplasm could be mistaken for metastatic prostatic adenocarcinoma based on positive NKX3.1 staining. A larger study to also include other tumor subtypes (e.g., carcinoma

ex-pleomorphic adenoma) would be useful to further define NKX3.1 expression in salivary gland neoplasms.

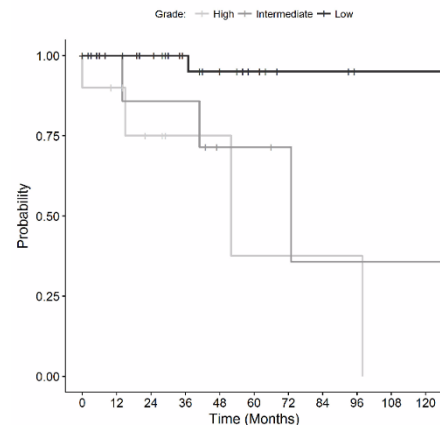
1357 Formal Histologic Grading Provides Accurate Risk Stratification in Acinic Cell Carcinoma

Lisa Rooper¹, William Westra², David W Eisele³. ¹Johns Hopkins Hospital, Baltimore, MD, ²Johns Hopkins, Baltimore, MD, ³Johns Hopkins University

Background: In the absence of overt high grade transformation, acinic cell carcinoma (AcicC) is regarded by definition as a low grade salivary gland malignancy. However, a subset of apparently well-differentiated AcicC still develop recurrence or metastases. While older studies cast doubt on the prognostic value of histologic features in AcicC, more recent literature suggests that grading correlates with progressive disease. However, this issue has not been extensively evaluated since the exclusion of secretory carcinomas from the AcicC category. This study aims to assess the prognostic value of a formal histologic grading system in a strictly-defined cohort of AcicC.

Design: All cases of primary AcicC diagnosed between July 1985 and June 2017 were identified from the surgical pathology archives of a large academic medical center. All available histologic sections were reviewed for each case, and the diagnosis of AcicC was confirmed based on the presence of unequivocal serous acinar differentiation. Tumors were evaluated for the presence of ≥ 4 mitoses/10 high-power fields (HPF), infiltrative borders, necrosis, and nuclear pleomorphism. Tumors with 0-1 of these features were defined as low grade, 2 as intermediate grade, and 3-4 as high grade. Disease-free survival was estimated using Kaplan-Meier analysis.

Results: Based on the proposed grading criteria, 40 AcicC (67%) were classified as low grade, 10 (17%) as intermediate grade, and 10 (17%) as high grade. Of these, 1 low grade (3%), 4 intermediate grade (40%) and 4 high grade (40%) tumors developed recurrence or metastasis over follow-up intervals of 0-330 months (median 32 months). Likelihood of progressive disease was significantly associated with histologic grade ($p < 0.001$). The estimated 5-year disease-free survival was 95% for low grade, 71% for intermediate grade, and 38% for high grade AcicC (Figure 1).



Conclusions: Histologic grading using a mitotic rate $\geq 4/10$ HPF, infiltrative growth, necrosis, and nuclear pleomorphism highlights a subset of AcicC that harbor a significantly higher likelihood of recurrence or metastases. Close attention to mitotic rate and infiltrative growth in particular helps identify those otherwise well-differentiated AcicC that develop progressive disease in the absence of other conventional risk factors. Although formal histologic grading does not account for all variability in outcomes, routine use of this proposed grading system has the potential to provide valuable additional prognostic information in AcicC.

1358 Adamantinoma-Like Ewing Sarcoma of the Salivary Glands

Lisa Rooper¹, Vickie Y Jo², Cristina R Antonescu³, Vania Nosé⁴, William Westra⁵, Brandon R Swartz⁶, Raja Seethala⁷, Justin Bishop⁸. ¹Johns Hopkins Hospital, Baltimore, MD, ²Brigham & Women's Hospital, Boston, MA, ³Memorial Sloan Kettering Cancer Center, New York, NY, ⁴Boston, MA, ⁵Johns Hopkins, Baltimore, MD, ⁶UT Southwestern Medical Center, Dallas, TX, ⁷University of Pittsburgh School of Medicine, Pittsburgh, PA

Background: Ewing sarcoma (ES) is a round cell sarcoma typically seen in young patients and characterized by *EWSR1-FLI1* fusions. Adamantinoma-like ES (ALES) is a newly described variant that aberrantly exhibits squamous epithelial differentiation, resulting in

diagnostic confusion. We report 9 cases arising in the salivary glands.

Design: Cases of salivary gland ALES were pulled from the authors' files. Immunohistochemistry (IHC) was performed along with molecular studies for *EWSR1-FLI1* fusions.

Results: Nine cases of ALES of salivary glands were found. Seven arose in the parotid and 2 in the submandibular gland. ALES presented as face/neck masses in 5 men and 4 women ranging from 32-77 yrs (mean 52). Original diagnoses included poorly differentiated carcinoma (n=4), basal cell adenoma/adenocarcinoma (n=2), and high-grade neuroendocrine carcinoma (n=1). Histologically, ALES consisted of highly permeative lobules of basaloid cells separated by prominent bands of fibrosis. Mitotic rates were high and necrosis was common, but tumor cells were highly monotonous. Rosette-like structures were seen in most tumors; keratinization was present in only 1 case. By IHC, ALES showed consistent positivity for membranous CD99 (9/9), NKX2.2 (7/7), pancytokeratin (9/9), and p40 (9/9). Positivity for synaptophysin (7/9) was common with focal chromogranin in 2/9. S100, actin, desmin, and NUT were negative. All cases were confirmed to harbor *EWSR1-FLI1* fusions. Treatment information was available for 5, all of whom were treated with surgery and chemoradiation. For 2, chemotherapy protocols were altered after a revised diagnosis of ALES. With limited follow-up (0-18 months, mean 5), 7 patients were alive without disease, 1 alive with persistent disease, and 1 died as a complication of treatment.

Conclusions: ALES is a rare variant of ES that may unexpectedly arise in the salivary glands, where it is highly susceptible to misclassification as carcinoma due to strong positivity for cytokeratin/p40 and a propensity to affect adults. When compared to ALES elsewhere, salivary ALES is more often positive for synaptophysin and less likely to show keratinization, further confounding the correct diagnosis crucial to guiding appropriate therapy. ALES should be considered for any salivary tumor with a basaloid appearance and high-grade histologic features. Diffuse positivity for p40 with synaptophysin staining is a useful clue. IHC for CD99 and NKX2.2 is a helpful screen, and molecular testing for *EWSR1-FLI1* is confirmatory.

1359 Most Salivary Adenocarcinomas, Not Otherwise Specified, can be Reclassified Using Current Morphologic, Immunohistochemical, and Molecular Criteria

Lisa Rooper¹, William Westra². ¹Johns Hopkins Hospital, Baltimore, MD, ²Johns Hopkins, Baltimore, MD

Background: Salivary gland adenocarcinomas that do not fit a specific histological category are classified as not otherwise specified (ACA-NOS). While these tumors historically comprised the second most common salivary malignancy, this diagnosis has been used less frequently as new entities have been defined. Although this shift suggests that ACA-NOS is a heterogeneous group, there is still a tendency to regard it as a discrete biologic entity. This study aims to re-evaluate all cases previously classified as ACA-NOS using current diagnostic criteria and ancillary techniques to better ascertain the true prevalence and nature of this diagnosis.

Design: All cases of salivary ACA-NOS diagnosed between 1986 and 2017 in routine (non-consultation) resection specimens at a large academic medical center were identified, and available histologic sections were reviewed. Immunohistochemistry for androgen receptor, S100, mammaglobin, p63, p40, SOX10, SMA, c-kit, and DOG1 and fluorescence in-situ hybridization for ETV6 and EWS rearrangements was performed. Tumors were reclassified according to 2017 World Health Organization guidelines if morphology and ancillary testing supported a concordant diagnosis.

Results: The 74 ACA-NOS comprised 12% of all salivary malignancies during the study period, ranging from 21% in 1986-90 to 6% in 2010-present. 52 (70%) could be reclassified, including 29 salivary duct carcinomas (39%), 7 epithelial-myoepithelial carcinomas (9%), 6 polymorphous adenocarcinomas (8%), 5 myoepithelial carcinomas (7%), 3 secretory carcinomas (4%), 1 clear cell carcinoma (1%), and 1 squamous carcinoma (1%). Notably, 15 (29%) such cases represented variant histologies within these categories. The remaining 22 ACA-NOS included a morphologically and immunohistochemically diverse spectrum of 10 high-grade, 9 intermediate-grade, and 3 low-grade neoplasms comprising 4% of salivary malignancies.

Conclusions: Most tumors historically classified as salivary ACA-NOS can be assigned to a more specific category using current diagnostic criteria and ancillary tests, potentially facilitating more precise prognostication and treatment. These findings not only demonstrate that rigorous morphologic, immunohistochemical, and molecular analysis should be considered before diagnosing ACA-NOS, but also highlight the value of such techniques in salivary tumor diagnosis. Remaining ACA-NOS are much less common than previously reported and comprise a heterogeneous group without uniform biological characteristics.

1360 EGFR Mutations in Sinonasal Squamous Cell Carcinoma

Eiichi Sasaki¹, Yasushi Yatabe¹. ¹Aichi Cancer Center Hospital, Nagoya, Aichi, Japan

Background: Recently, inverted sinonasal papilloma (ISP) and its associated sinonasal squamous cell carcinoma (SNSCC) have been reported to show frequent EGFR mutations. The aim of this study is to clarify the spectrum of EGFR mutations in head and neck cancer and papilloma.

Design: Genetic analysis of hot spot mutations (exon 19 deletion, exon 20 insertion and L858R point mutations) in the EGFR gene was conducted for 281 head and neck squamous cell carcinomas that were enriched for SNSCC (n=73). Additionally, we analyzed 56 head and neck papillomas or polyps.

Results: The results are shown in Table 1. In ISP-associated SNSCC cases, the genotypes were concordant between ISP and associated SNSCC.

Histology		n	EGFR mutations	
Squamous cell carcinoma				
	Sinonasal	Inverted papilloma-associated	15	87% (13/15)
		Non-inverted papilloma associated	58	14% (8/58)
	Non-sinonasal		208	0
Papilloma or polyp				
	Sinonasal	Inverted papilloma	19	89% (17/19)
		Oncocytic papilloma	4	0
		Exophytic papilloma	2	0
		Nasal polyp	7	0
	Non-sinonasal	Squamous cell papilloma	24	0

Conclusions: We identified EGFR mutations in SNSCC (29%, 21/73) and ISP (89%, 17/19). Although EGFR mutations were detected in a subset of SNSCC cases without any papilloma component, the detection of EGFR mutations suggest an association with an ISP in terms of their origin.

1361 Molecular Pathways Involved in Epithelial-myoepithelial Carcinomas and Myoepithelial Carcinomas. Implication of the HRAS Activating Mutations and Identification of Different Tumor Profiles

Marion Schmitt-Boulanger¹, Jerome Cros², Marion Mandavi³, Marie Thriller⁴, Emmanuelle Uro-Coste⁵, Bertrand BAUJAT⁶, H el ene Blons⁷, Cecile Badoua⁸. ¹H opital Europ een Georges Pompidou, APHP, Paris, France, ²H opital Beaujon, APHP, Paris, France, ³INSERM, Paris, France, ⁴H opital St Joseph, Paris, France, ⁵Toulouse University Hospital, Toulouse, France, ⁶Hopital Tenon, APHP, Paris VI University, Paris, France, ⁷H opital Europ een Georges Pompidou, Paris, France, ⁸G Pompidou Hospital, Paris, France

Background: Few data are available about the molecular description of salivary glands carcinomas. In a first study we have shown that some rare mutations (KRAS, PI3K, CKIT...) could be found in some specific histological subtypes. Epithelial-myoepithelial carcinomas (EMC) and myoepithelial carcinomas (MC) seemed to be particularly concerned. The aim of this study was to address the molecular pathways involved in EMC and MC carcinogenesis

Design: The French head and neck cancer database REFCOR was queried for 59 cases of EMC and MC. Expression of p63, Ki-67, cKIT, PD-L1 and PD-L2 was assessed by immunohistochemistry and computer-assisted quantification. The presence of mutations in a panel of key cancer genes was assessed by next generation sequencing using the Ion AmpliSeq™ Cancer Hotspot Panel v2 panel from ThermoFisher scientific. Expression levels of 2559 genes were assessed with the HTG EdgeSeq Oncology Biomarker Panel.

Results: 42 EMC (21 males, 62.2 y.o (+/-16.5)) and 17 CM (12 males, 48.6y.o (+/-22.2)) cases were collected. Tumors were mostly located in the parotid gland (47 cases, 79.7%). 16 EMC (38.1%) and 5 CM (29.4) showed histological signs of dedifferentiation or aggressiveness. c-KIT and p63 expression was significantly higher in EMC than CM but Ki-67 index was similar in both tumor types. *HRAS* activating mutation was the most prevalent alteration (22 cases) and was significantly more frequent in EMC (20/22; 47.6%). *HRAS* mutation was not associated with the dedifferentiation pattern but was associated with a significantly higher index of proliferation, especially in EMC (3.4 vs 8.9%; *p*=0.04). *PI3K* mutation was the second most frequent

event (7 cases, 6 EMC) and always co-occurred with *HRAS* mutations. Unsupervised transcriptomic analysis revealed 3 clusters of EMC: one with a high prevalence of *HRAS* mutation (10/13) and an infrequent aspect of dedifferentiation or aggressiveness and one with a low prevalence of *HRAS* mutation (0/6) and frequent dedifferentiation. The remaining cluster was heterogeneous and may be related to a more important stromal compartment. Gene Set Enrichment Analysis showed that *HRAS* mutated EMC had increased proliferation and mTOR-related gene signatures.

Conclusions: EMC and MC are distinct entities at the molecular level. *HRAS* activating mutations, present in half of EMC, seem to define a subtype with increased proliferative capability.

1362 Consistent LEF-1 Expression in Human Papillomavirus-related Multiphenotypic Sinonasal Carcinoma: a Potential Diagnostic Pitfall

Akeesha A Shah¹, Bahram Olia², Justin Bishop³. ¹Cleveland Clinic, Cleveland, OH, ²ProPath, Dallas, TX, ³UT Southwestern Medical Center, Dallas, TX

Background: Human papillomavirus-related multiphenotypic sinonasal carcinoma (HMSC), previously referred to as HPV-related carcinoma with adenoid cystic carcinoma-like features, is a newly-described sinonasal neoplasm that demonstrates a prominent basaloid morphology. While HMSC is commonly associated with squamous dysplasia and thus is presumably surface-derived, it exhibits histologic and immunophenotypic features of a salivary gland carcinoma including a biphasic pattern of ducts and myoepithelial cells. Lymphoid enhancer binding factor 1 (LEF-1), a nuclear transcription factor, is a downstream mediator of the Wnt/ β -catenin signaling pathway, but it can also modulate gene transcription independently. Limited data has suggested that among salivary gland tumors, LEF-1 expression is relatively specific for basal cell adenoma and basal cell adenocarcinoma. Here we examine the immunohistochemical expression of LEF-1 and β -catenin in HMSC.

Design: Seven HMSCs were retrieved from our case files. Immunohistochemistry for LEF-1 and β -catenin was performed on formalin-fixed paraffin embedded tissue. Nuclear staining was recorded in both the surface derived and salivary gland components. Positivity was defined as strong nuclear staining in greater than 50% of tumor cells.

Results: All HMSCs exhibited a prominent basaloid morphology, with evidence of myoepithelial and ductal differentiation along with surface squamous dysplasia. Each HMSC (7 of 7) exhibited diffuse and strong LEF-1 immunostaining in both ducts and myoepithelial cells. The surface dysplasia component was negative. All tumors lacked nuclear expression of β -catenin in all tumor components (0 of 7 positive).

Conclusions: Although a small cohort, our preliminary data demonstrates that HMSC consistently expresses LEF-1 in a strong and diffuse manner independent of β -catenin, which consistently lacks nuclear labeling in HMSC. LEF-1 positivity may be a useful diagnostic adjunct when considering HMSC. However, it may also be a pitfall, because LEF-1 expression is common in basal cell adenocarcinoma, a tumor with features that overlap with HMSC.

1363 Accuracy of Tumor-specific Cytologic Classification of Malignant Salivary Gland Aspirates: A Cyto-histologic and Clinical Correlation Study

Yesha P Sheth¹, Kamal Khurana². ¹SUNY Upstate Medical University, ²SUNY Health Science Center, Syracuse, NY

Background: Fine needle aspiration (FNA) cytology of salivary glands plays a critical role in preoperative diagnosis of lesions. Although the FNA of salivary gland is highly accurate in identifying a malignant neoplasm, the correlation between the specific malignant diagnosis on FNA and the final outcome remains to be determined. The aim of the study was to determine the accuracy of classification of cases diagnosed as malignant on FNA of salivary glands by comparing it with surgical/clinical follow up.

Design: A computerized search was performed for "malignant" salivary gland aspirates between May 1994 and June 2017. Only cases with available histologic follow up or clinical follow up were reviewed. Accuracy of malignant diagnosis and specific type of malignancy was determined by comparing the cytologic diagnosis to final outcome.

Results: Of the 1,065 salivary gland aspirates, 107 cases (10.1%) were diagnosed as malignant. Follow up available on 88 (82.2%) of the 107 cases correlated with initial cytologic diagnosis of "malignancy". Specific salivary gland sites included the parotid glands (49 cases) and submandibular glands (39 cases). Based on surgical or clinical follow up, 44 cases were primary salivary gland neoplasms (50%) and 44 were metastatic (50%). Table 1 shows the concordance rate between the tumor-specific cytologic diagnosis of malignant neoplasms and surgical/clinical follow up. Overall concordance rate

for tumor specific cytologic classification of primary and metastatic malignant neoplasms involving salivary gland was 81.8% and 100%, respectively. Discordant classification (17.2%) was noted in cases of poorly differentiated carcinoma and was attributable to heterogeneity of morphologic patterns and lack of adequate cell block material.

Cytologic Diagnosis (n=88)	Final Diagnosis (n=88)	Concordance (%)
Metastatic squamous cell carcinoma (37 cases)	Metastatic squamous cell carcinoma (37 cases)	100%
Metastatic adenocarcinoma (2 cases)	Metastatic adenocarcinoma (2 cases)	100%
Metastatic thyroid carcinoma (2 cases)	Metastatic thyroid carcinoma (2 cases)	100%
Metastatic small cell carcinoma (1 case)	Metastatic small cell carcinoma (1 case)	100%
Metastatic melanoma (2 cases)	Metastatic melanoma (2 cases)	100%
Lymphoma (21 cases)	Lymphoma (21 cases)	100%
Poorly differentiated carcinoma (10 cases)	Poorly differentiated carcinoma (2 cases) Salivary duct carcinoma (2 cases) Squamous cell carcinoma (2 cases) Undifferentiated lymphoepithelial carcinoma (2 cases) Mucoepidermoid carcinoma (1 case) Metastatic melanoma (1 case)	20%
Acinic cell carcinoma (8 cases)	Acinic cell carcinoma (8 cases)	100%
Mucoepidermoid carcinoma (3 cases)	Mucoepidermoid carcinoma (3 cases)	100%
Basal cell adenocarcinoma (1 case)	Basal cell adenocarcinoma (1 case)	100%
Carcinoma Ex-pleomorphic adenoma (1 case)	Carcinoma Ex-pleomorphic adenoma (1 case)	100%

Conclusions: Tumor specific characterization of malignant aspirates of salivary gland is highly accurate to allow clinicians to plan definitive management in majority of cases. Poorly differentiated carcinomas may be difficult to classify requiring additional histologic examination for tumor type-specific characterization.

1364 Hyalinizing Clear Cell Carcinoma of Head and Neck: Histologic, Immunophenotypic and Genetic Characterization and its Differentiation from other Clear Cell Mimics

Namita Sinha¹, Samir El-Mofty². ¹Washington University in St. Louis, St. Louis, MO, ²Washington University School of Medicine, Saint Louis, MO

Background: Hyalinizing clear cell carcinoma (HCCC) is an uncommon carcinoma that usually involves salivary glands of the head and neck. Similar tumor in the jaw bones is called clear cell odontogenic carcinoma (CCOC). These tumors usually have indolent course and are usually treated by surgery. On the other hand, other clear cell neoplasms of head and neck origin or metastatic tumor with clear cell features (clear cell squamous cell carcinoma, mucoepidermoid carcinoma, myoepithelial carcinoma, calcifying epithelial odontogenic carcinoma, renal cell carcinoma [Rcc], Ewing's sarcoma and chordoma) have aggressive course that commonly recur or metastasize and therefore, require aggressive management. EWSR1-ATF1 fusion has been found to be consistent finding in HCCC and CCOC. However, EWSR1 rearrangement is not always specific and can be seen in other tumors including Ewings sarcoma. Complete immunophenotypic characterization of the tumor is therefore necessary to differentiate HCCC and CCOC from other clear cell neoplasms.

Design: We performed a retrospective study of 10 patients with a diagnosis of HCCC or CCOC, which was confirmed by EWSR1 rearrangement and analyzed their immunohistochemical profiles in order to differentiate them from other clear cell neoplasms.

Results: HCCC and CCOC occurred in 6 male and 4 female patients (age range 4 to 81 years) and originated in the oral cavity (6), sinonasal mucosa (2), maxilla (1) and mandible (1). The tumors expressed pancytokeratin (9/9, 100%), CK7 (5/6, 83%), HMWK (3/3 100%), P63 (8/8, 100%), CD10 (3/7 43%, 1 diffuse, 2 focal and strong), CAIX (3/7, 43%, 1 diffuse, 2 focal and strong). Ki-67-labeling index ranged from <5% to 20%. All tested tumors were negative for CK20, synaptophysin, RC, PAX8, S100, brachyury and SMA.

Conclusions: HCCC and CCOC can be differentiated from clear cell mimics based on their EWSR1 rearrangement in addition to immunoreactivity for pancytokeratin, CK7, HMWK, P63 and lack for expression of CK20, synaptophysin, RCC, PAX8, S100, brachyury, and SMA. It is of importance to point out that HCCC and CCOC may be focally or diffusely positive for CAIX and CD10 but are negative for

RCC and PAX8 as opposed to clear cell Rcc which are usually positive for CAIX, CD10, RCC and PAX8. EWSR1 rearrangement in HCCC and lack of MAML2 rearrangement differentiate them from the clear cell variant of mucoepidermoid carcinoma.

1365 Molecular Profiling of Intraductal Carcinoma of Parotid Gland Revealed a Subset of Tumors Harboring a NCOA4-RET and a Novel TRIM-RET Fusions: Report of 3 Cases

Alena Skalova¹, Jan Laco², Emmanuelle Uro-Coste³, Petr Martinek⁴, Lester D Thompson⁵, Cecile Badoua⁶, Thalita Santana⁷, Marketa Miesbauerova⁸, Tomas Vanecek⁹, Michal Michal¹⁰. ¹Charles University, Faculty of Medicine in Plzen, Plzen, Czech, ²Charles University and University Hospital Hradec Kralove, Czech Republic, ³Toulouse University Hospital, Toulouse, France, ⁴Bioptical Laboratory, Pilsen, Czech Republic, ⁵Southern California Permanente Medical Group, Woodland Hills, CA, ⁶G Pompidou Hospital, Paris, ⁷University of São Paulo, São Paulo, Brazil, ⁸Charles University, Faculty of Medicine in Plzen, Plzen, Czech Republic and Bioptical Laboratory, Ltd., Plzen, Czech Republic, ⁹Bioptical Laboratory, Pilsen, Czech Republic, ¹⁰Bioptical Laboratory, Plzen

Background: Intraductal carcinoma (IC) is the new WHO designation for tumors previously called low grade cribriform cystadenocarcinoma. The relationship of IC to salivary duct carcinoma (SDC) is controversial, but they are considered to be distinct entities. IC is rare low grade malignant salivary gland neoplasm with features similar to mammary atypical ductal hyperplasia or ductal carcinoma in-situ, that shows diffuse S100 protein and mammaglobin positivity and is genetically largely undefined. Secretory carcinoma (mammary analogue) (SC) harboring *ETV6-NTRK*, and in rare cases a novel *ETV6-RET* fusion, shares histomorphology and immunoprofile with IC. Here, we used genetic analysis to examine the differences between the two morphologically close tumor entities.

Design: 13 cases of IC were analyzed by NGS using the Fusion Plex Solid Tumor kit (ArcherDX). Identified fusions were confirmed using FISH break apart probe of *RET* gene and a RT-PCR designed specifically to the detected breakpoints. All cases were originally tested for *ETV6* breakapart by FISH and for common *ETV6-NTRK3* fusions using RT-PCR.

Results: NGS analysis detected a *NCOA4-RET* fusion transcript joining exon 6 and 7 of *NCOA4* gene and exon 12 of *RET* gene in 2 cases and a novel *TRIM27-RET* fusion transcript between exons 3 and 12 in one case of salivary gland tumors displaying histological and immunohistochemical features typical of IC. All three cases were negative for *ETV6-NTRK3* gene fusion by the Fusion Plex kit, RT-PCR, and *ETV6* gene was found intact by FISH.

Conclusions: A novel finding in our study has been a discovery of a subset of IC patients with *NCOA4-RET* and *TRIM27-RET* fusions who may benefit from *RET*-targeted therapy.

The study was in part supported by the grant of Charles University (SVV 2017- 260 391).

1366 Giant Cell Lesions of Gnathic Bones Express RANKL and May Be Responsive to Denosumab Therapy

Anna Stagner¹, Dipti Sajed², G. Petur Nielsen¹, Vikram Deshpande¹. ¹Massachusetts General Hospital, Boston, MA, ²University of California at Los Angeles

Background: Central giant cell lesions (CGCL) are benign but potentially locally aggressive tumors of the jaw seen most often in young patients. Many are definitively treated with surgery, but a subset recur and can be destructive. Behavioral predictions based on histology have been unsuccessful. CGCLs share many histopathologic features with giant cell tumors (GCT) of long bones, which have been successfully treated with denosumab, a monoclonal antibody with high affinity for receptor activator of nuclear factor-kappa B ligand (RANKL). Stromal cells of GCT express high levels of RANKL, and expression of this receptor could make CGCLs also potentially amenable to treatment with denosumab.

Design: Cases were retrieved from the surgical pathology archives of Massachusetts General Hospital and independently reviewed by two subspecialty pathologists. Clinical information was obtained via chart review. Tumors were classified as aggressive or nonaggressive based on clinical behavior and radiographic characteristics using a previously described system. Tumors were characterized histopathologically as 1) resembling GCT or 2) non-GCT, the latter characterized by fewer/unevenly distributed giant cells and spindle stromal cells. Given the lack of robust antibodies, a chromogenic in situ hybridization (ISH) assay using a probe against RANKL was performed and scored semi-quantitatively based on the magnification at which the signal was first detected.

Results: 17 patients were identified (median age, 15 years). 11 patients did not have an associated syndrome and 6 were syndromic.

9/11 non-syndromic tumors were clinically aggressive. 10 tumors were characterized as GCT-like and 7 as non-GCT-like. No clinical or radiologic differences were identified between histologic patterns. 15 of 17 tumors, both syndromic and non-syndromic, showed high expression of RANKL mRNA (10/10 GCT-like and 5/7 non-GCT-like). RANKL expression was restricted to the mononuclear cells. Two patients with clinically aggressive CGCL, GCT-like histology and high tumor RANKL expression were identified as candidates for a trial of denosumab with notable clinical response.

Conclusions: CGCL express RANKL in mononuclear stromal cells, regardless of histology, clinically aggressive behavior, or sporadic/syndromic status. Two patients with clinically aggressive tumors and high RANKL expression were successfully treated with denosumab. RANKL expression in CGCL may support a new therapeutic application for denosumab and warrants further investigation. <

1367 Prognostic Value of 1p36 Deletion in Adenoid Cystic Carcinoma of the Salivary Gland

Petr Steiner¹, Simon Andreassen², Katalin Kiss³, Alena Skalova⁴. ¹Charles University in Prague, Faculty of Medicine in Pilsen and Bioptical Laboratory, Ltd, Pilsen, Czech Republic, ²Rigshospitalet, Copenhagen, ³Diagnostic Centre Rigshospitalet, Copenhagen, University Hospital, Copenhagen, ⁴Charles University, Plzen, Czech

Background: Adenoid cystic carcinoma (AdCC) of the salivary gland is characterized by slow but relentless clinical progression with poor clinical outcome in most patients. Chromosomal rearrangements result in formation of *MYB-NFIB* and, more rarely, *MYBL1-NFIB* fusion genes, which are robust ancillary markers in routine diagnosis of salivary gland tumors, but does not carry prognostic value. Therefore, in lack of molecular markers of prognostic value, the major purpose of this study was to determine if 1p36 locus deletion, known as adverse prognostic marker in various other tumor types, is of prognostic value in salivary gland AdCCs.

Design: Thirty-one AdCCs of the major and minor salivary glands were retrieved from the Salivary Gland Tumor Registry of Šikl's Department of Pathology and Bioptická laboratory Ltd. in Plzen, Czech Republic. Sixty-four additional cases were selected from Rigshospitalet, Copenhagen, Denmark. All 95 cases had available tumor material and clinical data. FISH analysis using ZytoLight® SPEC 1p36/1q25 Dual Color Probe (ZytoVision GmbH, Bremerhaven, Germany) was performed to detect 1p36 locus deletion. The results were correlated with clinical data.

Results: The study included 88 patients with analyzable tissue material (48 female [54.5 %]; 40 male [45.5%] with a mean age of 56.9 years (range: 14-85)). Thirteen patients [14.8 %] with 1p36 locus deletion were identified. A statistically significant correlation between 1p36 locus deletion and high tumor stage, reduced overall survival, disease-specific survival, recurrence-free interval and recurrence-free survival was found (p values: 0.0042, <0.0001, <0.0001, <0.0001 and 0.0001, respectively).

Conclusions: Deletion of 1p36 is associated with an aggressive clinical course of salivary gland AdCC.

The study was in part supported by the grant of Charles University (SVV 2017- 260 391).

1368 High-risk Human Papillomavirus is Associated with Sinonasal Non-keratinizing Squamous Carcinoma NOT-ex-Inverted Papilloma

Jihong Sun¹, Margaret Brandwein-Weber². ¹Mount Sinai Health System, New York, NY, ²Mt. Sinai Hospital, New York, NY

Background: High-risk human papillomavirus (HPV) has been etiologically associated with non-keratinizing oropharyngeal squamous carcinomas (SCC), which has tremendous clinical importance due their improved outcomes. Recent studies have suggested that HPV positive sinonasal SCC, especially non-keratinizing type, may also be associated with better outcomes. Here we study a large group of sinonasal SCC, with no association to inverted papillomas, and HPV DNA testing, with p16 expression and histological subtype.

Design: 24 cases of sinonasal SCC (2011 - 2017) were studied, comprised 16 males and 8 females (M:F=2:1), aged 40-90 years (median 64.5 years). SCC were classified as either keratinizing, non-keratinizing, papillary, or basaloid. HPV DNA testing was performed by PCR (22 cases) or in-situ hybridization (ISH) (2 cases). PCR was performed by using HPV L1 consensus primers, followed by real-time PCR with HPV16/18 E6 PCR primers and type specific probes. Non-HPV16/18 genotypes are determined by sequencing method. The HPV DNA ISH was performed in a commercial laboratory by using probes for HPV 6, 11, 16, 18, 31 and 33 from Dako (USA). Standard immunohistochemistry for p16 were performed on all cases.

Results: Among the 15 non-keratinizing SCC cases, 12 (80%) showed p16 overexpression. High risk HPV DNA were detected in all 12 cases: HPV 16 in 6 cases, HPV 18 in 2 cases, and HPV 33, 35, 45 and 56 in 1 case

each. There is one papillary SCC case with p16 positivity and HPV16 detection. One basaloid SCC case was found with p16 positivity and both HPV 16 and 33 detection. Seven cases were diagnosed as keratinizing SCC with at least focal keratin formation, five cases were p16 overexpressed, but only 1 case was HPV 16 positive and rest 4 cases were HPV DNA negative. Comparing these 12 HPV DNA positives in 15 non-keratinizing SCC with only 1 HPV DNA positive in 7 keratinizing SCC, the outcome is statistically significant ($p < 0.05$).

Table 1: Sinonasal SCC histology, HPV DNA and p16 status

HPV DNA / p16 status	HPV type	Histology
HPV DNA +/p16 + (n=15)	HPV16 (n=8)	6 NK *
		1 papillary
		1 K **
	HPV16/33 (n=1)	1 basaloid
	HPV18 (n=2)	2 NK
	HPV33 (n=1)	1 NK
	HPV35 (n=1)	1 NK
	HPV45 (n=1)	1 NK
HPV56 (n=1)	1 NK	
HPV DNA - / P16 + (n=4)	N/A	4 K
HPV DNA - / P16 - (n=5)	N/A	3 NK, 2 K

*non-keratinizing, **keratinizing

Table 2: Sinonasal SCC histology, HPV DNA positivity and types, p16 IHC status

Histology	HPV DNA+ (%)	HPV type	P16 IHC+ (%)
Non-keratinizing (n=15)	12 cases (80%)	16(x6), 18(x2), 33, 35, 45, 56	12 cases (80%)
Keratinizing (n=7)	1 case (14%)	16	5 cases (71%)
Papillary (n=1)	1 case (100%)	16	1 case (100%)
Basaloid (n=1)	1 case (100%)	16/33	1 case (100%)

Conclusions: Our study further confirmed the previous observation of other groups, High risk HPV may be etiologically associated with non-keratinizing SCC in the sinonasal tract. Our study showed 80% of non-keratinizing SCC harbored high risk HPV DNA, most type is HPV 16, whereas only 14% of keratinizing SCC had high risk HPV DNA detected. We also found the closer association between p16 expression and HPV status in non-keratinizing SCC compared with its much lower rate of association with keratinizing SCC. Further clinical outcome correlation is to be conducted.

1369 Lack of UV-Signature Mutations Distinguishes Primary Salivary High-Grade Neuroendocrine Carcinoma from Metastatic Merkel Cell Carcinoma

Lulu Sun¹, James S Lewis², Eric J DUNCAVAGE³, Rebecca Chernock⁴. ¹Barnes Jewish Hospital/Washington University, Saint Louis, MO, ²Vanderbilt University Medical Center, Nashville, TN, ³Washington University, St Louis, MO, ⁴Washington University School of Medicine, Saint Louis, MO

Background: Primary salivary high-grade neuroendocrine carcinomas (NECs) are rare, occur predominantly in the parotid gland and are difficult to differentiate from metastatic cutaneous NECs, known as Merkel cell carcinomas (MCCs), which may metastasize to the parotid. Morphology, immunohistochemistry and molecular profiles overlap. Even Merkel cell polyomavirus (MCPyV) has been reported in both, although it is much more common in MCC than in salivary NEC (~80% versus <30%). Recently, highly prevalent UV-signature mutations have been found in MCPyV-negative MCCs, supporting a sun damage-induced mechanism of pathogenesis. Salivary NECs have not been evaluated for UV-signature mutations nor for gene fusions. Salivary-type gene fusions in NECs could suggest high-grade transformation from another salivary neoplasm (such as carcinoma ex pleomorphic adenoma) in the appropriate context and thus favor salivary origin. Here, we examine UV-signature mutations and gene fusions as potential molecular markers to distinguish salivary NEC from MCC.

Design: Targeted next-generation DNA sequencing results of 151 cancer-related genes previously performed on 4 primary MCPyV-negative high-grade salivary NECs were examined for UV signature mutations, defined in the literature as $\geq 60\%$ of total mutations being C-to-T transitions at dipyrimidine sites or $\geq 5\%$ CC-to-TT substitutions. RNA sequencing was also performed on formalin-fixed paraffin-embedded tissue from the 4 tumors. RNA reads were aligned to the human genome to detect fusion transcripts.

Results: UV-signature mutations were not detected in any primary salivary high-grade NEC. The average percentage of total single base pair mutations that were C-to-T transitions at dipyrimidine sites was $28.2\% \pm 10.9\%$, with a range of 15.4% to 42.1% (<60% in all 4 cases). There were no CC-to-TT substitutions. RNA-sequencing showed no evidence of canonical gene fusions, including those found in salivary tumors.

Conclusions: Reliable markers to separate primary salivary NEC from metastatic MCC are lacking. Recent evidence indicates that 90% or more of MCPyV-negative MCC harbor UV-signature mutations. Here, we show that absence of UV-signature mutations may distinguish primary salivary NECs from most MCPyV-negative MCCs and therefore may have diagnostic utility. UV-signature mutations strongly favor a skin primary. Tumor-associated gene fusions were not detected in salivary NEC, indicating that transformation from lower grade salivary neoplasms is likely uncommon.

1370 Prevalence of Oral and Cervical Human Papillomavirus Infections in Women Attending Colposcopy Clinics in Ireland

Prerna Tewari¹, Stephen Reynolds², Christine M White², Tom D'Arcy⁴, Cliona Murphy⁵, Cara Martin², John O'Leary². ¹Dublin, ²Trinity College Dublin, Dublin, Ireland ³Trinity College Dublin, Dublin, Leinster, ⁴St James's Hospital, Dublin, ⁵Tallaght Hospital, Dublin

Background: HNSCC is the sixth most common cancer worldwide and HPV has been recently recognised as one of the primary causes of Oropharyngeal squamous cell cancers (OSSCs). The increasing incidence of HPV-associated OSSCs worldwide has been ascribed to a "viral epidemic".

Despite the recognised importance of HPV in OSSCs, the epidemiology of oral HPV infection is not well understood. The natural history of oral HPV infections and the risk factors for persistent HPV infection in the oropharynx may differ from cervical HPV infection. There is currently limited data available on oral HPV incidence, persistence and clearance in healthy individuals in the Irish population.

Design: A prospective observational cohort study was undertaken on selected at-risk populations which comprises of women referred with abnormal cytology to the Colposcopy units at The Coombe Women and Infants University Hospital and the Adelaide & Meath Hospital, Dublin, Ireland.

An oral rinse sample was taken from the women referred with abnormal cytology at the baseline visit and at subsequent six-month follow-up visits following informed written consent. HPV testing was carried out on the Cobas 4800 platform with the Cobas HPV DNA test. Where oral samples tested positive, a cervical biopsy/LLETZ treatment sample from the same patient was retrieved for HPV testing. All positive samples were genotyped with the INNOLIPA HPV genotyping assay.

Questionnaires were also administered to all participants to assess socio-demographic characteristics, sexual and contraceptive history, alcohol and tobacco use, and relevant clinical history.

Results: 200 women were tested for HPV of which 12% were positive. Majority of the oral samples were HPV 18 positive. The cervical biopsy/LLETZ samples were all HPV positive.

Conclusions: We observed a high prevalence of oral HPV infections in women referred with abnormal cytology.

1371 CAIX and PAX8 Commonly Immunoreactive in Endolymphatic Sac Tumors: Differential with Renal Cell Carcinoma in von-Hippel Lindau Patients

Lester D Thompson¹, Kelly R Magliocca², Edward Stelow³, Bruce Wenig⁴, Justin Bishop⁵. ¹Southern California Permanente Medical Group, Woodland Hills, CA, ²Emory University, Atlanta, GA, ³Univ of Virginia Health System, Charlottesville, VA, ⁴Moffitt Cancer Center, Tampa, FL, ⁵UT Southwestern Medical Center, Dallas, TX

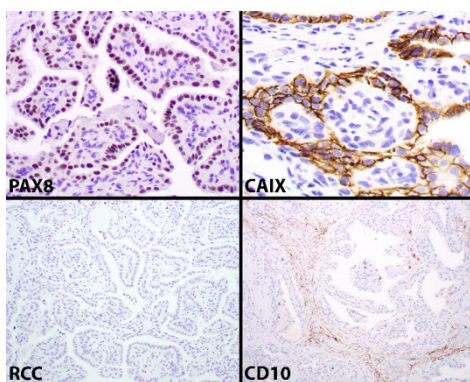
Background: Endolymphatic sac tumors (ELSTs) are rare, slowly growing temporal bone neoplasms which show a high association with von Hippel-Lindau (VHL) disease. The immunohistochemistry evaluation of these papillary-cystic neoplasms frequently raises the differential diagnosis with renal cell carcinoma, among other metastatic neoplasms, whether in VHL patients or not.

Design: A cohort of 19 patients with ELSTs were evaluated for

histologic features, immunohistochemistry findings, and association with VHL. Standard immunohistochemistry evaluation was performed.

Results: 14 females and 5 males ranging in age from 10 to 69 years at initial presentation comprised the cohort of patients. Most experienced hearing changes or inner ear symptoms (vertigo, dizziness), with an average duration of symptoms for 50 months. The tumors were an average of 3 cm (range, 0.8 to 8 cm), with 11 left and 8 right sided tumors. Bilateral tumors were not recorded. Six patients had documented VHL, with 3 patients having a concurrent or subsequent renal cell carcinoma (RCC). Patients were followed an average of 7.2 years (13 alive for 9.2 years; 2 dead without disease 1.2 years; and 2 alive with disease, 3.3 years). The neoplastic cells show the following immunohistochemistry findings:

Immunohistochemistry	% Positive	Pattern
CK-pan (AE1/AE3)	100	Strong, cytoplasmic
EMA	100	Strong, membranous
PAX8	87	Nuclear
CAIX	100	Strong, membranous
CK7	100	Strong, cytoplasmic
CD10	0	n/a
RCC	0	n/a
S100 protein	16	Delicate, nuclear and cytoplasmic



Conclusions: Based on this cohort of 19 patients with ELST, 6 of whom had VHL, the strong PAX8 and CAIX must be used in conjunction with negative CD10 and RCC to help exclude a metastatic renal cell carcinoma. As CAIX is an enzyme overexpressed in hypoxia and hypoxia inducible factor is what VHL protein regulates, this is an expected, although previously unreported finding. Whether part of VHL or not, VHL mutations may be a somatic rather than germline finding in the tumors, a possible further explanation for the CAIX reaction.

1372 Low Neck (Level Vb) Disease Predicts a Worse Prognosis in Oropharyngeal Squamous Cell Carcinoma: An Analysis of 390 Patients

Lester D Thompson¹, Hannah Herrera², Shawn Igane², Onita Bhattasali².
¹Southern California Permanente Medical Group, Woodland Hills, CA, ²SCPMG, ³Southern California Permanente Medical Group

Background: The AJCC 8th edition TNM classification for oropharyngeal squamous cell carcinoma (OPSCC) does not consider low neck (Level Vb [5b]) as a factor within the nodal staging groups. Patient survival outcomes when controlled for p16-positive (HPV-associated) tumors are compared.

Design: All patients in the Southern California Permanente Medical Group diagnosed with OPSCC between 2006 and 2012 with a minimum of 5 years of follow-up were included. Radiographic studies and pathology diagnoses with central p16 evaluation were compared for stage-matched patients with and without level Vb lymph node involvement.

Results: 341 males and 49 females ranging in age from 35-83 years comprised the cohort of 390 patients. The tonsil (n=201) was the most common site, followed by base of tongue (n=169), pharynx (n=12), and soft palate (n=8). Overall, 342 patients had p16-positive tumors, while 48 patients had p16-negative tumors. Nonkeratinizing (n=290 p16-positive; n=20 p16-negative), with maturation (n=35 p16-positive; n=3 p16-negative) and keratinizing (n=17 p16-positive; n=25 p16-negative) histologies were categorized. Overall mean survival was 71.0 versus 50.8 months for 342 p16-positive versus 48 p16-negative patients, respectively. Among the entire cohort, level Vb disease was a poor prognostic factor for survival (HR=2.70 [1.71-4.27]); p<0.001).

Analyzing only those patients with p16-positive disease, level Vb disease remained prognostic for worse survival (HR=3.47 [2.11-5.70]; p<0.001). Stage-matched analysis of p16+ cases demonstrated worse survival among patients with level Vb disease compared to patients in the same stage group without level Vb disease (HR=1.02 [1.67-4.65]; p<0.001). The prognostic impact of level Vb lymph node involvement in p16+ disease remained significant on multivariate analysis (HR=2.50 [1.42-4.43]; p=0.002).

Stage	# of patients	Mean overall survival (months)
I	149	75.7
I-Vb	13	48.3
II	81	78.3
II-Vb	13	64.9
III	64	62.5
III-Vb	19	47.0

Conclusions: Based on this cohort of 342 patients with HPV-associated OPSCC, irrespective of histologic type or tumor site, level Vb lymph node involvement predicted a worse outcome when compared with otherwise similar stage patients. This suggests the N categories may need to be modified or upstaged to account for level Vb lymph node disease.

1373 Histologically Significant Features in 390 Oropharyngeal Squamous Cell Carcinomas

Lester D Thompson¹, Hannah Herrera², Shawn Igane², Onita Bhattasali².
¹Southern California Permanente Medical Group, Woodland Hills, CA, ²SCPMG, ³Southern California Permanente Medical Group

Background: Numerous histologic characteristics identified in oropharyngeal squamous cell carcinoma (OPSCC) may portend a worse patient outcome. This study evaluates the prognostic impact of many factors controlling for p16 status (HPV-associated) and stage (AJCC 8th edition).

Design: All patients in Southern California Permanente Medical Group diagnosed with OPSCC between 2006 and 2012 with a minimum of 5 years of follow-up were included. Review of all pathology materials combined with central p16 evaluation was conducted for tumor site, histology classification, tumor grade, pattern of growth, surface versus crypt centered tumor, anaplasia, multinucleation, dyskeratosis, comedonecrosis, tumor ulceration, desmoplastic reaction, concurrent dysplasia, type of lymphocytic infiltrate (mild, moderate, brisk) and mitotic counts (in 20 count increments/10 high power fields).

Results: The cohort of 390 patients included 342 p16+ and 48 p16-tumors. On univariate analysis, the following factors, when present, were associated with a **better** patient prognosis: nonkeratinizing histology (n=290; p<0.001); with maturation (n=35; p<0.001); basaloid pattern (n=264; p=0.004); crypt rather than surface centered (n=312; p=0.004); presence of dyskeratotic cells (n=331; p=0.04). These factors **failed** to show a statistically significant difference in patient outcome when evaluated: tumor site (tonsil, base of tongue, pharynx, soft palate; p=0.32); histology pattern: lymphoepithelial (n=52; p=0.44), papillary (n=22, p=0.39), keratinizing (n=42; p=0.54), spindle (n=5; p=0.76); neuroendocrine (n=2, p=0.08); keratin pearl formation (n=219; p=0.97); tumor ulceration (n=76, p=0.89); tumor cell anaplasia (n=109, p=0.89); tumor cell multinucleation (n=73, p=0.74); desmoplastic stroma (n=229, p=0.20); comedonecrosis (n=255, p=0.34); lymphocytic infiltrate (mild, moderate or brisk, p=0.16); mitotic groups (based on 20/10 HPF groups, p=0.57). After controlling for p16 status and tumor stage, the following remained favorable prognostic factors for overall survival: nonkeratinizing (p=0.01) and with maturation histology (n=0.03); dyskeratotic cells (p=0.03); with a trend towards better survival for basaloid pattern (n=0.065).

Conclusions: Based on this cohort of OPSCC patients, controlling for p16 status and tumor stage, nonkeratinizing and with maturation histology, and the presence of dyskeratotic cells are significantly prognostic for better survival. All other histologic features do not show any significant differences in outcome.

1374 Exploring the Mismatch Repair Protein Loss in Head and Neck Squamous Cell Carcinoma

Kartik Vasan¹, Laveniya Satgunaseelan², Sunaina Anand², Christina Selinger², Kan Gao¹, Tsu-Hui (Hubert) Low¹, Rebecca Asher¹, Carsten E Palme², Jonathan Clark¹, Ruta Gupta².
¹Chris O'Brien Lifehouse, ²Royal Prince Alfred Hospital, ³Royal Prince Alfred Hospital, Sydney, NSW

Background: The incidence of non-Human Papilloma Virus (HPV) associated Head and Neck Squamous Cell Carcinoma (HNSCC) in young patients (<50 years) is increasing globally. The molecular pathways involved in the development of HNSCC remain unexamined

in this cohort. There are anecdotal reports of mismatch repair (MMR) protein loss in HNSCC. Also MMR deficient patients have been shown to have better response to immunotherapy. This study explores the incidence and clinicopathologic features of MMR deficient HNSCC using 516 cases with long term follow up.

Design: Immunohistochemical staining of 516 cases was conducted to assess the expression of MMR proteins (hMLH1, hMSH2, hMSH6, and hPMS2), as a well-characterised surrogate marker of microsatellite instability (MSI) was performed using tissue microarrays. This included 312 cases of non-HPV mucosal SCC and 204 cases of cutaneous HNSCC (1995-2016). A designation of MSI-low-like (MSI-L) status was given for those cases where one MMR protein was lost. MMR-high-like (MSI-H) status was designated for those cases where two or more MMR proteins were lost based on the 1997 National Institute of Health Consensus Panel guidelines for MSI testing. Polymerase Chain Reaction (PCR) testing of MMR deficient cases is being performed. Clinicopathological details were obtained.

Results: The 516 cases include 358 males and 158 females (M:F 2.26). The median age was 67.9 with 56 patients less than 50 years of age. MMR deficiency was seen in 31 patients (6.0%); 15 cutaneous SCC (7.4%) and 16 mucosal SCC (5.1%). Of these 31 patients, 30 (6.5%) were older than 50 years at the time of diagnosis of HNSCC. Loss of MLH1 and MSH6 were seen in 19 and 14 patients respectively. 17 cases showed MSI-H-like status and 14 MSI-L-like status. Amongst the MSI-H patients, 5 showed poorly differentiated morphology. Further clinical information of these patients is being obtained to understand the familial association of MMR in HNSCC and their response to treatment. The median overall survival was 4.38 in MSI-H patients as compared to a median overall survival of 8.98 years in the entire cohort.

Conclusions: Less than 10% of HNSCC are MMR deficient. MMR deficient patients were found to have significantly shorter overall survival as compared to the rest of the HNSCC cohort. This is in contrast to the findings observed in colorectal carcinoma. Future larger cohort studies as well as genetic evaluation is essential to explore the prognostic significance of MMR in HNSCC.

1375 Conventional and High Grade Transformation in Head and Neck Adenoid Cystic Carcinoma: a Single Tertiary-Care Oncology Centre Experience

Prerna Walecha¹, Asawari Patil¹, Munita Baf¹. ¹Tata Memorial Hospital, Mumbai, Maharashtra, India

Background: Adenoid cystic carcinoma (ACC) is an uncommon salivary gland tumor characterized by indolent growth, frequent local recurrences, late distant metastases and rare high grade transformation (HGT). This study presents a clinicopathologic spectrum of a large cohort of conventional ACC and HGT in ACC diagnosed at a single tertiary-care oncology centre. Adenoid cystic carcinoma (ACC) is an uncommon salivary gland tumor characterized by indolent growth, frequent local recurrences, late distant metastases and rare high grade transformation (HGT). This study presents a clinicopathologic spectrum of a large cohort of conventional ACC and HGT in ACC diagnosed at a single tertiary-care oncology centre.

Design: A retrospective review of clinical and pathologic findings of all ACC cases diagnosed from 2013-2015 was undertaken.

Results: A total 170 ACC cases including 17 (10%) with HGT were studied. Median age was 45 years; commonest sites included paranasal sinuses and oral cavity (23%, each). Median tumor (T) size was 4 cm. There were 3%, 73% and 24% cases of grade 1, 2 and 3, respectively. Perineural invasion (PNI), lymphovascular invasion (LVI), nodal metastasis and margin positivity (R1) was seen in 56.2%, 6.2%, 15.4% and 59% cases, respectively. Local recurrence and distant metastasis was seen in 29% and 25% patients, respectively. The 3-year and 5-year estimated overall survival (OS) was 91.8% and 83.4%, respectively. The most important predictors of progression-free survival (PFS) and OS were T size, T stage and R1; and tumor grade for PFS alone. In the HGT cohort, maxilla was the commonest site. Median T size was 3.9 cm. Grade 2 (53%) was the commonest backdrop seen in HGT. Micropapillary (13%), squamoid (13%), signet vacuoles (20%) and oncocytic (13%) change were observed in HGT cases. PNI, LVI, nodal metastasis and R1 was seen in 93.3%, 26.7%, 33.3% and 80% cases, respectively. Comedo necrosis was noted in 47%. For HGT cases, the median value of PFS and OS could not be reached.

Conclusions: ACC is an uncommon salivary gland tumor with a tendency to undergo high grade transformation in a small proportion of cases. T size, T stage, R1 and histologic grade are associated with prognosis in ACC. High grade transformation encompasses a wide morphologic spectrum and is associated with increased biologic aggressiveness in the form of augmented rate of PNI, LVI, nodal metastasis and margin positivity.

1376 PLA2R1 May Be a Novel Diagnostic Marker for Salivary Gland Tumors: A Multi-institutional Immunodiagnostic Utility Analysis of 145 Cases

Christina Wei¹, Lester D Thompson², Anna Mathew³, Philip Carpenter⁴. ¹USC/LAC and USC Pathology and Laboratory Medicine, Los Angeles, CA, ²Southern California Permanente Medical Group, Woodland Hills, CA, ³Keck School of Medicine of USC, Pasadena, CA, ⁴University of Southern California

Background: Salivary gland tumors are highly diverse with varied biologic and clinical outcomes. They are frequently diagnosed on small biopsy specimens, posing diagnostic challenges. As management is predicated on the accuracy of histological diagnosis, novel immunohistochemical markers are critically needed. Autoantibodies against the receptor for secretory phospholipase A2 (PLA2R1), are present in most cases membranous nephropathy, and diagnostic immunohistochemical (IHC) antibodies against PLA2R1 are routinely used in nephropathology. In this study, we investigated its immunodiagnostic utility in salivary gland tumors.

Design: PLA2R1 expression was investigated in a microarray of 145 resected primary salivary gland tumors diagnosed by the authors. PLA2R1 expression was determined by IHC. In parallel, PLA2R1 expression was evaluated in a separate microarray of 44 somatic carcinomas, including the following sites: breast, hepatobiliary, gastrointestinal, gynecologic, kidney, prostate, testes, thyroid. Two pathologists evaluated the cytoplasmic expression of PLA2R1 by the standardized semi-quantitative approach of H-score (% positive cells x staining intensity). Mean intertumoral H-score differences were evaluated by Tukey's pairwise multiple comparison test.

Results: The interobserver kappa for H-score is 0.40. PLA2R1 expression was observed in normal salivary gland ducts and in 86% of the primary salivary gland tumors (Figure 1 and 2). PLA2R1 expression was highest in pleomorphic adenoma (PA) and polymorphous adenocarcinoma (PAC), and lowest in adenoid cystic carcinoma (ACC) and salivary duct carcinoma (SDC). Tukey's pairwise comparison showed that PLA2R1 is differentially expressed between PAC vs ACC (p < 0.001), PA vs ACC (p < 0.01), PAC vs SDC (p < 0.002), and PA vs SDC (p < 0.01). PLA2R1 was not expressed in the somatic carcinomas surveyed, except to a minor degree in breast and prostate cancers.

Figure 1: Averaged H-Score for Various Primary Salivary Gland Tumors

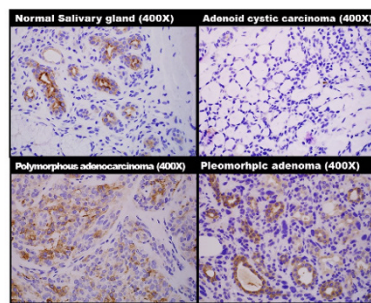
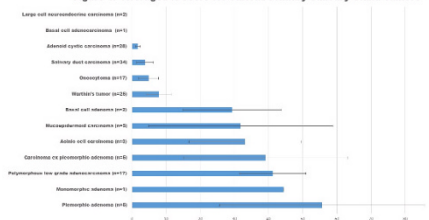


Figure 2: PLA2R1 immunohistochemical staining in selected salivary gland tumors

Conclusions: PLA2R1, a clinically available IHC marker, shows potential for application in primary salivary gland tumors with tubular-ductal like differentiation. It may be helpful in distinguishing various salivary gland tumors, especially on small biopsies, and as a marker to differentiate primary salivary gland tumors from other somatic carcinomas.

1377 Morphologic Comparison of SMARCB1 (INI-1)-Deficient Sinonasal Carcinoma and Sinonasal Undifferentiated Carcinoma Nominates Mitotic-Apoptotic Index as a Potential Diagnostic Discriminator

Steven C Weindorf¹, Jonathan McHugh², Aaron M Udager³. ¹Michigan Medicine, Ypsilanti, MI, ²University of Michigan Health System, Ann Arbor, MI, ³University of Michigan Medical School, Ann Arbor, MI

Background: SMARCB1 (INI-1)-deficient sinonasal carcinoma is a recently described diagnostic entity in head and neck pathology that may show overlapping morphologic and/or clinical features with other poorly-differentiated or small round cell tumors of the sinonasal tract, including sinonasal undifferentiated carcinoma (SNUC). To date, no definitive morphologic differences have been described that reliably distinguish SMARCB1 (INI-1)-deficient sinonasal carcinoma from SNUC

without the use of ancillary studies [i.e., INI-1 immunohistochemistry (IHC)]. Therefore, we sought to explore potential diagnostic clues to the diagnosis of SMARCB1 (INI-1)-deficient sinonasal carcinoma.

Design: All undifferentiated sinonasal carcinomas at a single large academic institution between June 2013 and June 2017 were retrospectively identified. Blinded to the specific diagnosis, available H&E slides were reviewed concurrently by two study pathologists to assess morphologic features, including cytoplasm, nuclei, nucleoli, chromatin, and architecture; in addition, the presence and qualitative extent of cytologic pleomorphism and rhabdoid features was recorded. Counts of mitotic and apoptotic figures in ten high-power (40X) fields were performed independently by two study pathologists and averaged. INI-1 IHC was subsequently performed by the clinical IHC laboratory on sectioned tissue from all tumors, and cases were grouped for comparison based on the presence or absence of nuclear INI-1 staining. Clinical information was manually extracted from the electronic medical record.

Results: A total of 8 undifferentiated sinonasal carcinomas were identified, of which 2 (25%) showed loss of nuclear INI-1 staining by IHC [i.e., SMARCB1 (INI)-1 sinonasal carcinoma]. Comparison of clinical information and morphologic features showed significant overlap among all cases, however, the mitotic count, apoptotic count, and mitotic-apoptotic count were relatively lower in INI-1-deficient tumors (Table 1); in addition, these INI-1-deficient tumors were more likely to show rhabdoid features and lack significant cytologic pleomorphism (Table 1).

	SNUC (n = 6)	SMARCB1 (INI-1)-Deficient Sinonasal Carcinoma (n = 2)
Cytologic Pleomorphism	No = 2 Yes = 4 (Anaplasia = 1)	No = 2 Yes = 0
Rhabdoid Features	None = 4 Focal = 1 Non-focal = 1 Extensive = 0	None = 0 Focal = 0 Non-focal = 1 Extensive = 1
Mitotic count per ten 40X fields (mean)	57 (range: 41-121)	26 (range: 13-38)
Apoptotic count per ten 40X fields (mean)	60 (range: 34-139)	17 (range: 8-25)
Mitotic-apoptotic count per ten 40X fields (mean)	111 (range: 84-260)	42 (range: 21-63)

Mitotic-apoptotic count per ten 40X fields (mean)

Conclusions: Although SMARCB1 (INI-1)-deficient sinonasal carcinoma shares many clinical and morphologic features with SNUC, our preliminary data indicate that the mitotic-apoptotic index (MAI) is a potential diagnostic discriminator. If this finding is confirmed in larger studies, MAI assessment may allow for more judicious use of INI-1 IHC in the work-up of undifferentiated sinonasal carcinomas.

1378 TOP2A, ERCC1, and NTRK Expression in Papillary Thyroid Carcinoma in Hispanic Population

Ciara Wisecup¹, Frank Wians¹, Alireza Torabi². ¹Texas Tech University Health Science Center, ²Yosemite Pathology Medical Group, Modesto, CA

Background: Papillary thyroid carcinoma (PTC) is the most common type of thyroid cancer and it is more common in women than men. Previously (CAP 2017), our data failed to demonstrate any significant relationship between tumor staging and BRAF V600E and PD-L1 expression. TOP2A is a key factor enzyme in DNA replication and cell cycle progression and its amplification is associated with higher response to anthracyclin-based neoadjuvant therapy. ERCC1 enzyme participates in DNA repair pathway and its mutation make cells more sensitive to DNA damaging agents and chemicals such as cisplatin (high expression of ERCC1 correlates with resistance to platinum based chemotherapy). NTRK is a tyrosine kinase receptor that is involved in cell differentiation and survival and its translocation has been reported in PTC. In the current study, we looked at the expression of TOP2A, ERCC1 and NTRK by immunohistochemistry in PTC and compared the data to the BRAF mutation PD-L1 expression.

Design: We chose 47 patients who had total thyroidectomy for well-differentiated PTC and constructed a 3mm wide core tissue microarray (TMA). Anaplastic and undifferentiated cases were excluded. The adjacent normal thyroid tissue in the TMA was used as control. All patients were Hispanic; all but one was female; 24 were older than 45 and 23 younger. Tumor staging was based on TNM and age. The array was stained with anti-TOP2A (clone 3F6), anti-ERCC1 (clone 8F1), and anti-TRK A/B/C (clone EPR17341) by Caris life science laboratory.

Results: Of the 4 cases (8%) that were positive for TOP2A, 3 happened

in stage I PTC (p-value of 0.01). 23 cases were negative for ERCC1 (49%) with no significant correlation to the tumor staging. Only 2 cases were positive for NTRK (4%), one in stage I and the other stage II (p-value of 0.0006). There was no significant relationship between the BRAF V600E mutation and PD-L1 with expression of these 3 proteins.

Conclusions: Total thyroidectomy and radioiodine are the main and definite treatment for PTC, while locally advanced disease is usually treated by external beam radiotherapy. TOP2A and NTRK could be the potential targets for PTC treatment; however, in our experience only 8% and 4% of the cases express these 2 proteins, respectively, and all occur in lower stage. Although 49% of the cases were negative for ERCC1 (which make them susceptible to platinum based chemotherapy), there was no significant correlation with tumor staging.

1379 Characterization of Features of Bluntly Invasive Well-differentiated Oral Squamous Cell Carcinoma

Sook-Bin Woo¹, Reshma S Menon², Chia-Cheng L². ¹Brigham and Women's Hospital, Boston, MA, ²Harvard School of Dental Medicine, Boston, MA

Background: Oral squamous cell carcinoma (SCCa) has many histological subtypes. However, some tumors do not show the conventional pattern of infiltration of the stroma by detached tumor islands and single cells. The aim of this study is to report cases of tumors that exhibit a "blunt" pattern of invasion and yet because of substantial cytologic atypia/dysplasia, is not strictly a verrucous carcinoma.

Design: Cases diagnosed as "atypical endophytic squamous proliferation suspicious for at least bluntly invasive squamous cell carcinoma (BISCCA)" were identified from a single laboratory. All cases had to show bulky endophytic epithelial proliferation with a broad "pushing" front without evidence of conventional infiltration of the stroma, but with at least mild-to-moderate dysplasia.

Results: There were 38 cases (20 female, 18 male) with a median age of 70 years. Sixty-five per cent of cases occurred on the gingiva (15) or ventrolateral tongue (10); the rest were on the buccal/labial mucosa (9), vestibule (3) and hard palatal mucosa (1). All 38 cases exhibited a bulky epithelial proliferation with an endophytic growth pattern. The histopathologic features included a papillary or verrucous surface in 27 cases (71.0%). Most cases (78.9%) showed thick parakeratosis; five cases demonstrated both ortho and parakeratin and 3 only hyperkeratosis. Rete ridges were bulbous in almost all case and the bulkiness of the epithelium was 3-5 times that of the adjacent normal mucosa. The epithelium showed mild to moderate grades of dysplasia in all cases. There were micro abscesses at the tips of rete ridges in 42.1% of case. Eosinophils were noted in both the epithelium and connective tissue in 22 cases (57.9%). As expected, there was no evidence of perineural or lymphovascular invasion.

Conclusions: We believe that BISCCA is a form of SCCa that resembles verrucous carcinoma in its pattern of invasion but yet shows significant cytologic atypia. Many pathologists are unwilling to use the term invasive squamous cell carcinoma when there is no stromal infiltration by single cells or detached tumor islands. We believe the term BISCCA is appropriate for such lesions. It may be that these tumors like verrucous carcinoma may have a lower propensity for metastases and "depth of invasion" may not have the same significance as for conventionally invasive SCCa.

1380 Anaplastic Thyroid Carcinoma: Three Cases with Novel Histologic and Immunohistochemical Features Simulating Chondroblastoma But Without Evidence of H3F3A or H3F3B Hotspot Mutations

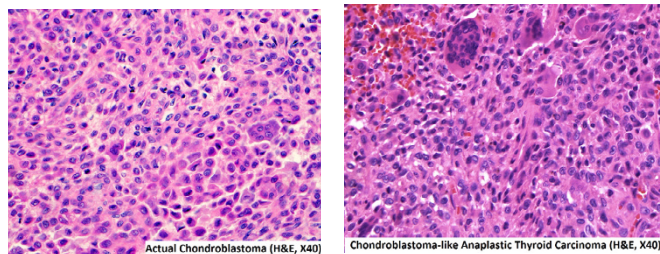
Meng-Jun Xiong¹, Brian S Husen², Von Samed³, Jin Wu⁴, Therese J Bocklage⁵, David Martin⁶. ¹University of New Mexico School of Medicine, Albuquerque, NM, ²University of New Mexico School of Medicine, Albuquerque, NM, ³Albuquerque, NM, ⁴UNM SOM, ⁵University of Kentucky College of Medicine, Lexington, KY, ⁶Univ. of New Mexico, Albuquerque, NM

Background: Anaplastic thyroid carcinoma (ATC) is aggressive with variable histologic features but typically with high grade morphology. In a review of 26 cases, we observed 3 tumors that histologically and by IHC reactivity closely resembled chondroblastoma, a low grade tumor of bone with characteristic reactivity for SATB2, DOG1 and S100 protein. Recently, mutations of H3F3A and H3F3B have been reported as specific and sensitive for giant cell tumor of bone and chondroblastoma. We evaluated the 3 chondroblastoma-like (CB-like) cases of ATC for these mutations and compared clinical, histologic, IHC and molecular genetic findings with 23 additional cases of ATC.

Design: CB-like features were identified in a recent case of ATC prompting review of 26 cases identified through searching surgical pathology databases at our institution. We found 2 more cases histologically resembling chondroblastoma, and performed additional antibody staining including SATB2, DOG1 and S100 protein antibodies

using standard methods. Cases of giant cell tumor of bone and chondroblastoma were used as positive controls. Two to 10 sections at 10µm thickness were obtained by micro-dissection per case. Genomic DNA was isolated from formalin-fixed paraffin-embedded tissue. PCR was performed using *H3F3A* and *H3F3B* gene-specific primers and further evaluated by Sanger sequencing to examine for *H3F3A* codon 34 (exon 1) and *H3F3B* codon 36 (exon 2) hotspot mutations.

Results: The 26 patients comprised 18 females and 8 males with age range (25 to 85 years [yr]) and mean (65 yr). Survival was poor (<1 yr: 19; ≥1 yr: 4; unknown: 3). Patients with CB-like features included 2 females and 1 male, aged 49, 69, and 73 yr. By IHC, 3/3 tumors strongly expressed SATB2, 2/3 tumors expressed DOG1, and 1/3 expressed S100 protein. NanoDrop-100 demonstrated good DNA concentration and high quality (range: 114 to 2,751 ng/µl) and A260/280 ratio (range: 1.92-2.04). All 26 ATC cases were aligned and compared in forward and reverse sequences with known *H3F3A* (Genbank NM_002107.4) and *H3F3B* (NM_005324.4), respectively. All ATC cases lacked an *H3F3A* or *H3F3B* mutation.



Conclusions: We found 3 cases of ATC with histologic and IHC features resembling chondroblastoma of bone. However, behavior of these deceptively low grade tumors did not seem to differ from typical high grade ATC. Hotspot mutations of *H3F3A* and *H3F3B* were absent. Variant mutations could be detected by a more sensitive assay such as NGS combined with targeted IHC for protein expression.

1381 Misdiagnosed Myoepithelial Carcinoma of Salivary Gland: A Challenging and Potentially Significant Pitfall

Bin Xu¹, Wadad Mneimneh², Dianne Torrence³, David Klimstra⁴, Ronald Ghossein⁴, Nora Katabi⁴. ¹Sunnybrook Health Sciences Centre - University of Toronto, Toronto, ON, ²University of South Alabama, Mobile, AL, ³University of Florida, Gainesville, FL, ⁴Memorial Sloan-Kettering Cancer Center, New York, NY

Background: Myoepithelial carcinoma (MECA) is an underrecognized challenging entity with a broad spectrum of morphologies. Misdiagnosing MECA is not uncommon as distinguishing it from its other mimics, especially cellular myoepithelial-rich pleomorphic adenoma (PA) can be difficult. Such distinction seems significant as adverse outcomes can be seen in MECA.

Design: In this study, we described 19 histologically challenging cases of MECA in which a benign diagnosis was initially rendered or strongly considered, including 14 MECA ex-PA and 6 MECA *de novo*, and analyzed their clinicopathologic features.

Results: The tumor sites included parotid (n=12), submandibular (n=5) and minor salivary glands (n=2). All MECAs ex PA were intracapsular or minimally invasive except for two cases. Sixteen out of nineteen (84%) cases had an initial diagnosis of benign neoplasms, including 9 PAs, 5 atypical PAs, and 2 myoepitheliomas. The other three cases were initially diagnosed as malignant (MECA ex PA) but were histologically challenging. Among the 15 patients with available follow up (median=45 months), one had distant metastasis to the contralateral temporal skin/soft tissue at time of diagnosis and 12 (80%) developed recurrence, including 9 with local recurrence and 4 with distant metastases to lung (n=2) and bone (n=2). The initial diagnoses of the 5 cases with distant metastases were PA (n=1), atypical PA (n=2), and intracapsular MECA ex PA (n=2). Ten out of twelve patients with recurrence had an initial benign diagnosis. Histologic features that were helpful to recognize malignancy included a uniformly cellular myoepithelial proliferation with an expansile nodular pattern (seen in all cases) and alternating hypocellular and hypercellular zonal distribution (seen in 74% of cases). Compared to the primary, the recurrent/metastatic tumor was more cytologically atypical in 3 cases. Two patients with MECA ex PA (intracapsular and minimally invasive) died of their disease; one had an initial diagnosis of PA.

Conclusions: MECA is a histologically challenging entity that closely mimics PA. Distinguishing PA from MECA is important since the later seems to carry a significant risk of distant and local recurrence even when it is intracapsular/minimally invasive CA ex PA. Areas of myoepithelial overgrowth with an expansile nodular pattern and zonal cellular distribution distinguish the majority of MECAs and may serve as useful diagnostic histologic features for this entity.

1382 Expression of Cancer Testis Antigen PRAME, PD-L1, and PD-1 in Salivary Duct Carcinoma

Bin Xu¹, Achim Jungbluth², Nathaniel Aleynick², Ronald Ghossein², Nora Katabi². ¹Sunnybrook Health Sciences Centre - University of Toronto, Toronto, ON, ²Memorial Sloan-Kettering Cancer Center, New York, NY

Background: Salivary duct carcinoma (SDC) is an aggressive salivary malignancy that is often resistant to chemotherapy and has high mortality rates. Immunotherapy involving the checkpoint PD-L1 (programmed cell death ligand 1) and or PD1 (programmed death protein1) has led to occasional dramatic improvement in the treatment of various aggressive cancer types. Interestingly, the presence of PD1/PDL1 in SDC has not been analyzed yet. Besides immuncheckpoint blockade, other immunotherapeutic approaches such as cancer vaccines have shown promising results. Cancer testis antigens (CTAs) are regarded as promising vaccine targets due to their tumor-specific expression pattern, since they are present in a wide variety of malignancies while in normal tissue solely expressed in testis. PRAME (Preferentially Expressed Antigen in Melanoma) is a highly immunogenic CTA and preliminary analyses indicate that it shows a higher incidence and more homogeneous expression than other classical CTAs. Since little is known about the expression of PD1, PD-L1 as well as PRAME, this study analyzes the protein expression of PD-L1, PD-1, and CTA in SDC.

Design: 44 cases of SDCs were available for analysis. The following parameters were documented: percentage of tumor cells (TC) with CTA PRAME (mAb EPR20330) immunopositivity, number of immune cells (IC) that were positive for PD1 in one high power field (HPF), and percentage of TC and IC that were positive for PD-L1. PD-L1 positivity was defined using two sets of criteria: 1) ≥25% TC; and 2) ≥25% TC or IC.

Results: PRAME expression was observed in 25/44 (76 %) of SDCs, staining 43±6% of TC (mean ± standard errors of mean) displaying nuclear and/or cytoplasmic positivity. No staining was present in normal salivary gland tissue. PD-L1 was positive in 3/44 (7%) cases using criterion 1 and in 8/44 (18%) cases using criterion 2. Among the negative cases, PD-L1 was completely absent in TC in 33 cases (75%) and had 1-5% staining in TC in 8 (18%) cases. PD-1-positive staining in IC was noted in 18/37 (49%) of cases, staining 37±6 IC per HPFs. There was no significant correlation among PD-1 in IC, PD-L1 in TC, and CTA in TC.

Conclusions: 1) PRAME is frequently expressed in SDC which makes it a promising candidate as target for vaccine-based immunotherapy. 2) PRAME may also serve as a diagnostic marker for malignancy. 3) PD1 staining is noted in 49% of SDCs but the frequency of PD-L1 positivity seems to be low.

1383 Expression of Androgen Receptor Splice Variant-7 (AR-V7) in Salivary Duct Carcinoma: Implications for Treatment with Androgen Deprivation Therapy (ADT)

Richard Yang¹, Pei Zhao², Changxue Lu³, Rong Hu⁴. ¹Madison, WI, ²Johns Hopkins University, School of Medicine, Baltimore, MD, ³Johns Hopkins University, Baltimore, MD, ⁴University of Wisconsin Hospital and Clinics

Background: Salivary duct carcinoma (SDC) is a high grade salivary gland malignancy. Standard treatment for SDC is surgical resection with or without radiation. Androgen deprivation therapy (ADT), the mainstay treatment for metastatic prostate cancer, has been used to treat SDC. Despite the initial response, many patients have had disease recurrences and a small portion of androgen receptor (AR) positive SDCs do not respond to ADT. The androgen receptor splice variant 7 (AR-V7) constitutively activates AR signalling in absence of ligand, due to truncation of the ligand-binding domain. AR-V7 has been implicated in castration resistance in prostate cancer. We hypothesize that AR-V7 may also play important roles in resistance to ADT in AR-positive SDC. This study aims to determine AR-V7 expression status in SDC prior to ADT.

Design: We searched our Institutional Tumor Bank database for the diagnosis of "salivary duct carcinoma" between Jan 2000 to Jan 2017. Immunohistochemical (IHC) staining of AR was performed on formalin-fixed, paraffin-embedded specimens. Semi-quantitative RNA in situ hybridization (RISH) was used to assess both total AR (AR-T) and mature AR-V7 mRNA level. Prostate cancer cell line LNCaP95 and PC-3 were used as positive and negative controls. Quantitative RT-PCR was performed on a subset of frozen tumors.

Results: Twenty-four cases diagnosed with SDC from 23 patients (13 men, 10 women) were retrieved. All tumors were located in the parotid gland except one in the submandibular gland; five tumors were carcinoma ex pleomorphic adenoma. Using IHC, 21 cases (88%) were positive for AR, which correlated with AR-T mRNA levels by RISH. Among AR-positive SDCs, 13 cases (62%, 3 from women, 10 from men) were positive for AR-V7 by RISH. The expression level of AR-V7 varied from weak (1+) to very strong (3+) and two cases demonstrated AR-V7 levels exceeding those detected in androgen-

independent LNCaP95 cells. Positive AR-V7 was also detected in one out of three frozen tumors by RT-PCR.

Conclusions: Traditional IHC and RISH for AR expression showed excellent concordance. A significant proportion of AR positive SDCs were positive for AR-V7, with a few demonstrating levels comparable to castration resistant prostate cancer. These data support incorporation of AR-V7 assessment via RISH, IHC, or RT-PCR in clinical trials evaluating the therapeutic benefit of ADT in SDC patients. These test results may be useful in selecting SDC patients who would likely benefit from ADT.

1384 Targeted Genomic Profiling Reveals Highly Recurrent Molecular Alterations in the Malignant Progression of Sinonasal Papilloma to Sinonasal Squamous Cell Carcinoma, including CDKN2A Mutation/Deletion and TP53 Mutation

Osman Yilmaz¹, Komal Kunder², Jonathan McHugh³, Bryan L Betz⁴, Scott Tomlins¹, Noah Brown¹, Aaron M Udager⁴. ¹University of Michigan, Ann Arbor, MI, ²University of Michigan, ³University of Michigan Health System, Ann Arbor, MI, ⁴University of Michigan Medical School, Ann Arbor, MI

Disclosures: Scott Tomlins: *Employee, Strata Oncology*

Background: Inverted sinonasal papilloma (ISP) and oncocytic sinonasal papilloma (OSP) are benign tumors that may be associated with sinonasal squamous cell carcinoma (SNSCC). Our group recently identified frequent somatic *EGFR* mutations in ISP and *KRAS* mutations in OSP and demonstrated concordant mutations in associated SNSCC components, confirming a clonal relationship between these tumors. In the present study, we utilize targeted next-generation DNA sequencing (DNAseq) to characterize the landscape of molecular alterations involved in malignant progression from papilloma to SNSCC.

Design: ISP-SNSCC ($n = 18$) and OSP-SNSCC ($n = 2$) at a single large academic institution were retrospectively identified from previously published tumor cohorts. Representative formalin-fixed paraffin-embedded tissue was selected for targeted DNAseq using the OncoPrint Comprehensive Assay and an Ion Torrent Proton sequencer; when available, tissue from the corresponding papilloma component was also selected. Somatic variants and copy number alterations (CNA) were identified via in-house bioinformatics pipelines, and prioritized alterations were nominated by manual curation using previously established criteria.

Results: ISP-SNSCC demonstrated a total of 70 prioritized somatic variants (median per tumor = 3; range = 1-12). All tumors harbored *EGFR* mutations, including a previously unreported exon 6 hotspot variant; other recurrently mutated genes included *TP53* ($n = 13$), *CDKN2A* ($n = 8$), *NFE2L2* ($n = 4$), *PIK3CA* ($n = 3$), *FBXW7* ($n = 3$), and *NOTCH1* ($n = 3$). A total of 36 CNA were identified in ISP-SNSCC (median per tumor = 1.5; range = 0-5). *CDKN2A* (loss; $n = 8$) was the most frequent CNA, with 6 tumors showing two-copy loss ("deep deletion") and 2 showing single-copy loss; other recurrent CNA include *TERT* (gain; $n = 5$) and *SOX2* (gain; $n = 3$). All ISP-SNSCC harbored at least one *TP53* or *CDKN2A* alteration, with >85% of tumors having at least one *CDKN2A* alteration; all 7 matched ISP were negative for *TP53/CDKN2A* mutations and showed no CNA. Both OSP-SNSCC demonstrated *KRAS* G12D mutations with concurrent *TP53* mutations. *EGFR* was amplified in two ISP-SNSCC, and *KRAS* was amplified in one OSP-SNSCC.

Conclusions: Malignant progression of sinonasal papilloma to SNSCC involves highly recurrent molecular alterations, including *TP53* mutation and *CDKN2A* mutation/deletion. Common molecular alterations in head and neck squamous cell carcinoma also occur in subsets of sinonasal papilloma-associated SNSCC.

1385 PanCancer and MicroRNA Analysis of Cystic Adenoid Carcinoma Patients using NanoString Technology

Maicon F Zanon¹, Leticia F Leaf², Adriana Carloni², Rui Reis², Adriane F Evangelista², Cristovam Scapulatempo Neto³. ¹Barretos Cancer Hospital, Barretos, São Paulo, ²Barretos Cancer Hospital, ³Barretos, SP

Background: Adenoid cystic carcinoma (ACC) is a relatively rare tumor, constituting only 2–3% of all tumors. This malignancy arise mostly from salivary glands, being the second more frequent in this tissue. Regarding to the molecular signatures of ACC, the oncogenic fusion MYB/NFIB, accounts for approximately 79% of the cases. Despite of these findings, molecular biology of ACC remains largely unknown. The main goal of this study is to analyze the PanCancer and microRNA panels of ACC patients intending to find new biomarkers associated with the most relevant clinical-pathological characteristics and also to evaluate the regulation patterns according to microRNA-mRNA networks.

Design: A total of 19 patients samples from ACC salivary gland tissue

from FFPE was submitted to RNA extraction using RecoverAll Total Nucleic Acid isolation kit and following to NanoString PanCancer and microRNA panels, which analyzes 800 cancer hallmarks and functional microRNAs, respectively. A commercial pool of human salivary gland total RNA (Clontech) was used as control. Data were analyzed using R and bioconductor packages, for filtering, batch adjust, normalization and statistical analysis. MicroRNA-mRNA association was performed using miRDip database and networks were constructed using Cytoscape bioinformatics tool.

Results: It was possible to identify molecular signatures from PanCancer genes and microRNAs targets according to salivary gland type, solid and growth patterns, tumor grade, sex, angiolymphatic and perineural invasion. Several putative interactions between differentially expressed microRNAs and mRNAs have been identified in salivary glands (major compared with minor), including *MET* and *NR4A3* and the microRNAs hsa-miR-23b-3p and hsa-miR-590-3p. The transcripts *MET* and *NR4A3* and the microRNA hsa-miR-23b-3p were also identified as differentially expressed in topography (solid tumors compared with the other types).

Conclusions: Differentially expressed PanCancer genes and microRNAs in ACC can vary according to the major clinical features of the disease and their regulation pattern can be associated in microRNA-mRNA networks.

1386 Somatic Mutations in Head and Neck Cutaneous Squamous Cell Carcinoma

Catherine Zilberg¹, Ruta Gupta², Matthew W Lee¹, Bruce G Ashford³, Marie Ranson⁴, Tsu-Hui (Hubert) Low², Sydney Ch'ng³, Mark Cowley⁵, N Gopalakrishna Iyer⁶, Carsten E Palme³, Jonathan Clark³, Bing Yu⁷. ¹The University of Sydney, ²Royal Prince Alfred Hospital, Sydney, NSW, ³Chris O'Brien Lifehouse, ⁴University of Wollongong, ⁵Garvan Institute of Medical Research, ⁶Singhealth Duke-NUS Head and Neck Centre, ⁷Royal Prince Alfred Hospital

Background: The genomic landscape of head and neck cutaneous squamous cell carcinoma (HNCSCC) is poorly characterized. High tumor mutation burden, a predominance of tumor suppressor genes and a typical UV mutation signature have been reported for HNCSCC. *TP53*, *ATM*, *APC*, *NOTCH1* and *CDKN2a* mutations have been described in HNCSCC. Additionally, well-characterized oncogene mutations in *BRAF*, *HRAS*, *EGFR*, *KIT* and *SMO* amenable to targeted therapy have been identified in HNCSCC. This study evaluates the genetic alterations in primary HNCSCC and studies and compares the mechanisms of carcinogenesis associated with clinicopathologic characteristics of patients.

Design: Highly cellular areas of 10 high risk HNCSCC that did not metastasize at a follow up of at least 24 months underwent targeted gene sequencing with the TruSeq Amplification Cancer Panel (Illumina, San Diego, USA). The somatic mutations were analyzed for functional significance utilizing SIFT, PolyPhen, FATHMM and Qiagen OCl Database. Associations with clinicopathological variables were evaluated. Pathway analysis was performed for individual patients.

Results: The study included 10 patients with primary non-metastatic HNCSCC (38-92years, 8 Males, 2 Females, tumor diameter 7-160mm). A UV signature was seen. 436 known or predicted significant mutations in 45 genes were identified across 10 samples. 56 mutations present at a variant allele frequency >5% within the tumors have been functionally validated and of these 80% were tumor suppressor genes. Of the 380 mutations with a frequency <5%, 66% were tumor suppressors. The cell cycle/apoptosis pathway and APC pathway were altered in 100%. Other commonly altered pathways were DNA damage response (90%), MAPK (80%) and PI3k/Akt/mTOR (80%). The youngest patient in this cohort was immunosuppressed and demonstrated the maximum number of somatic mutations seen in this cohort. Loss of function mutations in *SMAD4* were seen only in patients with a higher mutation burden. *CDKN2a* mutations were only seen in tumors >50mm in diameter. Alterations in *CTNNB1* and *FGFR2* were associated with peri-neural invasion.

Conclusions: HNCSCC demonstrated a predominance of loss of function mutations in tumor suppressor genes. Multiple mutations in oncogenes were also seen, particularly at low variant allele frequency. These factors, coupled with the high mutation burden seen in HNCSCC present challenges for the development and use of targeted therapies for this disease.